MOVEMENT SEQUENCES BASED ON TEMPORAL INTERVAL DURATION AND SPATIAL POSITION AND NEURONAL ACTIVITY IN MACAQUE DORSOLATERAL PREFRONTAL CORTEX

A THESIS
SUBMITTED TO THE FACULTY OF THE
UNIVERSITY OF MINNESOTA
BY

STEPHEN KERRIGAN

IN PARTIAL FULFILLMENT OF THE REQUIREMENTS
FOR THE DEGREE OF
DOCTOR OF PHILOSOPHY

JAMES ASHE

November, 2014

Acknowledgements

It would like to acknowledge and thank Dr. James Ashe; thank you for the space and trust to complete this work, it has been my pleasure. I would also like to acknowledge and thank the Department of Neuroscience; you are a wonderful community of good scientists and I have benefitted greatly from interactions with almost all of you.

To my family: Michael, Nancy, James, & JJ; you are each special, and have contributed uniquely to the completion of this thesis. Thank you for your tireless support, your encouragement, and your proud reckless bragging. To my wife JJ, you are the volunteer in this group; I am lucky everyday. And to Nona, we all owe you everything, thanks for a lifetime of jokes, stories, and food.

Dedication

This thesis is dedicated to my wife and children, my family, and the loving memory of our Nona, Francis Amelia Landolfi.

Table of Contents

List of Tables

List of Figures

Prologue

The greatly expanded prefrontal cortex is one of the distinctive features of the primate brain. Although there are many competing theories about the specific functional properties of granular prefrontal cortex (PFC), there is a general agreement that its development conferred a significant evolutionary advantage on primates. One specific proposal is that the fundamental function of PFC is to enable primates to generate and prospectively encode goals (targets for action) based on a combination of the animal's biological motivations and its perception of the current behavioral context, and to be able to do so on the basis of single experiences (Passingham and Wise 2012). There are several functional subdivisions within the PFC, each of which has a distinct set of physiological properties. The dorso-lateral region of the prefrontal cortex (dlPFC) is the most strongly connected to both motor control structures and the dorsal visual steam, and because of these connections it is able to influence visually guided behavior. The dlPFC encodes goals for movement based on the duration, order, and visuo-spatial location of recent events, amongst other features (Mushiake, Saito et al. 2006, Tanji and Hoshi 2008, Genovesio, Tsujimoto et al. 2009, Genovesio, Tsujimoto et al. 2011). The objective of this thesis is to describe the properties of single neurons in macaque dlPFC, as far as they are currently understood, and to add to that knowledge by describing neuronal activity during movements that are well-defined by the conjunction of their timing, order, and direction.

In order to speak, play music, or dance, it is important that each movement be both properly timed and sequenced. For instance, when playing a sequence of notes on a piano, each key must be struck in the right order, at just the right moment, and then held in place for a specific amount of time, before it is released. How does dlPFC contribute to the neural control of spatio-temporal sequences such as this? To address this question we trained two macaque monkeys to perform a behavior that combined a sequential movement task with a temporal interval production task, and then we recorded the activity of single

neurons in dlPFC. Specifically, the subjects made a series of directional movements of a cursor, and between the movements they performed self-timed delays of specific durations. During this challenging task, each visually-guided movement was described by the conjunction of its timing, serial order, and spatial location. Complex tasks like this one are important to study because it is impossible to predict what neural activity will be observed based on how the same neurons behave during more simplified behaviors such as the much used center-out task.

To succeed at this task the animals had to solve several problems. First, the subjects needed to keep track of time. The neural representation of time is the subject of the first section in the introduction, and the results in Chapter 3. Second, the subjects needed to move to the right targets in the right order; we called this the 'spatial sequence', and we called the sequence of three different self-timed temporal interval durations the 'temporal sequence'. The neural control of movement sequences is the subject of the second section in the introduction, and the focus of the results in Chapter 4. Third, the subjects needed to produce the correct spatio-temporal sequence while also keeping track of time during the delays. Attention-dependent behaviors in which voluntary, rather than habitual or stimulus-driven, thoughts and actions are performed are thought to depend on the PFC (Shallice 1982, Miller and Cohen 2001). The anatomical structure and contingent theoretical functions of the PFC are the subject of the third section of the introduction. Finally, there were many possible ways that neurons in dlPFC might have encoded movement information while the animals performed the task. We employed an information theoretic analysis to address the subject of neural coding. Information theory and its application to neural data is the subject of the fourth and final section of the Introduction, and contributes to the final results in Chapter 4.

Chapter 1: Introduction

Section 1.1: The Neural Representation of Interval Timing

Time is one of the fundamental contexts for behavior; any movement occurs at a specific time and lasts for a certain duration. Sometimes, the moment at which a movement is made is especially important. For instance, some movements must be made to coincide with the elapsed or remaining amount of some temporal interval. Examples of this kind of timed movement are common in daily life, and include playing a musical instrument, dancing, speaking, and responding to a yellow traffic signal while driving. The accuracy and effectiveness of a movement is dependent on what is done, and also when it is done. Where in the brain are timed movements generated, and how is time represented in relation to the rest of the movement parameters? In the following sections, we review the brain structures involved in interval timing, theoretical models of neural clocks, and the general principles of temporal processing that can be gleaned from behavioral studies and from neural recordings in non-human primates.

1.1.1: Brain Structures Involved in Interval Timing

Temporal processing in the brain spans an enormous range of time, from microseconds to days and months. There is a consensus that specialized neural mechanisms process timing signals at different portions of this scale; in other words, the set of brain structures involved in interval timing is dependent on the range of time intervals being discussed. In this thesis research we focus on the generation of timed motor responses and the perception of interval duration in the range of a few hundred to a few thousand milliseconds, further references to ‘interval timing’ will refer to this range. It remains a matter of debate whether or not the brain has specialized circuits for interval timing (Buhusi and Meck 2005), but is it known that no single structure is essential to the neural control of interval timing; there are no diseases or lesions that have been shown to stop subjects

from either recognizing or producing timed intervals (Buonomano and Karmarkar 2002). Instead, the combined activity of large neural networks contribute to the neural control of interval time, and these networks are distributed across several cortical regions, the cerebellum, and the basal ganglia. For example, a meta-analysis of interval timing studies that imaged human subjects showed that during interval timing tasks the right dorsolateral prefrontal cortex, the right posterior parietal cortex, the bilateral supplementary motor areas, the left hemispheric sensorimotor cortex, and the cerebellum in the right hemisphere are recruited (Lewis and Miall 2006). Interestingly, during tasks that minimized movement during the timed interval; or excluded predictable, regular, and repeated intervals; only the two association cortices remained preferentially active, namely the dorsolateral prefrontal cortex and the posterior parietal cortex. The learning and production of conditioned reflexes in the range of tens to hundreds of milliseconds has been conclusively determined to depend on the cerebellar cortex (Ivry and Spencer 2004). The cerebellum may also participate in timing in the range seconds, and the feed-forward control of other, more complex ‘cognitive’ behaviors, but the well-known participation of the cerebellum in the coordination and control of movement may have thus far obscured observation of these functions. In addition to the prefrontal cortex and the cerebellum, the basal ganglia also appear to be involved in the neural control of interval timing. For example, interval timing is disrupted in subjects with Parkinson’s disease and Huntington’s disease, both of which are degenerative diseases of the dopaminergic projections to the basal ganglia (Ivry and Spencer 2004). Drugs that modulate dopamine in the basal ganglia, such as dopamine agonists and antagonists cause overestimations and underestimations of the passage of time (Rammsayer and Lima 1991, Rammsayer 1999).

1.1.2: Clock Models for Internal Estimates of Elapsing Time

There are many brain regions that participate in interval timing, but the specific roles they play and the mechanisms they use are unknown. However, theoretical 'clock' models suggest potential solutions to the problems intuitively posed by interval timing tasks. Interval timing tasks, such as determining which of two stimuli lasted longer, require neural timing mechanisms that can be started or reset at any moment, can count elapsed time, and compare the duration of elapsed time to a previously encountered duration held in memory. To produce a timed movement, in which the subject needs to time a specific interval duration that needs to elapse before the movement begins, a slightly different set of control mechanisms (or processes) are required; the appropriate interval duration must first be retrieved from memory, then the clock must be started, the right amount of time must pass, and then the movement must be generated.

There are two popular types of theoretical clocks that describe the neural mechanisms used to perform interval timing tasks. The most common is the pacemaker and integrator type (Gibbon, Malapani et al. 1997, Buonomano and Karmarkar 2002, Ivry and Spencer 2004, Mauk and Buonomano 2004, Buhusi and Meck 2005). The pacemaker represents the ticking clock, and the integrator counts the number of ticks. In this model, additional cognitive processes would be required to represent recall from memory, to determine the best bin sizes at which the integrator should operate, and a comparator would be necessary to make judgments of relative duration. Clearly separated clock, memory, and decision stages are specified in models of this type, and there are many variants; various pacemaker signals have been proposed, ranging from single neural oscillators, oscillating neuronal populations, and distributed neural oscillations in thalamo-cortical circuits (Buonomano and Karmarkar 2002, Buhusi and Meck 2005). Some models specify neural oscillators operating at a single rate, while others tune the oscillator to the interval, rather than in integrator or bin size (Buhusi and Meck 2005). Other model variants adjust the memory and decision

stages, such as specifying different levels of independence between the integrators used for different timing bin sizes, and various additional processes, such as reinforcement learning signals. The effects of stimulant drugs have been interpreted to support the pacemaker/integrator hypothesis. Dopamine agonists and antagonists cause characteristic distortions in the perceptions of time, as if caused by speeding up or slowing down the pacemaker (Rammsayer 1999). Alternatively, these same studies have been interpreted to suggest that rather than increasing the speed of the oscillator, the dopamine agonist might lower the threshold that the accumulator needs to reach before signaling the time has elapsed (Buhusi and Meck 2005). The second type of theoretical clock model is the 'population clock' that posits the ability to track ongoing time is a natural consequence of signal processing by simple neural networks is (Buonomano and Karmarkar 2002, Buonomano and Maass 2009). The idea is that if one could observe all the neurons in a network, then spatio-temporal patterns in the network's activity will emerge that uniquely encode each passing moment during a temporal interval (Buonomano and Merzenich 1995). To decode the time-dependent information, the population activity is first transformed into a single point in the 'state space', which represents all the possible ways the network could be active. Following the 'neural trajectory', the path of that point through the state space as it tracks the network activity over time, has been shown to be sufficient to keep track of ongoing time in theoretical, and in-vitro neural networks (Salinas 2009, Buonomano and Laje 2010). An important consideration is that the networks require training and the same initial conditions to make the activity patterns repeatable, and thereby allow the passage of time to be decoded. These results show that relatively small, simple neural networks can represent the passage of time and they suggest that the representation of ongoing time may be common in the more complicated and highly interconnected networks of the brain that are primarily known for signal processing related to other functions.

Despite the existence of the several plausible hypotheses reviewed above, there is no consensus either on the brain areas involved or the specific neural mechanisms used to encode interval timing. The theoretical models mentioned above are both compatible with single or multiple clocks and with either a narrowly focused or a widely distributed process. If multiple 'clocks' are used to perform interval timing behaviors, they may be segregated based on the length of the timed interval, the modality of the temporal signal, or the type of movement. In terms of the spatial distribution, the neural representation of interval time might span the whole brain, or be localized to distinct physiologically or anatomically defined circuits, such as somatotopically organized thalamo-cortical-striatal loops. In the following section, I review the experimental results from human behavior and macaque neurophysiology, but these do not unequivocally support any particular model. There is no consensus about which, if any, model best describes the neural mechanisms for interval timing, how each model's elements map onto actual brain structures, or where in the brain time-dependent signals originate.

1.1.3: Interval Timing: Behavioral Studies

In interval timing experiments, subjects are asked to estimate, re-produce, or compare temporal intervals. Over many trials the behavioral results are used to build psychophysical curves that illustrate the subjects' internal estimates of duration. There are several principal observations in how subjects judge, and mis-judge, the passage of time that are common to humans, macaque monkeys, and some other animals (Gibbon, Malapani et al. 1997, Lewis and Miall 2009). The first observation is that the precision of temporal interval estimation is relatively low when compared with other physiological processes such as sound localization, reflex conditioning, and circadian rhythm. The mechanistic reasons for this finding are not understood, but the common understanding is that it is somehow a consequence of the conscious, flexible nature of interval timing

compared to these other processes (Gibbon, Malapani et al. 1997, Buonomano and Karmarkar 2002, Ivry and Spencer 2004, Mauk and Buonomano 2004, Buhusi and Meck 2005). Subjects can decide at will when to start and stop their internal clock during interval timing, and can apply it to any sensory modality or in any motor task. This conscious control seems to come at the price not only of precision, but with a requirement for sustained attention, especially in the longer 1000 ms range (Rammsayer and Lima 1991). For instance, distractor tasks such as mental arithmetic and variable loudness degrade temporal interval discrimination, consistent with attention-based cognitive models of human timing.

The second observation is that the variability of temporal interval duration estimates scales almost linearly with the length of the duration (Gibbon, Malapani et al. 1997, Buhusi and Meck 2005, Lewis and Miall 2009). This is referred to in the literature as the scalar property or conformation to a power law. Gibbon originally proposed that the scalar property (or scalar expectancy model) was an extension of Weber's law, which refers to an increase in the size of the just-noticeable-difference between two stimuli that is proportional to their magnitude. The underlying mechanisms for this observation are not understood, but again, the assumption is that it is somehow a result of the flexibility of interval timing mechanisms. The 'coefficient of variation' is a metric that describes the proportional relationship between interval estimate variability and interval duration; over a certain range of intervals it tends to remain constant, because the variability increases linearly with duration. In a meta-analysis of many psychophysical studies (Gibbon, Malapani et al. 1997), noted that the coefficient of variation remained relatively constant for interval durations between 100 and 1500ms; the authors suggested that interval timing in this range is controlled by a common neural mechanism with the corollary that timing in other ranges might be governed by different neural mechanisms or substrates.

The third observation is that the results of many behavioral studies support the proposal of Gibbon that different neural mechanism may operate for different temporal interval durations when temporal intervals are defined by two different sensory signals, such as when an interval begins with a somatosensory cue but ends with an auditory cue, sub-second interval timing performance is significantly worse (Buonomano and Karmarkar 2002). The differential effects on sub-second and supra-second interval timing suggest that different neuronal mechanisms operate at these two ranges. However, it is also possible that it is more difficult to bind incongruent cues to a single percept in only a few hundred milliseconds and this may account for the observation without having to invoke different neural mechanisms. Yet another alternative is that shifting attention is more difficult on the shorter intervals. Studies of learning transfer also suggest multiple interval timing mechanisms. Differences between sub-second and supra-second timing require further study, as all studies do not differentiate between the two; a related set of experiments failed to detect differential effects of÷ several distractor tasks, such as mental arithmetic or variable loudness, on very. short (50 ms) versus 1000 millisecond timing (Rammsayer and Ulrich 2005).

Fourth, timing processes seem to be centralized and common to many different overt behaviors. For instance, the perception and production of temporal intervals seem to be related; for example, practice on a sensory timing task at some interval, say 400 ms, tends to produce improvement on a movement task for the same interval (Gibbon, Malapani et al. 1997). However, these results could directly relate to timing due to improving the precision of a centralized timer for that duration, or ancillary neural processes, such as improvements in the recall from memory of the specific duration that is desired.

Finally, the accuracy of temporal interval estimates has recently been shown to depend on the timing context (Jazayeri and Shadlen 2010). During an interval estimation task, subjects timed test intervals that ranged in duration from

approximately 500 to 1,200 ms. Importantly, the overall range was broken down into three overlapping subdivisions of about 350 ms in width, and the test durations were sampled from only one subdivision during each block. The authors found that human subject's interval estimates regressed toward the mean stimulus duration in each block. This meant that an individual test duration was more often overestimated or underestimated depending on the block. The authors were able to model the temporal interval estimates by combining a naïve estimate of the test stimulus that included scalar variability, with a prior expectation for the test interval's duration that depended on the current block. These results suggest that human subjects had implicit knowledge about the variability in their sense of passing time, and adjusted their interval estimates using learned implicit expectations about the timing context.

In summary, interval timing mechanisms enable the neural representation of passing time in the range of hundreds to thousands of milliseconds, which subjects use to judge interval durations and produce timed movements. Human subjects, and other animals, can perform many kinds of interval timing tasks, but their neural representations of elapsing time are imprecise. Psychophysical studies of behavior have defined several principles governing the variability of temporal interval estimates, and so these observations implicate which neural mechanisms might generate neural representations of interval time. The neural representation of interval time is variable, and an interval estimate's variability grows with the duration of the timed interval. However the rate of growth may change at 100 ms, and again at 1500 ms (Gibbon, Malapani et al. 1997, Lewis and Miall 2009). Intermodal timing tasks in the range of a few hundred milliseconds increase interval estimate variability, but not in the range of seconds (Buonomano and Karmarkar 2002). Psychophysical results suggest that different neural mechanisms might operate on different periods of time, but it is hard to determine the specific processes responsible. Besides keeping track of ongoing time, there are other stages during temporal estimation tasks that might have led

to the psychophysical observations, such as storage or retrieval of duration from memory, or the comparison of measured durations to experimental or memorized standards. I review data from pharmacology and invasive electrophysiology below that further expand upon the accuracy and precision of neural representations with which subjects perceive and produce temporal intervals.

1.1.4: Interval Timing: Pharmacology and Behavior

The pharmacological effects of dopamine agonists implicate differences in the interval timing mechanisms used for sub-second and supra-second timing. In the previous behavioral results both time ranges were consciously estimated. The following experiments contrast temporal intervals of 50 ms versus 1000 ms in duration; and the results obtained using temporal intervals of 50 ms in duration may not be consciously estimated, and so seem unlikely to be comparable to sub-second intervals of 500 ms in duration. In any case, it seems that dopaminergic signaling is important to timekeeping of any duration, systemic administration of dopamine agonists causes human subjects to overestimate the passage of time, while dopamine antagonists cause them to underestimate how much time has passed (Rammsayer and Lima 1991). If dopamine played a role in either the rate of a pacemaker or the level of a decision threshold, it could cause these behavioral results. Administration of Haloperidol, a D1 and D2 receptor antagonist, to human subjects was found to impair interval discrimination at 50 and 1000 ms durations, but Remoxipride, a more selective antagonist for D2 receptors, only impaired interval discrimination for 1000ms intervals (Rammsayer and Classen 1997, Rammsayer 1999). The same authors also found that Midazolam, a benzodiazepine agonist of GABAa receptors, impaired interval timing tasks that used a 1000 ms standard interval, but not tasks using a 50 ms standard interval (Rammsayer 1999). These results show different requirements for dopamine signaling and overall activity level during 50 ms versus 1000 ms interval timing tasks. Importantly, Midazolam also impaired

performance during a short-term memory test of immediate word recall, but was not shown to cause significant sedation or motor impairment. These effects support the idea that short-term, or working, memory is important for interval estimation in the range of seconds, and reflects the requirement that subjects maintain sustained focus in order to perform interval timing tasks within this range. In summary, the effects of systemic drug administration support the idea that there are multiple interval timing mechanisms that operate on separate interval durations; and that longer durations, in the range of seconds, rely on working-memory-like cognitive processes that depend on D2 dopamine receptors.

1.1.5: Interval Timing: Macaque Cortical Neurophysiology

To perform interval timing tasks, the brain must estimate elapsing time. To understand this process we must first understand how the activity of single neurons is modulated by the passage of time. Extracellular recordings of single neurons in macaque cortex have begun to catalogue neuronal activity related to the passage of time that is distributed across the regions of the brain most highly recruited during interval timing tasks (Lewis and Miall 2006), which include the posterior parietal cortex (Leon and Shadlen 2003, Janssen and Shadlen 2005, Maimon and Assad 2006, Schneider and Ghose 2012), the dorsolateral prefrontal cortex (Niki and Watanabe 1979, Onoe, Komori et al. 2001, Brody 2003, Sakurai, Takahashi et al. 2004, Roesch and Olson 2005, Genovesio, Tsujimoto et al. 2006, Tsujimoto and Sawaguchi 2007, Sakamoto, Mushiake et al. 2008, Genovesio, Tsujimoto et al. 2009), the supplementary motor area (Mita, Mushiake et al. 2009, Merchant, Zarco et al. 2012), and other regions of frontal cortex (Lucchetti and Bon 2001, Lucchetti, Ulrici et al. 2005, Oshio, Chiba et al. 2006, Lebedev, O'Doherty et al. 2008, Ohmae, Lu et al. 2008)

Recordings of single-cell activity that paralleled a macaque subject's perception of elapsing time were made in the lateral intra-parietal area (LIP) of the posterior parietal cortex (Leon and Shadlen 2003). During an interval discrimination task, subjects indicated whether a stimulus duration was longer or shorter than a memorized standard by making a saccade. As time passed during the test interval, the likelihood that the subject would choose the 'longer' or 'shorter' target changed accordingly. The activity of single neurons in LIP was found to represent this likelihood, and so reflected the subject's neural estimate of elapsing time. Neurons in LIP have also been shown to represent the likelihood of observing a visual 'go' cue, which was possible given an internal estimate of how much time had passed during the previous delay (Janssen and Shadlen 2005). These studies demonstrate that neuronal activity in LIP represents a decision process that was based on the animals' internal estimate of elapsing time.

Neuronal activity in LIP has also been found to relate to movement timing. During a task in which subjects were required to saccade every 1000 ms, neuronal activity during the interval between movements either increased or decreased monotonically with the passage of time, and was predictive of the interval duration, but not other metrics of the eye movements (Schneider and Ghose 2012). During another task, in which subjects pressed a key to reverse the direction of a moving dot before it hit an obstacle, neuronal activity increased at a rate that predicted the timing of the button press, and reached a threshold level at reliable times before the movement (Maimon and Assad 2006, Maimon and Assad 2006). These results show that in LIP the rate of change and threshold level of activity are involved in movement timing.

Several areas in frontal cortex participate in the control of timed movements. For instance, the primary motor cortex (M1) and dorsal premotor cortex (PMd, located just rostral to M1) encode the passage of time for several seconds prior

to a self-timed movement. During a self-timed delay task, in which macaque subjects held a button down for 2.5 to 4.5 seconds, neurons in M1 and PMd exhibited near monotonic increasing or decreasing activity, the duration of which was scaled to the length of the delays, but the overall pattern and magnitude of which remained virtually unchanged (Lebedev, O'Doherty et al. 2008). The time at which the peak (or trough) neuronal firing rate was reached was closely correlated with the time of the movement, and many neurons were also phasically active at the start of the self-timed intervals. The authors were able to decode single trial predictions of both the amount of time passed since last movement, and the amount of time remaining until the next movement, using the activity of neuronal ensembles that was recorded before the overt motor behavior. The PMd has also been shown to prepare timed responses based on the duration of a visual stimulus (Lucchetti, Ulrici et al. 2005). Pre-motor activity in PMd was timed in accordance with the learned durations of a visual stimulus, and occurred at a reliable delay before movement. These studies show that activity in M1 and PMd is sufficient to trigger movement based on a neural representation of elapsing time.

The pre-supplementary motor area (Pre-SMA), located on the medial surface of frontal cortex, categorizes temporal intervals, tracks the passage of time, and generates signals sufficient to time interval-dependent movements. In one task, subjects were required to press and hold a button down for one of three visually-instructed delay durations, and then to release the button (Mita, Mushiake et al. 2009). Neurons in Pre-SMA signalled the temporal interval duration at the beginning and the end of the delays; for some their activity was modulated in reponse to only one duration and provided a catagorial signal, while for others it was graded, or tuned to preffer one duration more than the rest. During a finger-tapping task, that was at first synchronized to a metronome and then continued without it, several different increasing and decreasing activity profiles were recorded from neurons in the Pre-SMA that encoded either the time since the last

tap, or the time until the next tap (Merchant, Zarco et al. 2012). The neuronal activity observed during this repetitive timed-movement task seem qualitatively similar to the push/pull process suggested to operate in LIP during a similar task (Merchant, Zarco et al. 2012, Schneider and Ghose 2012). These studies show that the Pre-SMA encodes temporal interval durations categorically and is sensitive to the passage of time, thus it is specialized to organize and trigger precisely timed movements.

Neurons in dlPFC encode the duration of visual stimuli, and integrate this information with other stimulus features, such as order and color. Neurons in dlPFC encode the delay duration indicated by visual stimuli; during a delayed saccade task some neurons encoded the durations categorically (short, intermediate, long) (Genovesio, Tsujimoto et al. 2006). Similarly, in an adjacent region of lateral frontal cortex known to contribute to eye movements, the supplementary eye field, or SEF, neurons were found whose phasic activity prior to a saccade was dependent on the duration of the previous delay (Ohmae, Lu et al. 2008). When neuronal activity in dlPFC related to ongoing time was dissociated from response planning during a duration discrimination task, that included two visual stimuli that were shown in two colors, red and blue, the authors found that some neurons only encoded stimulus duration, whereas a greater number of neurons encoded the relative duration of one stimulus versus the other, and did so in combination with other stimulus features. For instance, some neuronal activity was selective for ‘first stimulus longer’ or ‘red stimulus shorter’ (Genovesio, Tsujimoto et al. 2006, Genovesio, Tsujimoto et al. 2009). These results show that dlPFC participates in the control of visual behaviors by jointly representing the decision variable, duration, in combination with other salient stimulus features. Under some conditions dlPFC has been shown to be required for interval timing. During a duration discrimination task in which the subjects memorized the shorter of a pair of reference durations, with a different pair used in each imaging session, and determined if it was the same or different

from a test interval, regional cerebral blood flow in the dlPFC was correlated with the duration of the visual stimuli, and reversible inactivation of the dlPFC using bicuculline significantly reduced subjects performance during the task (Onoe, Komori et al. 2001). The interval durations used in this experiment ranged from 400 to 1,500 ms, and so these findings support the idea that timing intervals of 1000 ms or longer requires working memory and sustained attention, that in turn depends on activity in the dlPFC.

In summary, neuronal activity related to the neural control of interval time has been recorded in the dorsolateral prefrontal cortex, the medial and lateral pre-motor cortex, the primary motor cortex, and the posterior parietal cortex of non-human primates. Neurons in some of these areas have been shown to represent the passage of time directly, and in others to participate in neural processes that use an internal estimate of elapsing time as an input value, such as: signaling the moment to execute a timed movement, encoding the duration instructed by visual stimuli, and reporting a perceptual decision based on duration. The coordinated activity of a distributed visuo-motor neural network that includes these areas enables subjects to estimate elapsing time and perform interval timing tasks. The signature trait of neuronal activity representing the passage of time common to these studies was monotonically increasing or decreasing discharge rate that was scaled to the duration of the temporal interval. Additionally, the neuronal activity reached peaks (or troughs) whose magnitude and timing were consistent with respect to movement and/or visual stimuli, and so might be use to trigger timed movements or mark the timing of stimuli.

It is very difficult to prove that signals are causally related to the neural control of interval or elapsing time. The first reason is because there are many other processes that may be correlated with the passage of time, including but not limited to the decay of a physical stimulus, such as an odorant, the neural adaptation to static sensory stimuli, the growing intention to move, or the

anticipation of a reward. Interval timing experiments, such as those discussed in detail above, have been designed to exclude as many of these possibilities as possible, but it is hard to design a timing experiment that is completely resistant to alternative interpretation. The second reason is that it is hard to prove neural activity is causal in the neural control of interval time, even if it has been shown to represent the passage of time, (e.g. the time until the beginning of a movement can be decoded from neuronal data (Lebedev, O'Doherty et al. 2008, Merchant, Zarco et al. 2012, Schneider and Ghose 2012). This is because neuronal activity that represents time might be part of the timing mechanism itself, the theoretical neural clock, or it might simply have access to a timing input signal that is used to participate in another neurological process.

The distributed networks that control time are certainly not limited to the areas described above. Electrophysiological recordings during interval timing tasks need to be performed elsewhere in cortex, as well as the cerebellum, basal ganglia, and thalamus. Tasks that capture different perceptual and motor aspects of interval timing are likely to differentially engage temporal processing mechanisms, and so new signals related to time, and in new locations. The ubiquity of somatotopically organized thalamo-cortical-striatal loops, and the known participation of the cerebellum in timing movements and sensory stimuli, suggests that recordings of neuronal activity in these areas during interval-timing tasks will generate findings related to the cortical results described above.

1.1.6: Interval Timing Summary

In this section I provided a general introduction to the neural control of interval timing, as it is central to our experimental paradigm. I reviewed evidence that humans and other animals are able to estimate the passage of time, and that the variability of interval estimates conforms to several principles, the first among them being the concept of scalar variability. I have reviewed the brain structures known to be involved in interval timing, and presented a detailed account of the recent recordings of neuronal activity made in non-human primate cortex. I have also introduced theoretical models of neural clocks that might plausibly operate in the brain. I hope to have convinced the reader that the neural control of interval timing is performed by a distributed neural network, but that we do not yet know the full extent of the network, nor which nodes actively participate in the neural representation of ongoing time.

Section 1.2: Sequential Behaviors

In this section we explore the issues related to the neural control of sequential behaviors, and focus on sequences of arm movement made by non-human primates, as this paradigm was used to generate the experimental results in this thesis. ‘Sequential behaviors’ must be learned and contain discrete serial order positions. In the following sections, we will more specifically define sequential behaviors, introduce some general principles of sequential processing that can be gleaned from human and animal behavior, review the brain structures involved, and review the results from neural recordings in non-human primates related to the neural control of movement sequences.

1.2.1: Defining Sequential Behaviors

For behaviors that are performed over time single actions must be organized into logical sequences. The effect of each action in a sequence depends on which actions have already occurred, and in what order. Said another way, the associations between the real-world effects of one action and the next are the prime concern for the controller of an action sequence, because they determine whether or not the desired goal will be accomplished at the end of the sequence. But the associations between sequence elements cannot be used to control sequential behaviors. This is because sequential behaviors are created by repeated resampling from a limited set of actions, which means that many similar sequences will be a part of the animal’s normal repertoire, repeated patterns found in different sequences cause the associations between sequential elements in one sequence to interfere with the sequential associations in other sequences. For the generation of behavior, any system based on a representation of sequences, sequences chunks, or contextual associations between sequence elements will be plagued by such interference. The first realistic conception of a neural mechanism to produce flexible sequential behavior envisioned a representation of serial order that was integrated with

movement representations (Lashley 1951). Labeling sequence elements with serial order positions enables the integration of behavior over time. Specific properties are common to all sequential behaviors, including recognition of sequential stimuli, pre-activation and step-wise reactivation of movement sequences, and monitoring of sequential behavior for error correction and goal updating. Although drawn mainly from examples of human language, Lashley's framework has been supported by macaque neurophysiology, which has documented the neural correlates of many of the features he discussed (sequential goals, parallel pre-activation of sequence elements, and stepwise reactivation and serial order signals) in several regions in the frontal cortex, including the dlPFC, SMA, Pre-SMA (Mushiake, Inase et al. 1990, Tanji 2001, Averbeck, Chafee et al. 2002, Hoshi and Tanji 2004, Saito, Mushiake et al. 2005, Mushiake, Saito et al. 2006).

In this text we explore the issues related to the specification of movements during sequential behaviors. A 'sequential behavior' is not used as a blanket term referring to any series of movements, it must have well defined serial order positions, and a large set of possible movements that may be made at each position. Sequential behaviors are not innate, they must be learned by the animal, and cannot be described by simple syntactical rules such as alternation. Examples of sequential behaviors include written and spoken language, playing musical instruments, performing a choreographed dance, the song of birds, etc. Accordingly, locomotor movements such as swimming, crawling, walking, running, trotting, galloping and others are not sequential behaviors; these more automatic serial movements are performed innately by animals and controlled by oscillatory circuits in the spinal cord and brainstem (Brown 1914, Marder and Bucher 2001, Grillner, Wallén et al. 2008). The coordination and combination of movement segments into a continuous trajectory, such as those performed by a baseball player or gymnast, are also excluded here (Soechting and Flanders 1992, Bullock 2004). The important distinction is that the sequential behavior

must have well defined serial order positions; the complexity of the action performed at each position is immaterial.

Based on examples of human and animal behavior, Karl Lashley suggested that sequences of actions must be pre-activated in parallel, and that the ordinal position of each action could be encoded by the strength of its representation (Lashley 1951). For instance, movement sequences are generally performed too fast to be dependent on sensory or proprioceptive feedback; such as the skilled musician who can play an arpeggio on a musical instrument very quickly or the successive phonemes in speech. This suggests that sequences must be pre-activated in order to support their feed-forward, open-loop control. A common mistake during spoken language is a 'Spoonerism', such as "Let us not forget that waste makes haste." Verbal mistakes tend to misplace words, rather than omit them, and when misplaced, words tend to switch positions within syntactic rules; nouns switch with nouns, verbs with verbs, etc. This mistake reflects the presence of an idea, or goal, specifying the whole sentence, and parallel pre-activation of the words that are categorized by type. Lashley suggested that the strength a word's representation could encode its serial order position. In this scenario it would be possible to transpose 'haste' with 'waste' if the representation of 'haste' flagged in the early part of the sentence and the only other compatible verb readied was 'waste'. Neurophysiological studies to date have identified neuronal activity consistent with the general system postulated by Lashley. In reviewing the following findings related to serial order, I will focus on single neuron results from primate electrophysiology.

1.2.2: The Importance of Serial Order

The neural control of serial order is an important component of sequential behaviors. Ordinal position is an abstract numerical quantity, it enables humans and other animals to identify and categorize actions and events according to their rank, as either first, second, third, etc. (Nieder 2005). As an introduction to the neural control of sequential behaviors, I will first review behavioral results in which non-human primates performed tasks that required a robust neural representation of ordinal position.

The 'ordered object task' is a simple task that measures a subject's ability to remember the order of several actions and plan upcoming movements accordingly. On each trial three objects or pictures are placed in front of the subject; the task is to select one object at a time, and to pick a new one on each of three trials, in any order. Macaque monkeys can learn this task easily, but cannot perform the task better than chance with experimental electrolytic lesions made in the mid-dorsal prefrontal cortex (Petrides 1991, Petrides, Alivisatos et al. 1995, Petrides 2000). In a critical variation of the task, when monkeys were trained on a task that used three novel objects on every trial, extensive lesions in prefrontal cortex (dorsal convexity of the prefrontal cortex or the midlateral and postero lateral prefrontal cortex) had no effect of task performance (Levy and Goldman-Rakic 1999). These results show that the dlPFC is required to maintain a memory of serial order in the face of interference caused by repeated interactions with the same stimuli, and that when the interference was ameliorated by the use of novel stimuli, activity in dlPFC was no longer necessary. In the final variant of this task that I will discuss, a sequence of four novel objects was used in every trial, and then subjects were asked the order in which pairs of stimuli had been presented (Petrides 1991). If the first or fourth object was a member of the test pair, animals with or without dlPFC lesions learned the task in the same amount of time. But for test pairs that included the second and third objects, lesioned animals never reached criterion performance.

These behavioral results are important because sequential behaviors require that serial order be recalled and represented in the face of similar interference; to be recalled from memory and then performed movement sequences must be differentiated from similar sequences present in the behavioral history and future. Thus the neural mechanisms required for sequential behaviors are also likely to depend on the dlPFC.

More recently, extracellular recordings of single neurons in the dlPFC of non-human primates have found neuronal activity selective for the serial order of visual stimuli, both as a stand-alone categorical representation and in conjunction with other aspects of the stimuli, such as their color (Ninokura, Mushiake et al. 2004, Genovesio, Tsujimoto et al. 2009). In fact, neurons in DLPFC encode the serial order of visual, auditory, and tactile stimuli, with some cells encoding serial order without regard for modality, and other cells encoding the conjunction between serial order and modality (Saga, Iba et al. 2011). Interestingly, neurons in the primary motor cortex (M1) have also been found to encode the serial order of visual stimuli that indicated potential movements (Carpenter, Georgopoulos et al. 1999). Sequential movement tasks have not observed signals in primary motor cortex related to the ordinal position of movement in a sequence (Matsuzaka, Aizawa et al. 1992). In summary, behavioral and neuronal evidence shows that the dlPFC is important for the neural representation of serial order, which is one of the critical components required for the neural control of sequential movements.

1.2.3: Movement Sequences

The planning and execution of movement sequences may be divided into four steps. The behavioral goal must be prospectively encoded; the overall sequence and the set of action elements that will be used to achieve the goal must be prepared; serial reactivation of each element must be performed in the correct order; and serial outcomes must be monitored for error-correction and goal or rule-updating. There are compelling neural data that the dlPFC is engaged in all of these functions (Tanji and Hoshi 2008).

Neurons in dlPFC and other regions of frontal cortex encode the sequence in which multi-modal stimuli are presented (Ninokura, Mushiake et al. 2004, Genovesio, Tsujimoto et al. 2009, Saga, Iba et al. 2011), and can respond to these signals by planning and generating sequential movements with various effectors. Barone and Joseph found that neurons in the dlPFC integrated temporally and spatially discontinuous sequences of auditory and visual stimuli, prospectively encoded the instructed sequential eye and limb movements, and then encoded the unfolding behavioral states as the subjects responded (Barone and Joseph 1989). The dlPFC, SMA, and Pre-SMA have been shown to participate in the specification of movement sequences in the absence of outside stimuli; they contain neurons that are more active for self-guided, rather than visually guided sequential movements (Mushiake, Inase et al. 1990, Matsuzaka, Aizawa et al. 1992). As a comparison, neurons in M1 were found to participate in the movements, but did not differentiate between the visually-guided, and self-guided conditions (Mushiake, Inase et al. 1990).

One of the parameters used to prospectively encode a sequence is its goal. Because a variety of different movement sequences may accomplish any specific goal, goals do not specify specific sequences, or even specific movements. This means that goals also serve as an abstract categorical system for movement sequences, one that ultimately does not require sequences to share any

operational traits. Neurons in dlPFC specify and categorize movement sequences by encoding goals (Mushiake, Inase et al. 1990, Saito, Mushiake et al. 2005, Genovesio, Tsujimoto et al. 2012). In the case of spatial movement sequences through simple mazes, neurons in dlPFC were found to signal intermediate and final goal positions before any movements have been made, but not the path used to get there, nor the movements required to move along the path (Saito, Mushiake et al. 2005). Movement sequences may also be categorized by similarities in their structure, even when the structural similarities are at an abstract level. (Shima, Isoda et al. 2007) Shima and colleagues trained non-human primates to perform three specific actions (push, pull or turn a handle) which could then be combined in different sequential combinations; each action was instructed by a specific visual stimulus and successive stimuli determined the sequence of actions. The subjects were trained to perform four element sequences based on three abstract categories not defined by the component movements: four-repeating (e.g. *pull pull pull pull* or *push, push, push, push*), alternate (*pull turn pull turn*), and paired (*turn turn pull pull*). Neural activity in dlPFC was selective for the abstract categories independent of the component movements prior to movement initiation. In this task each movement sequence was performed in a block, and so the neuronal activity selective for sequence categories was distributed over several blocks. The prospective encoding of goals, or other abstract sequence categories, are also examples of the parallel activation of a set of movements.

During the planning and execution phases of a movement sequence, a few experiments have observed neuronal activity related to the parallel pre-activation followed by serial reactivation of each movement in the sequence (Averbeck, Chafee et al. 2002, Mushiake, Saito et al. 2006). Both studies recorded neuronal activity in macaque dlPFC during a sequential movement task. In the first study, non-human primates to drew simple multi-segment geometrical shapes, like triangles and squares based on a visual template. The strength of each

movement segment's neural representation was indicated by how often a decoding algorithm, which received the neuronal activity as an input variable, was able to guess the correct segment. During the planning phase of each trial all of the upcoming movement segments were represented for each shape. The strength of the representation for each segment was negatively correlated with the serial order of the planned movements; the first upcoming step in the sequence was the most robustly encoded, and the decoder's performance was increasingly decremental for each serial order position thereafter (Averbeck, Chafee et al. 2002). During movement execution each segment's representation was reactivated; the current segment was the most strongly represented, with each segment's signal strength falling off in both directions. During a movement sequence task that used simple mazes, the same as was mentioned in the previous paragraph, neurons were selective for specific sequences during the planning period (Mushiake, Saito et al. 2006). The results of a decoding analysis were the same to those in the Averbeck study just discussed: during the planning period the movement direction signal was graded from the first step to the last, and during the execution of the task the movement direction signal was strongest for the current step. Neurons in the lateral prefrontal cortex may also reflect the subjective knowledge of upcoming sequences of eye movements in conditions in which non-human primates are required to learn new sequences (Averbeck, Sohn et al. 2006). Similarly, the activity of neurons in this area can predict which of six sequences a subject was going to perform next and when errors would occur (Averbeck and Lee 2007). These results show that single neurons in dlPFC are engaged in the parallel pre-activation and serial re-activation of movement sequence elements.

The integration of organizational signals from dlPFC with more specific movement parameters occurs, at least in part, in the SMA and pre-SMA, two adjacent regions in the medial premotor cortex. The dlPFC does not project directly to M1, but it is strongly connected to the SMA and Pre-SMA, which are in

turn strongly connected to M1 (Matsuzaka, Aizawa et al. 1992, Tanji 2001). Bilateral injection of muscimol, a $GABA_A$ agonist, into either the SMA or pre-SMA prevents non-human primates from performing movement sequences from memory (Shima and Tanji 1998). Only with visual instruction were the animals able to perform the sequential task. During a version of the handle manipulation task, described above, that included six three-element sequences, neuronal activity during the planning period in the SMA and especially the Pre-SMA was selective for specific sequences, and during the execution period serial order, movement type, and their conjunction were encoded (Shima and Tanji 2000, Hoshi and Tanji 2004, Nakajima, Hosaka et al. 2009). Because of the relatively small set of movement types and serial order positions that could be included in this electrophysiological experiment, it is possible that the observed neuronal activity would have been best understood as tuned to the conjunction between movement type and serial order; but may have appeared to be tuned to one movement made in one position, or to link specific movement or serial order pairs. The presence of conjunctions between serial order and movement type allow these signals to believably contribute to the organization of a sequence of actions over time (Tanji 2001).

In summary, dlPFC encodes several important pieces of information related to the neural control of sequential behaviors; it specifies the actions to be included in a sequence according to a representation of the goal, the sequence category, and the specific set of actions that will comprise the sequence, and reactivates each movement in the set as the sequence unfolds. This process depends on the ability of dlPFC to identify and categorize actions and stimuli according to their serial order, and importantly, to integrate a representation of serial order with other aspects of the behavior, such as movement direction or stimulus color. The activity in the SMA and Pre-SMA is suited to the execution of movement sequences based on the more abstract information provided by dlPFC.

1.2.4: Sequential Behaviors Summary

In this section I provided a general introduction to the neural control of sequential behaviors, as a movement sequence task involving spatial and temporal parameters forms the basis for our experimental paradigm. I have described the properties that define sequential behaviors and reviewed evidence that humans and other animals are able to execute movement sequences of this type. I have also introduced the widely referenced ideas of Karl Lashley on this subject, and reviewed behavioral and neuronal results that have come to support his inferences. I hope to have convinced the reader that the dlPFC is importantly engaged in the control of movement sequences, and required for the representation of serial order on which movement sequences depend, hence we have chosen this is brain region from which we recorded neuronal activity during our behavioral task.

Section 1.3: The Primate Pre-Frontal Cortex

The highly adaptable general intelligence of primates is dependent on the prefrontal cortex (PFC), but there is not a single clear summary for how the PFC supports intelligent behavior. Humans and macaque monkeys with PFC lesions struggle to focus their attention and to behave in logical, predictable, or socially acceptable manners; but they typically retain the ability to perform single actions and well-learned daily activities (Shallice 1982, Passingham and Wise 2012). Depending on the region of the PFC affected, lesions may cause either unresponsiveness or distractibility (Shallice 1982). Single unit studies have shown that the PFC is engaged in many neural processes related to the organization of logical behavior, including: timing, action sequencing; response inhibition; task switching; rule encoding; rule switching; stimulus and response categorization; the direction of attention; the retrospective and prospective maintenance of remembered sensory, motor, and cognitive variables, goals, and rewards (Niki and Watanabe 1979, Shallice 1982, Petrides 2000, Duncan 2001, Fuster 2001, Miller and Cohen 2001, Saito, Mushiake et al. 2005, Shima, Isoda et al. 2007, Saga, Iba et al. 2011, Passingham and Wise 2012). These findings also show that the representations of single neurons in PFC highly adaptable; so adaptable that small differences between two behavioral tasks can substantially alter the neuronal activity in PFC, and therefore the associated neural processes used by the brain (Duncan 2001, Passingham and Wise 2012). In order to understand the motivation for our experiment, in which animals were required to satisfy several simultaneous constraints during a sequential task, and the relevance of our findings, the following sections introduce the prefrontal cortex in terms of its anatomical structure, putative function, and the most relevant previous results from macaque neurophysiology.

1.3.1: Anatomical Structure and Axonal Connectivity of the Macaque Prefrontal Cortex

The unique pattern of local and distributed reciprocal connections in the primate prefrontal cortex enable it to direct attention and coordinate behavior based on the highly adaptable encoding of behavioral information by its neurons. The granular pre-frontal cortex (PFC) is the most recently evolved portion of the primate brain, and reaches its largest relative size in humans (Passingham and Wise 2012). Like the rest of the cortex, the PFC is reciprocally and topographically connected with the thalamus and basal ganglia. But granular prefrontal cortex has been differentiated from non-homologous cortex, in rats for instance, based on an anterior shift in its topographically organized connections with the thalamus and its large cytoarchitectural layer four (Wise 2008). The fourth layer of primate prefrontal cortex is deeper than that of other animals, and densely packed with large cell bodies, which allows more input synapses. It is worth noting that the PFC layer 4 is not as large and well defined as the primate primary visual cortex (V1), which receives a massive number of incoming visual axons, and is often referred to as ‘granular’.

The PFC does not communicate directly with primary motor or sensory structures, it is instead reciprocally connected to the highest-level motor, sensory, and affective signal processing structures in the brain, including the medial and lateral premotor cortices, the posterior parietal cortex, the infero-temporal cortex, and the hippocampal and amygdalar complex. The incoming axons from these areas deliver signals to the PFC that are related to movement, perception, memory, and emotion. But the PFC does not only receive these signals, it is in fact an active participant in each of these neural processes, because its own axons project back to its inputs. Prominent reciprocal connections also define the structure within the PFC. Most of the neurons in the PFC are reciprocally connected to most of the other neurons in the PFC. These cortico-cortical connections are topographically organized, sometimes

interhemispheric, and exist both within and between the three main subdivisions of the PFC, the dorsolateral, orbital, and medial regions (Fuster 2001,Passingham, 2012 #897). This unique pattern of local and distributed reciprocal connections is massively parallel; it ranks the PFC as the highest level association area in the brain, and means that neural signals do not pass through the PFC, instead they are associated with each other, and joined together or abstracted, and then returned to their sources (Duncan 2001, Fuster 2001, Miller and Cohen 2001, Rigotti, Barak et al. 2013).

Three main divisions are typically recognized in the PFC: the dorsolateral, orbital, and medial regions. These areas are distinguishable on the basis of cytoarchitecture and the patterns of synaptic innervation, but might be better thought of as specialized rather than separate (Fuster 2001). Each of the three regions of the PFC receives some innervation from the same motor, sensory, and limbic structures, but the proportions are different. The dorsolateral PFC features especially prominent connections with pre-motor and posterior parietal cortices. Due to these connections dorsolateral PFC represents spatial variables from many modalities and supports temporally organized behaviors, such as speech. Lesions of this area cause problems planning and executing sequences of actions, such as preparing dinner, writing, and drawing (Shallice 1982). Difficulty maintaining attention is concomitant with sequencing issues. The orbitofrontal PFC is more strongly connected to the basal ganglia, hypothalamus, and amygdala, and due to these connections it represents not only the level of arousal and response to rewards, but the motivational significance of sensory stimuli. Orbitofrontal lesions release impulsive, reckless, and socially unacceptable behaviors and leave patients prone to distraction. The medial PFC is also strongly connected to the hippocampus and amygdala; it processes internal state, reward, and motivational signals. Medial PFC lesions cause a loss of spontaneity, difficulty initiating movements and speech, and an inability to concentrate. (Fuster 2001, Passingham, 2012 #897). Disorganized behavior and

an inability to direct attention result from lesions in each region of the PFC, but different syndromes result from lesions to each area. The partially overlapping inputs and highly interconnected structure of the PFC seems commensurate with the overall similarity in functions across the PFC, as well as the regional differences.

1.3.2: Functional Theories for Prefrontal Cortex

Purposeful, well-organized behavior requires that separate actions executed at different times are organized into coherent sequences, in which each action helps the animal to achieve its goal. The prefrontal cortex is involved in providing the supervision required to guide behavioral sequences that occur over time. Hence, functional theories for the prefrontal cortex describe its role in prospective goal selection, and the recall and maintenance of mnemonic information. While summarizing the functional role of the prefrontal cortex in behavior, Fuster describes the ‘perception-action cycle’, namely the interplay between ones actions and the changed sensory environment, and points out that the ability to integrate information over time is critical to an animals ability to exert control over the cycle. Fuster placed the prefrontal and posterior parietal cortices at the top of a hierarchical control structure for guiding behavior, in which more automatic behaviors are mediated by stimulus driven action selection which occurs on the lowest levels of the hierarchy, including primary sensory and motor cortices. Progressively higher hierarchical levels participate in processing more abstract features of sensory information, and selecting actions based on more complex rules or contingencies. At the top of the pyramid, pre-frontal cortex mediates contingencies across time between representations of sensory and motor events to prospectively encode goal-directed behavior. Fusters perception-action cycle and hierarchical model have since inspired many more ornate versions (Fuster 2001, Badre 2008, Botvinick 2008).

A more recent hierarchical model argued that increasingly complex rules for choosing the correct stimulus response associations occur at progressively rostral portions of the frontal cortex (Koechlin, Ody et al. 2003). Cross-temporal episodic associations required for behavior are represented in the highest levels or rostral prefrontal cortex, contextual signals are represented in the posterior prefrontal cortex, and stimulus response associations are represented in the premotor cortex. Considerable debate and diversity of hierarchical models persists, but hierarchical structure does appear to coincide naturally with hierarchical control of behavior (Botvinick 2007, Badre 2008).

Prospective encoding of future actions by PFC requires the creation of preparatory set and the active maintenance of a neural representation over time. Preparatory set includes the prospective, rather than retrospective, memory of future goals states. The dorsolateral PFC has been shown to plan movement sequences, and serially activate plans for sequential movements, discussed below. The active maintenance of neural activity representing remembered information was first called ‘working memory’ by Patricia Goldman-Rakic. Neurons in PFC represent visuo-spatial information in elevated firing rates which persist over delay periods in the absence of cue stimuli (Fuster, Bodner et al. 2000).

Shallice described the problem of action selection in terms of the competition between many possible actions, rather than the *de novo* specification of action based on first principles (Shallice 1982). Most of an animal’s daily tasks are routine and can be automatically performed without conscious attention. But sometimes mistakes occur, such as driving home after work, and then realizing you forget to stop for groceries. When multiple action representations are activated by the current internal state and sensory context, Shallice envisioned a two stage conflict resolution system, with routine control operating at all times by means of fast and simple heuristics, like recency or most frequently chosen, to

decide which of the triggered actions to execute, and a supervisory system engaged by attention to inhibit pre-potent responses or boost little used actions in novel situations. In the example above the routine drive home was executed, but distraction prevented the supervisory system from interrupting the trip to stop at the store. In this model the action performed is that with the most activated representation, control occurs by the introduction of a bias signal that boosts the representation of one action.

More recently, Miller and Cohen presented a mechanistic description of how bias signals originating in PFC might influence action selection downstream (Miller and Cohen 2001). Their idea is that when automatic responses must be inhibited and replaced, such as in novel or infrequent circumstances, a descending modulatory signal can be used to bias the competitive, mutually-inhibitory action selection process in favor of the underdog response. Like the ideas of others before, the act of remembering something is accomplished by activation of the representation for that thing, and so the amount of activity in the population of units selective for a given action encodes the strength of the neural representation for that action. The action-selection neural network contains mutual inhibitory units representing alternative actions, and so action representations compete with each other in order to become the dominant action. In their simple population model the bias signal must be sustained in order for the descending bias signal to drive the competitive neural process to select the more weakly activated action. The sustained working memory signals that are characteristic of the PFC are thus well suited to embody this descending control process. The need for sustained activation also conforms to result of errors caused by lack of sustained attention mentioned in Shallice's framework and observed in patients with PFC lesions. Miller and Cohen's mechanism allows an active memory in PFC exert descending executive control over behavior (Buschman and Miller 2007).

1.3.3: Functional Theories Based on the Activity of Single Neurons.
Single-neuron recordings during single experiments in prefrontal cortex highlight the representation of many different salient sensory and motor variables, while observation of the whole volume of literature emphasizes the adaptability of prefrontal cortex to the animal's current task (Duncan 2001). Single cell recordings in prefrontal cortex have also shown that heterogeneous, spatially mixed neuronal populations encode different task-related variables during many experiments (Duncan 2001). Duncan has argued that primate flexibility and success is directly related to the adaptability of distributed representations in PFC. In support of this thesis he presents evidence that the task variables encoded in pre-frontal cortex are determined by the locus of the animals attention (Duncan 2001, Wise 2008). Duncan went on to hypothesize that this centralized co-representation of multiple task variables is critical to coordinating brain-wide processing. For example, despite the fact that different features of a visual object, such as retinal position, body-centered position, velocity, distance, size, color, etc., are processed in separate and discrete regions of extra-striate cortex, attending to a visual object sharpens the perception of all of that object's visual features. The unification of activity related to the attended object might be driven by the activity in prefrontal cortex and its connections to parietal cortices. Duncan's ideas about the adaptability of prefrontal cortex, in combination with the mechanistic for sustained bias signals and action selection presented above, suggest that the adaptability of neuronal activity in prefrontal cortex enables the flexible behavior exemplified by primates.

Another important aspect of neural coding in prefrontal cortex is that single cells are simultaneously selective for many task variables. Typically, publications of neurophysiological recordings from primate prefrontal cortex focus on neuronal selectivity that appears to be related to a single task-related variable. However, two recent publications have shown that neurons in primate prefrontal cortex are

best described by multiplicative sensitivity to multiple task variables, and that this 'nonlinear mixed selectivity' is critical to the success of computational models of neuronal function in PFC, and thus may also be important for the actual computations performed in the brain. (Rigotti, Barak et al. 2013) showed that when the neuronal responses in a population were multiplicatively dependent on multiple task parameters, which they refer to as 'mixed selectivity', they naturally created high-dimensional representations that improved the ability of linear classifiers to guess the task variables being represented. This computational result may help explain actual brain function; relatively simple neuron models can act as linear classifiers, which output a response of either a 0 or 1 depending on whether their input activity is enough to excite them over a threshold. In addition, single cells have been shown to be capable of multiplication of their inputs (Gabbiani, Krapp et al. 2002). (Salinas 2009) showed that a model neuronal network could produce sequential actions if the activity of single neurons were multiplicatively related to serial order and movement type, which enabled neurons most sensitive to serial order to serve as building blocks for the movement sequences, and vice versa. In addition, multiplicative sensitivity to multiple task variables allowed the model to learn new sequences more quickly than alternative arrangements because the established selectivity could be more easily repurposed. In other neural systems multiplicative multiple selectivity may also help bind the results of parallel processing. Multiplicative sensitivity to the auditory cues inter-aural level difference and inter-aural time difference has been shown to be sufficient to allow single auditory neurons to create spatial maps in the owl brainstem (Pena and Konishi 2001). Models of multi-sensory integration also depend on neurons with nonlinear mixed selectivity; multisensory integration occurs in polysensory neurons in the posterior parietal cortex, which is strongly and reciprocally connected to the prefrontal cortex (Salinas 2009).

1.3.4: Conclusion

The prefrontal cortex enables primates to focus on the task at hand and behave in logical, effective, and socially acceptable manners. In this section I have reviewed evidence that the PFC contribute to the flexible, goal-directed behavior of primates by applying sustained, attention-directed bias signals though highly distributed reciprocal connections. These widely distributed bias signals are able to entrain distant neural processes and thereby coordinate brain-wide activity. Executive control by PFC is made possible because of the cellular and network characteristics of PFC. Neurons in PFC are highly adaptable, simultaneously sensitive to multiple features of their current behavioral context, and known to exhibit persistent firing during the recall and maintenance of information. Massively parallel local and distributed reciprocal connections to the PFC subserve both the distribution of top-down control by the PFC as well as the adaptability of the neurons located therein. This anatomical structure means that neural signals enter the PFC and then are associated with each other, both by conjugation and abstraction, and then re-distributed to other high-level motor, sensory, and affective signal processing structures in the brain.

1.3.5: Primate Prefrontal Cortex Summary

In this section I provided a general introduction to the prefrontal cortex. I have reviewed evidence that the PFC is required for well-organized behaviors, which are naturally sequential, and I have described how the cellular and network characteristics of the PFC make this possible. I hope to have convinced the reader that single neurons are PFC are multiplicatively selective for multiple task variables, sometimes referred to as ‘mixed selectivity’, and that this activity is worth studying in greater detail as we have recorded from PFC neurons during complex spatio-temporal movement sequences, and examine the task information encoded by their multiple selectivity using the information theoretic analysis reviewed below.

Section 1.4: Neural Codes and Mutual Information in PFC

What variables does the prefrontal cortex encode, and how does it encode them? Tuning curves based on firing rate have been used to describe neuronal selectivity to the levels of single variables, such as movement direction or stimulus orientation, in primary motor and visual cortex. But constructing tuning curves to describe how neurons in the PFC contribute to brain function would provide a less informative result. This is because, firstly, neurons in PFC encode multiple features or variables simultaneously, and secondly, the variables that neurons in PFC encode are highly dependent on the animals current goals and environment. Therefore, although creating a high dimensional tuning surface could be done, it would only describe the neuronal selectivity during one specific behavioral circumstance. In order to characterize neuronal coding in the PFC we turn instead to computational and information theoretic tools (Shannon 1948, Borst and Theunisson 1999, Nemenman, Bialek et al. 2004, Averbeck, Latham et al. 2006, Victor 2006, Quian Quiroga and Panzeri 2009, Victor and Purpura 2010, Rolls and Treves 2011). An information theoretic analysis does not require specific assumptions about what individual responses 'mean', i.e. that higher firing rates correspond to the neuron's preferred direction and lower rates correspond to anti-preferred directions. This allows an estimate of how much information a spike train carries about all the stimuli in an experiment, rather than an estimate of whether or not a particular stimulus is present (Quian Quiroga and Panzeri 2009). The well-known variability of neuronal responses to the same stimulus (or during the same movement) is taken into account by information theoretic methods in a rigorous way, and is in fact part of the estimate of the information carried by neural responses. Therefore these methods are well-suited to address questions related to behavioral variables that might be encoded in what is otherwise considered to be noise. Information theoretic estimates from spike trains quantify the information available to a post-synaptic observer on single trials, this is useful the brain actually operates on single trials, even though as experimenters we are often forced to average behavior and neural activity

over many trials. Information theoretic methods are also attractive because they can be used to quantify the information contained in neural responses to arbitrarily complex, naturalistic stimuli.

1.4.1: Computing Mutual Information from Spike Trains

In this section and the later results we focus on mutual information (*MI*), which can be thought of as the amount of information communicated from a transmitter to a receiver along some channel. As we focus on the activity of single neurons the neuron is the transmitter, its axon is the channel, and our extracellular recording electrode is the receiver. To compute *MI* by the direct method one measures the total probabilistic variability, or entropy, of the neural responses, and then subtracts the noise entropy, the remaining neural response variability after specifying each stimulus, shown in equation 1 (Strong, de Ruyter van Steveninck et al. 1998). The entropy is calculated using the probability of each response (2), and the probability of each response given the presence of each stimulus (3).

$$MI(R;S) = H(R) - H(R|S) \tag{1}$$

$$H(R) = -\sum_{r\in R} p(r)\log_2 p(r) \tag{2}$$

$$H(R|S) = -\sum_{s=1}^{N_s} p(s)\sum_{r\in R} p(r|s)\log_2 p(r|s) \tag{3}$$

A straightforward measurement of the transmitted information, or mutual information, requires one to know these probabilities explicitly, which requires many observations of every possible combination of stimulus and response. This method was developed for measurement on man-made communication systems

in which this goal was actually possible. But neuronal responses to identical stimuli are variable, and experimental data is limited; so the underlying statistical probabilities must be estimated from the data. Increasing the number of cells, or the number of letters allowed in each code 'word' requires an exponential increase in the amount of data required for the probability estimates. This is referred to as the sampling problem. Luckily for the part-time computationalist, several groups have made progressively more accurate probability estimates possible (Nemenman, Bialek et al. 2004, Victor 2006, Panzeri, Senatore et al. 2007, Magri, Whittingstall et al. 2009). The same groups have also addressed the 'bias' problem, which is the artifactual recovery of a (usually small) amount of extra information caused by the fact that the number of trials during which a particular stimulus or experimental condition is presented is smaller than the number of trials in the experiment.

1.4.2: General Principles for Applying Mutual Information to Biological Data

To understand *how* behavioral variables are encoded in the brain, one must first know *which* variables are encoded in the brain. The old adage 'garbage in, garbage out' applies here; failure to properly represent the variables actually used by the brain in a computational analysis is the most common way computational studies fail to produce useful insights about brain function. This can be difficult for many reasons. First, neural representations become increasingly complex as one moves further from sensory transducers. Neurons in parietal cortex can respond to visual, auditory, and somatosensory stimulation. Second, candidate variables may be deterministically related; for instance, is neuronal activity in primary motor cortex related to a movement's force, position, velocity, acceleration, or jerk?

The computations employed by neural networks in the brain depend on the sensory modality, brain region, and maybe even the behavioral context. When

comparing between information related to one sensory modality or another it is easy to see why this might happen; different sensory modalities vary over huge and different ranges of intensity, present different rates of attack and decay. In the high-activity environment of cortical neurons, a simplified neuronal model derived from cellular properties was unresponsive to and unable to generate precisely timed spikes (Shadlen and Newsome 1998). Their findings supported one common perspective in systems neuroscience, that population coding based on firing rate best describes cortical activity. In a study of single neurons in macaque V1 and V2 some of the visual stimulus-dependent information was found to be encoded in the precise timing and inter-spike interval, or spike patterning (Victor and Purpura 1996, Victor and Purpura 2010). Spike timing was also found to improve population coding of movement sequences in macaque pre-SMA neurons (Averbeck and Lee 2003). Whether cortical neurons rely on precision spike timing to encode information remains an open question. Many of the studies on the topic are theoretical, and caution must always be taken when considering the significance of their results, because a theoretical study determines what seems to be possible based on what we know about neurons and the brain, but an experimental study can show what does happen in the brain, even when we do not yet know how it is possible (Latham and Nirenberg 2005).

1.4.3: Measuring Nonlinear Mixed Selectivity using *MI*

Neuronal selectivity in primate prefrontal cortex is best described by multiplicative, or more generally nonlinear, sensitivity to multiple behavioral variables, as is explained in the previous section 1.3.3 (Duncan 2001, Rigotti, Barak et al. 2013). Nonlinear mixed selectivity naturally creates high-dimensional representations that enable simple linear classifiers, such as single neurons, to decode behavioral variables, and is a critical component of computational models of multisensory integration and action sequencing (Salinas 2009, Rigotti, Barak et al. 2013).

Recently, information theoretic analyses have been used to characterize the information encoded by cortical neurons that display nonlinear mixed selectivity. In macaque primary visual cortex (V1), neuronal responses were recorded during the presentation of three types of visual stimuli (a sequentially flashing checkerboard, a drifting grating, and a stationary grating) that were defined by two independently presented features (contrast and spatio-temporal sequence) (Reich, Mechler et al. 2001). The investigators then computed how much mutual information neurons in V1 transmitted about both features of each stimulus type. Because their computations allowed separate measurement of the information related to each simultaneously presented stimulus feature, the authors were able to show that the amount of spatio-temporal specific information encoded in the neuronal activity was dependent on the stimulus type, while the amount of contrast specific information was not. This meant that the average activity of neurons in V1 encoded information related to the two stimulus features simultaneously and independently.

(Reich, Mechler et al. 2001) also found that a fraction of the transmitted information couldn't be unambiguously assigned to either contrast or spatio-temporal pattern. This quantity is the amount of information that was dependent on the two stimulus features; dependence refers to information about the level of one variable may only be extracted from the spike train in relation to the level of another variable. This quantity does not contribute to the independent portions of the information, and can be created by nonlinear multiple selectivity, (but not linear multiple selectivity). Approaching this result from the perspective of a sensory discriminator, the authors termed this quantity 'confounded information' (Reich, Mechler et al. 2001). We will refer to the same quantity instead as 'synergistic information' because it is considered in addition to the sum of the independent portions, and might be used to combine them when specifying a conjunction, such as the performance of a motor act or unification of a percept. These results inspired three publications briefly reviewed below, as well as our

own. In each of the following examples an information theoretic analysis has been used to measure how much information cortical neurons encoded about either stimuli or movements that were described by either multiple ‘features’ or ‘parameters’. In our work we used mutual information to characterize neuronal encoding of spatio-temporal movement sequences, the results of which is presented in Chapter 5.

In the first report, the authors characterized the informational content of neuronal responses recorded from the cat inferior colliculus (IC) during the presentation of auditory stimuli. The experiment included three auditory stimulus types, each of which independently manipulated a two of the three auditory localization cues, namely intra-aural time difference, intra-aural volume difference, and spectral notch (Chase and Young 2005). By estimating the mutual information contained in the spike trains, the authors were able to separately quantify the neuronal response sensitivity to each cue. First, they found that the IC neurons were nonlinearly selective for multiple auditory localization cues. Second, they found that the majority of the transmitted information could be decomposed into independent portions related to the three cues. Third, although the overt selectivity of neurons with different membrane proteins suggested the existence of three cell types with unique sensitivity for the localization cues, their patterns of transmitted information were indistinguishable; neither the absolute nor relative amounts of information separately encoded about the localization cues could be used to discriminate between the three putative cell types. This result supports the need for further computational and information theoretic measurements of neural signals, because the patterns recognized by human observers are not necessarily representative of the actual informational content of neural signals. The authors next investigated whether the inclusion of spike timing in their information estimates could reduce or remove the synergistic information quantity (Chase and Young 2006). They found that incorporating spike timing increased

the amount of information recovered about two of the three auditory cues, but did not eliminate the synergistic information fraction.

In the third report, a similar analysis was used to characterize premotor activity in the anesthetized zebra finch. These birds learn a song from their fathers, and are used as a model system to study learned movement sequences. Neuronal responses were recorded from the premotor nucleus HVC of anesthetized zebra finches, while the animals listened to permutations of two-syllable recordings of their own songs (Nishikawa, Okada et al. 2008). The HVC neurons were broadly selective for many syllable pairs, including sequences that the bird never produced. The authors then separately estimated the mutual information encoded about the first syllables, second syllables, and the syllable pairs. They found a considerable amount of synergistically encoded information, which was derived from the dependent relations ships between the first and second syllables, and thus was related to the overall syllable sequences.

1.4.4: Neural Codes and Mutual Information Summary

In this section I provided a general introduction to the quantification of neuronal data using mutual information. I have reviewed the basic computations used to estimate the information encoded in spike trains, as well as the preliminary considerations that should be taken to ensure an estimate is accurate, and more importantly, useful. I hope to have convinced the reader that mutual information is an appropriate metric for neural coding, especially in the case of nonlinear multiple selectivity by single neurons, and I have reviewed four key publications that set the stage for our own results. In which we record from PFC neurons during complex spatio-temporal movement sequences, and examine the mutual information encoded by their nonlinear multiple selectivity.

1.4.5: Summary of Chapter 1

In this chapter I have focused on the primate prefrontal cortex, and shown that it is required for logical primate behaviors, with special emphasis placed in its role in movement sequential and timekeeping. I hope I have convinced the reader that based on the anatomy and physiology of the PFC, the neurons therein are highly adaptable the animals behavioral context, and capable of widespread dissemination of executive control signals. I also hope to have convinced the reader that multiplicative, or more generally nonlinear, multiple selectivity is likely important the neuronal adaptability and descending control in PFC, and that spike trains of this type are measureable using information theoretic analyses.

Chapter 2: Methods

2.1: The Spatio-Temporal Sequential Movement Task

We trained two non-human primates to perform movement sequences that combine spatial and temporal requirements. The spatio-temporal sequences comprised three consecutive movements punctuated by three internally-timed delays. The sequences were performed using a joystick which moved a cursor across a grid of targets on a computer screen. This task is directly related to the spatial and temporal control required to play a three-note sequence on the piano, and is quite different from more common sequence tasks in which time is merely an emergent property of the spatial sequence. The sequential behavior performed by the subjects comprised four different spatial sequences and six different temporal sequences (See Fig. 1), which where combined yielded a set of 24 distinct spatial-temporal sequences, referred to as 'trial types' or conditions in the text, each of which was repeated five times during an experimental session for a total of 120 correct trials. The fundamental building blocks of the behavior during a single session were movements in one of four directions {*Right*, *Left*, *Up*, *Down*}, internal timing for each of three different temporal interval durations {*500ms*, *1000ms*, *2000ms*} and the serial order {*First*, *Second*, *Third*} that defines the movement direction/temporal interval pairs. The task was presented to the monkeys on a flat screen monitor in a custom electrical noise-reducing recording room. Both monkeys used a joystick, unsprung, position sensitive, to control their cursor on the screen. A custom Microsoft Windows based program was written to control the task and to coordinate data acquisition with the National Instruments data acquisition board inside a PC computer. Eye movements were monitored using an infrared tracking system (iView).

A trial began when the subject moved the cursor into the circular central target (diameter) causing a grid of potential targets to appear on the computer screen and remain visible for the duration of the trial. After a one-second delay the first

of three instruction stimuli was displayed on the screen. Each stimulus comprised a colored rectangle and circle. The abstract geometrical stimuli were coded to instruct the direction of movement and the duration of self-timed delay for each of the three spatio-temporal segments (serial order) in a sequence. The first stimulus was presented alone for 800ms, the second stimulus appeared 800 ms after the first, and the third appeared 800 ms after the second; all stimuli remained visible until 800ms after the appearance of the third. When all stimuli were extinguished it marked the beginning of a pseudorandom delay (600-1000 ms). The appearance of a 20 pixel wide white ring around the central target signaled the end of the delay period instructing the subject to begin the first movement. Thereafter the subject completed the remaining movements and associated temporal interval delays. The beginning of each temporal interval was triggered when. Two hundred milliseconds after the cursor entered the target the 'clock' for the interval duration was activated and this was communicated to the subject by the appearance of a colored ring stimulus (diameter) around the target; these stimuli, which were interval-duration specific (black, brown and orange stimuli for durations of 2000, 1000, and 500 ms) remained visible until the end of the trial. It should be noted that the end of the temporal intervals was not indicated by any of the visual stimuli and thus needed to be internally-timed by the subject. The subjects were to perform the spatial-temporal sequence without error to receive a juice reward. Deviation from the spatial path or failure to time properly the interval resulted in the trial being aborted. For the temporal intervals, correct performance was defined to insure that there was no overlap between the allowed time ranges for the different temporal intervals: 500 ms (range 475-950 ms); 1000 ms (950-1900 ms); 2000 ms (1900-3800 ms). The movements between adjacent targets were confined to the direct path towards the correct target. The movement epoch is defined as the period of time between the cursors exit from one target and entrance into the next. The internally-timed delay epoch is defined as the period beginning with the appearance of the duration cue and ending with the cursor's exit from that target.

Figure 1. The Spatio-Temporal Sequential Movement Task

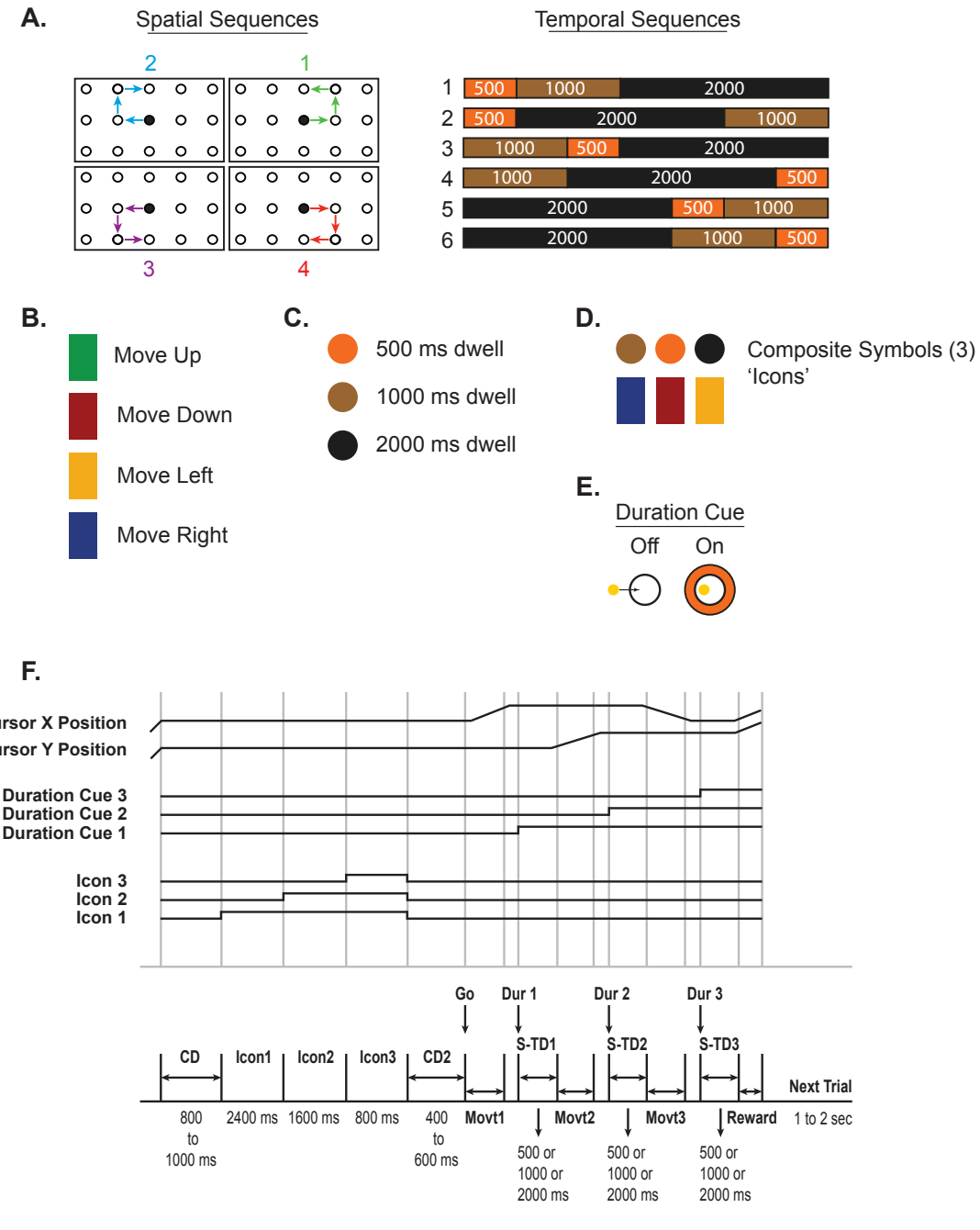

Figure 1. The Spatio-Temporal Sequential Movement Task**. A**. The four spatial sequences and six temporal sequences (showing the duration of temporal intervals in milliseconds) that the monkeys were trained to execute. Each trial was composed of one spatial sequence combined with one temporal sequence for a total of 24 unique spatial temporal sequences. **B&C.** Visual stimuli used to instruct the monkeys and their meaning. **D.** An example of a set of composite visual instruction stimuli, 'Icons', that appeared during the instruction period at the beginning of each trial. This triad instructs 'move right and then hold for 1000 ms, move down and then hold for 500 ms, move left and then hold for 2000 ms'. **E.** Duration cue signaling the beginning of the self-timed temporal interval. The 'Halo' appears two hundred milliseconds after the cursor is moved into the target and remains visible for the rest of the trial. **F**. Temporal sequence of visual stimuli and cursor movement during a single correct trial.

Both monkeys were required to perform 120 correct trials per day. Each of the 24 trial types had to be correctly performed 5 times. For monkey A, after carrying out a correct trial one of the other 23 'trial types' was chosen pseudorandomly for the next trial. If he made an error the trial type did not change. For monkey B each of the 24 'trial types' was performed in a block. After 5 successful trials had been computed, cumulatively, then the task moved on to the next block in the set sequence.

2.2: Surgical Procedures

Two male rhesus macaques were used in this study. All surgical and experimental procedures conformed to the animal care guidelines of the National Institutes of Health and were approved by an Institutional Animal Care and Use Committee at the VA Medical Center, Minneapolis. For each animal a 19-mm recording chamber and head restraint system (Nakasawa Works Co. Tokyo) were surgically implanted on the skull, under aseptic conditions, using general gas anesthesia (Lu and Ashe, 2005). Briefly, a hole in the skull was made over dorso-lateral prefrontal cortex using stereotaxic coordinates obtained from MR images of the head and brain. The hole was located directly over the principle sulcus, rostral to the arcuate sulcus, as depicted in Figure 2. The recording chamber was inserted and seated with dental cement. Then 3 or 4 titanium bone

screws were inserted in each of four titanium head posts. The head posts attached to a halo, enabling head holding and access to the recording chamber for later recording (Nakasawa Works Co. Tokyo). More bone screws were inserted in a grid over the exposed skull, and then the head posts, screws and the entire exposed skull were covered in a layer of dental cement, which became continuous with the cement around the recording chamber. Following surgery the animals were given acetaminophen with codeine orally and Xylocaine gel topically for analgesia.

Figure 2. Recording Chambers for Extracellular Neuronal Recordings

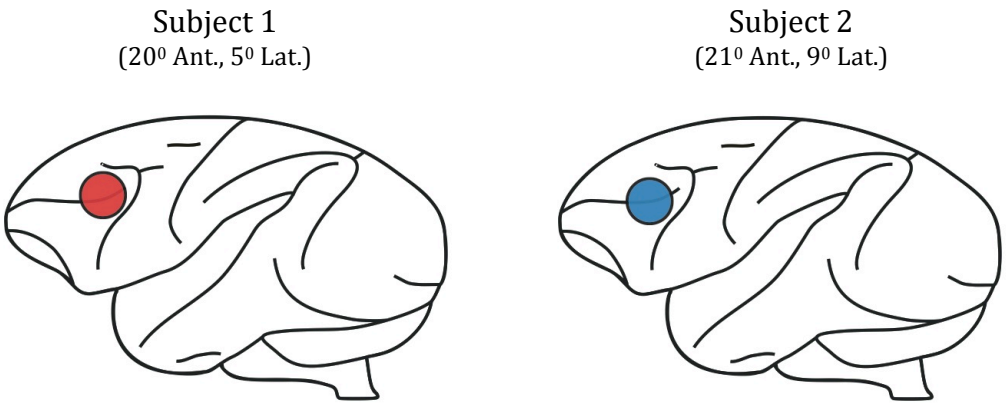

(Paxinos, Huang et al. 1999, Nieder 2005)

Figure 2. Composite image based on atlas coordinates and MRI measurements shows the location of the recording chamber in each primate subject over dorsolateral prefrontal cortex. (0,0) was defined as the most dorsal aspect of the cortex directly between the ears, and measured on the structural MRI images.

2.3: Neuronal Recordings

We recorded the extracellular electrical signals from single neurons in the macaque cortex during task performance using a 7 micro-electrode recording system (Thomas Recording, Marburg, Germany). This device allowed for independent control of each of the seven electrodes. The extracellular potentials were band-pass filtered (500 Hz – 7.5 KHz) and then sampled at 30 KHz. Impulses from single neurons were discriminated on-line using either a dual time-amplitude window discriminator (BAK electronics, MD) or semi-automatically with a template matching and self-trimming window discriminator (Alpha-Omega, Nazareth, Israel). The spike trains were digitized for storage at 0.1 ms and analyzed at 1 ms resolution. The recorded spike trains from single neurons are easier to interpret, in regards to their correspondence to behavior or cognition, compared to methods which average the activity from many cells. We have trained and recorded from macaque monkeys because they are the most homologues substitute to the human brain that may be ethically exposed to the invasive techniques that currently enable recording the electrical activity of single neurons.

2.4: Sequence ANOVA Methods

A comparative analysis of three possible high-level encoding schemes for the task parameters was performed for each neuron using three different analyses of variability (ANOVA's). We performed unpublished ANCOVA's earlier in the project and did not find a significant effect of the covariate firing rates from the beginning of each trial. We performed ANOVA 1 using trial type, also referred to as condition, as the only factor. Trial type contains 24 levels, formed by the combination of the temporal and spatial sequences. We performed ANOVA 2 using temporal sequence (6 levels) and spatial sequence (4 levels) as factors and including their interaction. We performed ANOVA 3 using movement direction, duration, and serial order as factors, with no interaction terms. ANOVA

3i used the same main effects with the addition of four interaction effects. To prevent correlation between direction and serial order data from the second movement segment was excluded from the analysis (see mutual information methods for further discussion). All analyses were performed with anovan.m in Matlab. All three ANOVA's used the average firing rate during two epochs, the last 300 ms of the movements and the 300 ms during the self-timed delay period beginning with the appearance of the duration cue, as dependent variables. Data is shared with the mutual information analysis and some of the population spike density functions.

2.5: Population Spike Density Functions by Parameter

We observed strong representations of movement direction, duration, and serial order in the neural recordings in DLPFC. For each movement parameter: (i) we identified single cells whose activity was significantly different across the levels of one parameter, (ii) for each cell, we rank-ordered the neural activity for the different levels of each parameters during epochs of interest, constructed a spike-density function (SDF) for each, and then averaged the ranked SDF's across the population of significant cells. The epochs of interest for each parameter were as follows: movement direction, 300 ms epoch at the end of the first three movements; temporal interval duration, 300 ms epoch at the end of the internally-timed delay interval; serial order, 300 ms epoch at the end of movement (same as for direction).

If the firing rate distributions corresponding to the levels of a single parameter were shown to differ significantly by ANOVA ($P<.05$), then a preferred level of the parameter was chosen by ranking-ordering the means of the normalized spike density functions. The spike density functions (SDF's) were computed by convolving a Gaussian kernel of 40 ms width with the spike times collected across all trials of a single parameter level. We used Matlab's native function ksdensity for this purpose. We then normalized the SDF's to the highest

estimated firing rate—the peak of the spike density function—across all levels within each parameter. This means that a cell included in the population SDF for multiple parameters was not required to be normalized to the same maximum activity level. We next computed the mean of the normalized SDF's for each level of the current parameter within the relevant 300ms window. The means were then ranked from high to low and the actual SDF curves were then ranked to match. After this procedure the preferred level of each parameter corresponded to the highest mean estimated firing rate and the anti-preferred corresponded to the lowest. Finally, the SDF's were averaged across the population of significant cells. In Figure 13, the preferred level of each parameter is always plotted in red, and the anti-preferred in blue.

2.6: Information Theoretic Analysis

We computed how neurons in dorsolateral pre-frontal cortex represented sequential movements defined by multiple independent high-level parameters during behavior. To do this we first calculated the minimum number of bits of mutual information that were separately transmitted about the direction, the duration, and the serial order of forearm movements during the performance of correct trials in the task. We then divided the total mutual information transmitted by each neuron that was jointly related to the three parameters into synergistic, independent, and redundant fractions.

Mutual information (*MI*) quantifies an observer's reduction in uncertainty about the value taken by one variable after they learn the value taken by another. Shannon originated this analysis to quantify the information sent between the input and output variables of communication channels such as telephone lines or television broadcasts (Shannon 1948). Werner and Mountcastle (1965) were the first to apply this method to information transmission in the nervous system, they used mutual information to quantify the stimulus-response functions of peripheral nerves to cutaneous stimulation.

2.7: The Design of the Information Theoretic Analysis

To measure how much information single neurons transmitted during behavior we reorganized firing rates according to three elemental movement parameters; direction, duration, and serial order. Computation of the mutual information related to each parameter was performed independently by resampling the neural recordings. To compute information related to self-timed delay duration firing rates were grouped according to their membership in either the 500, 1000, or 2000 ms delay duration. When averaging over many trials (n= 120) the delay duration is independent of the serial order of the delays, and also independent of the movement direction preceding or following the delay. The cell of interest might also encode serial order or direction, but those signals will only contribute to the noise entropy associated with self-timed delay duration, not the duration signal itself. It is critical to the independence of the three elemental terms that the state of one parameter is not predictive of the state of any other parameter.

To ensure the independence of the direction, duration, and serial order terms our information theoretic analysis was confined to only the *First* and *Third* serial order positions. Here movement direction {*Right*, *Left*}, self-timed delay duration {*500*, *1000*, *2000ms*}, and serial order {*First*, *Third*} are balanced in the experimental design. This means knowledge of the current state of one of the parameters is not predictive of the current state of either of the other two. We did not use data from the *Second* serial order position in the information theoretic analysis because this was the only time movements in the *Up* and *Down* directions occurred. There are 120 correct trials per recording, and 120 observations per state for the direction term and serial order terms, and 80 for the duration term.

$$MI_{DIR} = H(FR) - H(FR|Direction) \quad (4)$$

$$MI_{DUR} = H(FR) - H(FR|Temporal\ Interval\ Duration) \quad (5)$$

$$MI_{SO} = H(FR) - H(FR|Serial\ Order) \quad (6)$$

We also calculated the joint information, the total information simultaneously encoded about the current state of all three movement parameters. The joint term has twelve states, the result of individually specifying each possible combination of two directions, three durations, and two serial order positions. The first state of the joint term specifies when the first movement was to the right and moved the cursor into a target whose self-timed delay duration was 500 ms. Each state in the joint term has 20 observations. Reich, Mechler and Victor coined the term 'formal information' to describe a similar information theoretic measure in 2001. We refer to the 'joint information' in reference to a joint probability distribution for two or more statistically independent variables.

$$MI_{Joint} = H(FR) - H(FR|DIR, DUR, SO) \quad (7)$$

We collected firing rates for the information theoretic analysis from two 300 ms epochs during the spatio-temporal sequential movement task. Firing rates were used as a logical first step; this code is known to contain most of the information found in neural spike trains (Rolls and Treves 2011). We assume that spike timing, inter-spike intervals, and other spike metrics would encode some additional information. We chose to use epochs of 300 ms because they were wide enough to include a signal from cells with different preferred micro timing domains, but also small enough to be compatible with the neural processes required by the behavioral task. We chose to sample specific 300 ms portion of the movement and self-timed delay epochs of the task to ensure independence of the direction, duration, and serial order parameters. The first epoch was the last 300 ms of the first and third movements, the second epoch used was 300 ms

beginning with the onset of the duration cue during the first and third self-timed delays. We used the last 300 ms of the first and third movements to best resolve any signals related to planning the upcoming durations. We used the first 300 ms after the duration cue during the self-timed delay because movement direction was not controlled on the exit from the third target / self-timed delay, thus the last 300 ms of the first and third self-timed delays could not be used for this analysis. The last 300 ms of the first and second self-timed delays was not useful for our fractional characterization of parameter encoding, as it would have introduced a large correlation between the direction and serial order terms, as explained above. For the movement epoch duration refers to the upcoming instructed self-timed temporal interval. During the self-timed interval epoch the previous movement direction is used.

2.8: The Direct Method and 'Bias' Correction

We computed *MI* by the direct method, to perform the computations we used the 'information breakdown toolbox', an open-source toolbox written for Matlab (Magri, Whittingstall et al. 2009). To compute *MI* by the direct method one measures the total probabilistic variability, or entropy, of the neural responses, and then subtracts the noise entropy, the remaining neural response variability after specifying each stimulus (Strong, de Ruyter van Steveninck et al. 1998). In our case the neural signals were parsed according to parameters of the animals movement, rather than features of auditory or visual stimuli used by sensory physiologists.

$$MI(R;S) = H(R) - H(R|S) \tag{8}$$

$$H(R) = -\sum_{r\in R} p(r)\log_2 p(r) \tag{9}$$

$$H(R|S) = -\sum_{s=1}^{N_s} p(s)\sum_{r\in R} p(r|s)\log_2 p(r|s) \tag{10}$$

As stated above, to measure *MI* the set of all possible states of the stimuli and neural responses must be known. In experimental neurobiology this is not possible. The limited stability of extracellular recording arrays in awake behaving animals precludes the collection of enough data to actually measure the set of all possible neural responses to all stimuli. Neural response entropies must then be estimated; because neurophysiological experiments produce data sets of limited size, the true neural response entropies cannot be estimated with asymptotic accuracy. Further, limited data causes systematic overestimation of mutual information. This is referred to as 'bias', and it is endemic to *MI* estimation by the direct method because the noise entropy is more poorly estimated than the total entropy because the noise entropy is estimated from subsets of the total observations use to estimate the total response entropy. For further discussion see (Panzeri, Senatore et al. 2007).

We corrected for bias using a two-step process that has been shown to be effective for this purpose. (Panzeri, Senatore et al. 2007) Panzeri and Treves. 1996) Prior to the mandatory steps we sometimes employed response discretization. Each neural response must be observed more times than the number of different neural responses. In our analysis we compare the amount of information resolved by four terms; of those the joint term had the smallest number of observations per state, 20. Cells with more than 20 different neural responses were infrequent, when encountered these cells were discretized (which can only reduce the resolved information) to reduce their number of different neural responses to 20. The discretized data was then used for all information theoretic calculations; to preserve our ability to compare the information resolved from the Joint, Direction, Duration, and Serial Order terms. Following the optional discretization step, for all cells we corrected for bias by first including the Panzeri-Treves (1996) bias correction in the direct method computations that calculated the amount of mutual information related to each movement parameter. Neural response entropy estimation and bias correction

are core functions of the information breakdown toolbox (Magri, Whittingstall et al. 2009), which we used for this purpose. Second, we shuffled the data 1000 times, and each time we calculated the *MI* as above. Each shuffle was a pseudo-random resampling of the original data without replacement that preserved the original number of observations per stimulus. This distribution of 1000 *MI* values will be referred to as MI_{sh}. It represents the information resolved by chance, deflection of the mean of the MI_{sh} distribution above zero is a result of bias. To obtain the reported *MI* values the second step is to subtract the mean of the MI_{sh} distribution from the *MI* result resolved from the original experimental data calculated in step one. Naïve' mutual Information estimates must be greater than or equal to zero, following bias correction negative values are possible. All results are reported in 'bits', $\log_2$ units of information.

2.10: Significance Testing in the Information Theoretic Analysis

We also used the MI_{sh} distribution to test for mutual information significantly greater than would be expected by chance. Significance testing was performed prior to step two above. If the experimental *MI* result was greater than 95% ($P<.05$) of the MI_{sh} distribution then that cell was considered to have transmitted significant information related to the movement parameter in question. This procedure was used separately for each cell for each of the direction, duration, serial order, and joint terms.

Importantly, during the shuffling procedure described above we yoked the single parameter terms to the joint term to enable significance testing for synergistic information greater than would be expected by chance. Synergistic information is measured as the difference between the joint information and the sum of the three independent parameters. Synergistic information encodes the relationships between the three independent parameters; it cannot be used to reduce an observer's uncertainty about the state of any parameter in isolation. In 2001

Reich, Mechler and Victor contrived the term ‘confounded information’, to describe what we call synergy, because that fraction of the total mutual information could not be unambiguously related to one of the two visual stimulus ‘attributes’ that they had computed. To build the $MI_{\text{sh-syn}}$ distribution we subtracted each single parameter MI_{sh} from the $MI_{\text{sh-joint}}$ value after each shuffle.

$$MI_{sh-syn} = MI_{sh-joint} - MI_{sh-dir} - MI_{sh-dur} - MI_{sh-so} \quad (11)$$

This was done as follows, just prior to the information theoretic calculations the twelve-state joint data was duplicated and reorganized to produce each of the three single parameters. For instance, states {1,2,3,4,5,6} of the joint term were combined to make the {*First*} state of the serial order term, and states {7,8,9,10,11,12} were combined to make the {*Second*} state. Joint states {1,2,3,7,8,9} were combined to make the direction state {*Right*}, and {4,5,6,10,11,12} were combined to make the direction state {*Left*}. Joint states {1,4,7,10} were combined to make the duration state {*500ms*}, states {2,5,8,11} were combined to make the duration state {*1000ms*}, and states {3,6,9,12} were combined to make the duration state {*2000ms*}. Each of the twelve joint states has 20 observations. The direction and serial order single terms’ states each have 120 observations. The durations terms’ states have 80 observations. Mutual information was calculated for each term independently. The joint data was then shuffled 1000 times, and after each iteration the single parameter terms were reconstituted anew before the MI_{sh} values were calculated. This procedure ensured that distinct MI_{sh} distributions were created for each of the four terms, but that correlations within the 1000 pseudo-random shuffles were shared across the MI_{sh} distributions. We tested for synergy significantly greater than would be expected by chance by testing for experimental MI_{syn} results that were greater than 95% of a distribution of 1000 shuffled results ($MI_{\text{sh-syn}}$).

Chapter 3: Results Related to Timing

3.1 Temporal Interval Production and Neuronal Modulations Related to Elapsed Time in Dorsolateral Prefrontal Cortex.

Two non-human primates (NHP's) were trained to perform the spatio-temporal sequence task. The task comprised four movements of a cursor on a computer screen separated by three self-timed delays of specific duration. On each trial the animals were required to complete an entire sequence of movements and self-timed delays in order to earn a juice reward. Animal 1 performed the task in a block design, with trial type changing between each block, while animal 2 was presented with a new trial type after each correct trial. In this chapter we are only going to consider the behavioral performance and the neuronal activity as they relate to the animals internal estimation of the temporal intervals, and so we will largely ignore effects of serial order and movement direction, which will be discussed in chapter 4.

3.2: Behavioral Estimates of Temporal Intervals Conform to Scalar Representation of Time.

A scalar representation of time refers to the observation that the precision with which temporal intervals are measured 'scales' with the duration. An useful exercise is to imagine what would happen if time was measured with a rubber ruler that was stretched to fit any given temporal interval duration**.** Both monkeys performed the task with a success rate per trial near 42% (Monkey 1 = 41.5%, Monkey 2 = 43.8%). The duration of the self-timed delays took one of three nominal values, either 500, 1000, or 2000 milliseconds. In order to illustrate the animals' estimates of the three self-timed delay intervals we plotted a histogram of the time to the beginning of movement that ended each of the delays (Figure 3). Note: the duration cue ('Halo') appeared on the screen 200 ms after the

Figure 3. Behavioral Performance During the Spatio-Temporal Sequence Task

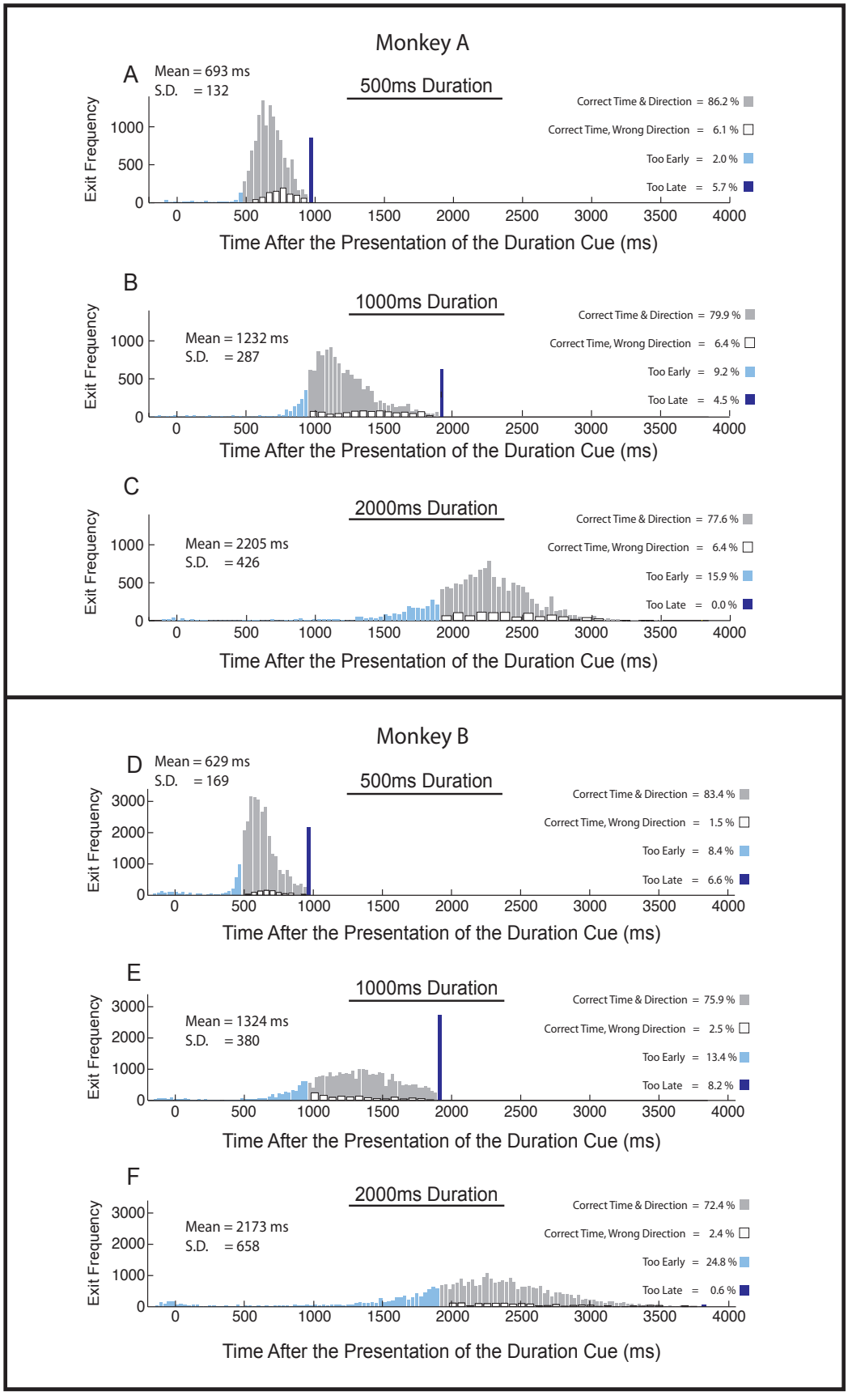

Figure 3. Frequency histograms of temporal interval estimates by interval duration for each animal. Data is cumulative over all neural recording experimental sessions. Movement times are relative to the appearance of the duration cue. Gray bars indicate correctly timed movements towards the correct subsequent target. White bars indicate correctly timed movements towards the wrong subsequent target. Light blue bars indicate movements that underestimated the target duration. Dark blue bars indicate failures to move within the time allowed. The means and standard deviations were computed regardless of outcome. Panels **A** & **D** show one monkey's performance on the 500 ms duration target interval. Panels **B** & **E** show the 1000 ms duration target interval. Panels **C** & **F** show the 2000 ms duration target interval.

cursor was placed inside the target, and indicated to the subjects when their internal estimate of the duration should begin. Overall, the distributions are unimodal, and slightly skewed towards the minimum estimate compatible with correct performance. Both animals performed the 500 ms duration delay above 80% correct. Doubling the delay length to 1000 ms in duration reduced the performance of each animal by about 5%. Doubling the delay length again, to 2000ms, reduced performance by another ~5% correct. We calculated the mean and standard deviation of each distribution using correct and error trials and found that the ratio of the standard deviation over the mean was approximately constant across all three durations for each monkey (Table 1). Both of these findings are consistent with a 'scalar' representation of time (Gibbon, Malapani et al. 1997). The monkeys' performance demonstrates that their internal estimates of the temporal intervals were adequate

3.3: Behavioral Estimates of Duration Regress Toward the Mean

Figure 3 shows that when the subjects failed to correctly estimate the 500 ms temporal intervals, they were more likely to underestimate the passage of time, and so stayed in a target too long. During the 2000 ms goal intervals one can see that the subjects tended to overestimate the passage of time, and so most of their errors occurred when they left a target too soon. We further investigated the apparent regression of the animals' interval estimates towards the mean interval

Table 1.

The Coefficient of Variation for the Behavioral Estimates of Temporal Intervals			
	Duration		
	500 ms	**1000 ms**	**2000 ms**
Monkey 1	5.25	4.29	5.17
Monkey 2	3.72	3.48	3.30

Legend. The coefficient of variation (COV), the ratio of the standard deviation of the temporal interval estimates over their mean, measures the relative precision with which each subject estimated the temporal intervals, given their duration.

duration by performing a multinomial logistic regression to determine the likelihood that the self-timed delays were performed correctly, underestimated, or overestimated. We found that duration had a significant effect on the likelihood of correct versus error trials, ($P< 0.001$). This corroborates the observation that making a temporal error increased with the duration of the self-timed temporal interval duration for both animals. We also found that when an error occurred the temporal interval duration had a significant effect on the likelihood of

underestimation, (P = 0.001). Specifically, the longer a self-timed delay was supposed to be, the more likely the subjects were to underestimate it. The beta value magnitudes indicate that temporal interval duration had a greater influence on the likelihood of underestimation errors than it did on errors in general. This result represents a statistically significant confirmation of the regression towards the mean of the interval estimates that was mentioned above. This regression towards the mean is likely to reflect a combination of the neural mechanisms for interval production and the distribution of temporal interval durations used in the experiment (Jazayeri and Shadlen 2010). The additional cognitive load required to plan and execute movements in various directions during the sequential task did not have any obvious effect on the temporal interval estimate distributions. For the purposes of this chapter we will ignore effects of the remaining experimental variables, namely serial order and movement direction.

Table 2.

Significant Slopes and Intercepts from the Logistic Regression Related to Behavioral Estimates of Different Durations.				
	Correct vs. Error		**Underestimate vs. Overestimate**	
	Slope	Intercept	Slope	Intercept
Monkey 1	1.00	N.S.	1.95	-2.88
Monkey 2	0.76	-0.70	1.26	-1.38

Legend. Beta values from the logistic regression indicate the strength of the influence of temporal interval duration on the behavioral outcomes during the spatio-temporal task, P < 0.05. Temporal interval duration had a significant effect on self-timed delay percent correct and underestimation versus over estimation error types.

3.4: Neuronal Activity Modulations Related to the Self-Timed Temporal Intervals.

We examined the activity of 397 neurons recorded in dorsolateral prefrontal cortex, 116 from monkey A and 281 from monkey B, that were found to be consistently active, fired on average more than 5 spikes per second, and did not present obvious signs of contamination from noise. All units were recorded during at least 5 repetitions of each of the 24 movement sequences, resulting in at least 120 trials per neuron. Here we describe our findings related to neural activity only during the temporal interval epochs.

We observed neuronal activity in DLPFC that was sensitive to the passage of time and the self-timed delay duration during the hold periods between the movements of the spatio-temporal sequential movement task. The typical neuronal response modulations related to timing consisted of either an increment in activity or a decrement that could generally be divided into two distinct phases. During the first phase, shortly after the cursor was moved into the self-timed delay target, steep phasic responses that lasted a few hundred milliseconds seemed to signal the start of the self-timed delay.

The second phase of the time sensitive neuronal response modulations typically began with a reset of the firing rate, that was followed by continuous ascending (Figure 4 and 5) or descending (Figure 6 and 7) rate modulation that reached a threshold at the end of the self-timed delay. The slopes of the continuous changes in firing rate were sometimes selective for the self-timed delay durations. The time that either maximal or minimal firing rates were reached signaled the beginning and the end of the time-dependent process. For single neurons these threshold discharge rates were fairly stable, in later analysis we take up their variability and possible relationship to other experimental variables in more detail.

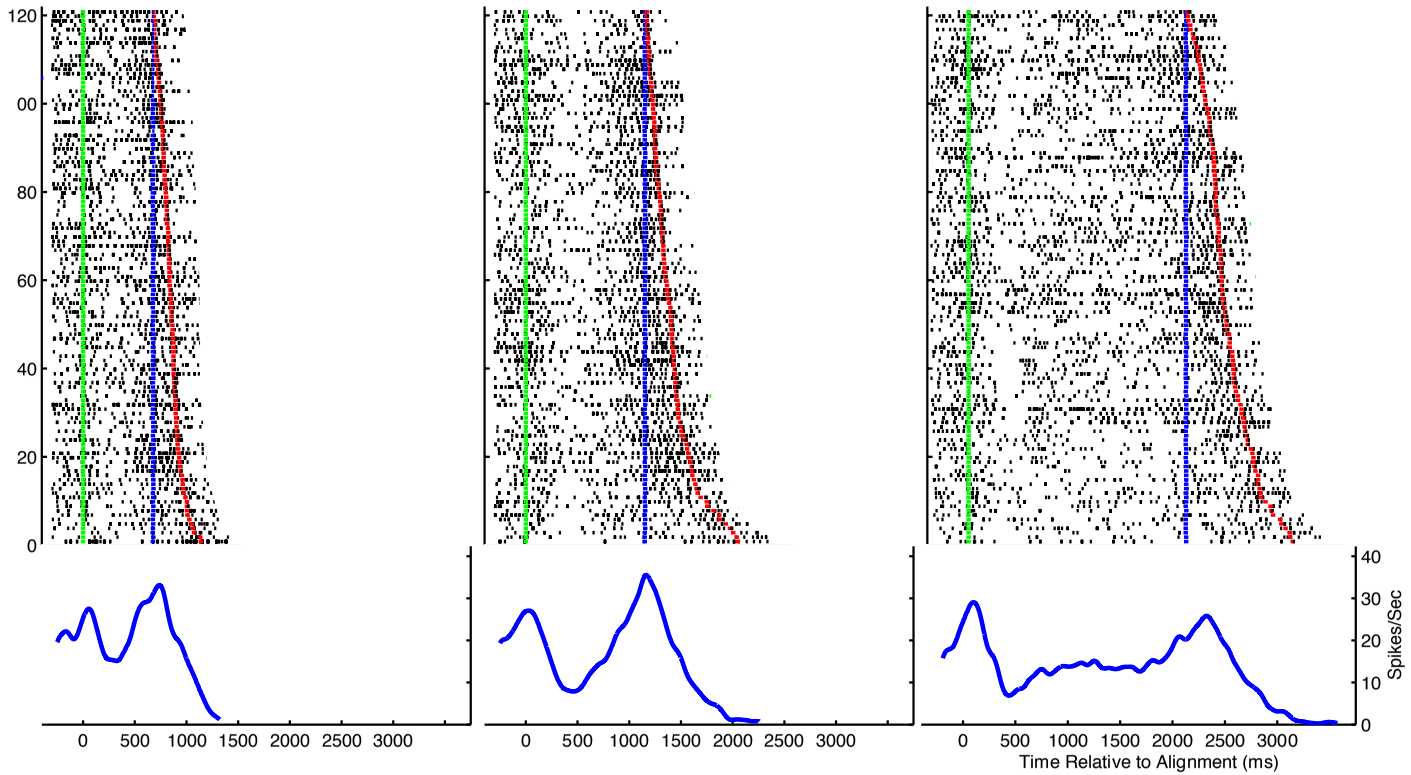

Figure 4A. An Ascending Type Neuron Modulated by Time. An example neuron in DLPFC (M2 052809 ch 9) showing neuronal activity modulated by time during the temporal interval. Raster displays and spike density functions depict average neuronal activity that reaches a peak once at the beginning of each self-timed temporal interval duration and once at the end. (**A**) The first peak seems to initialize the timing process; it occurs just after the cursor enters the target, indicated by the vertical green line. The average neuronal activity next reaches a phasic minima ~400 ms into each interval, and then ramps up toward the exit movement. Vertical green lines indicate the start of the temporal interval, when the cursor enters the target. Vertical blue lines indicate the minimum hold time, and red lines indicate the moment the cursor exited the target.

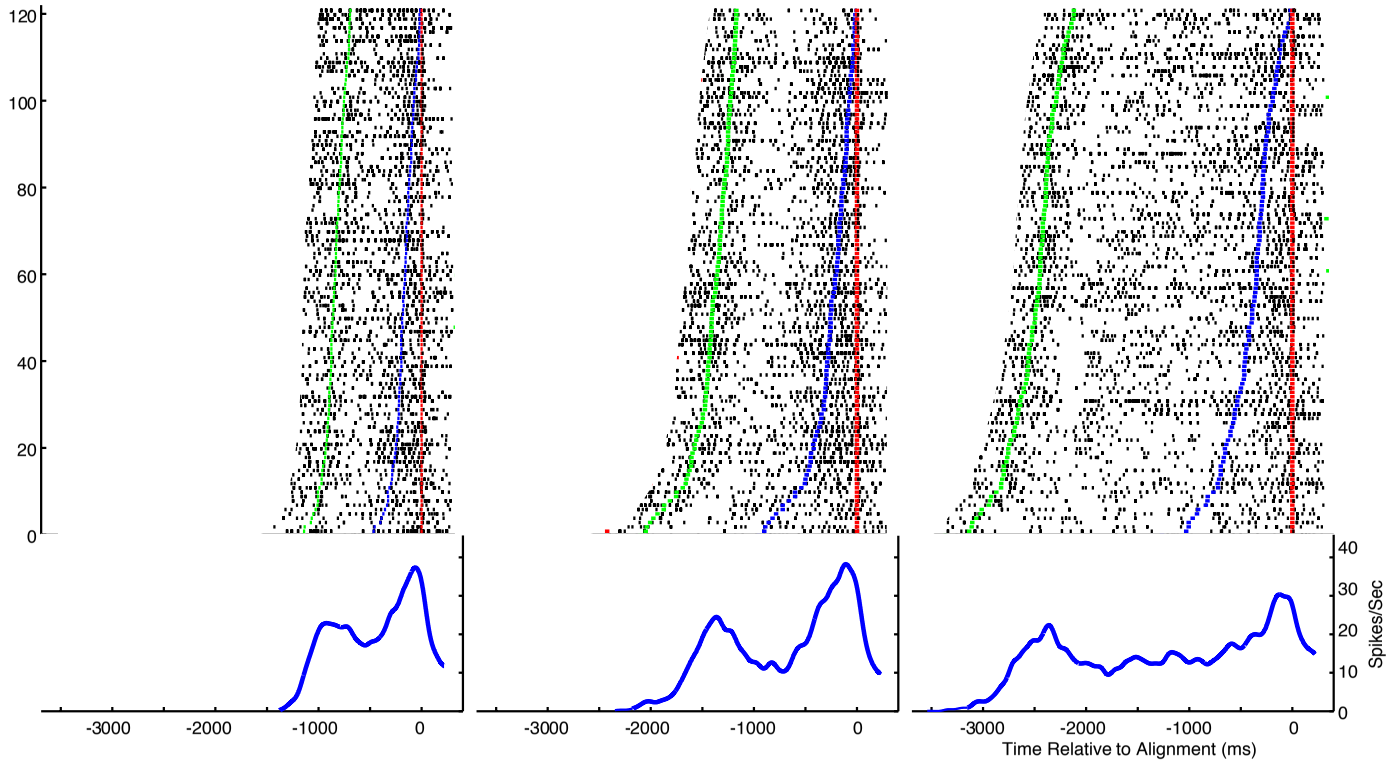

Figure 4B. The same neuron and formatting as is shown in 4A, except the activity is aligned to the end of the self-timed temporal intervals**.** The second peak consistently occurs just before the cursor is driven out of the target. The slope of the average activity from the minima to the second peak depends on the duration of the timed interval. Green lines indicate the start of the temporal interval,. Blue lines indicate the minimum hold time, and the vertical red lines indicate the moment the cursor exited the target, ending the self-timed temporal intervals.

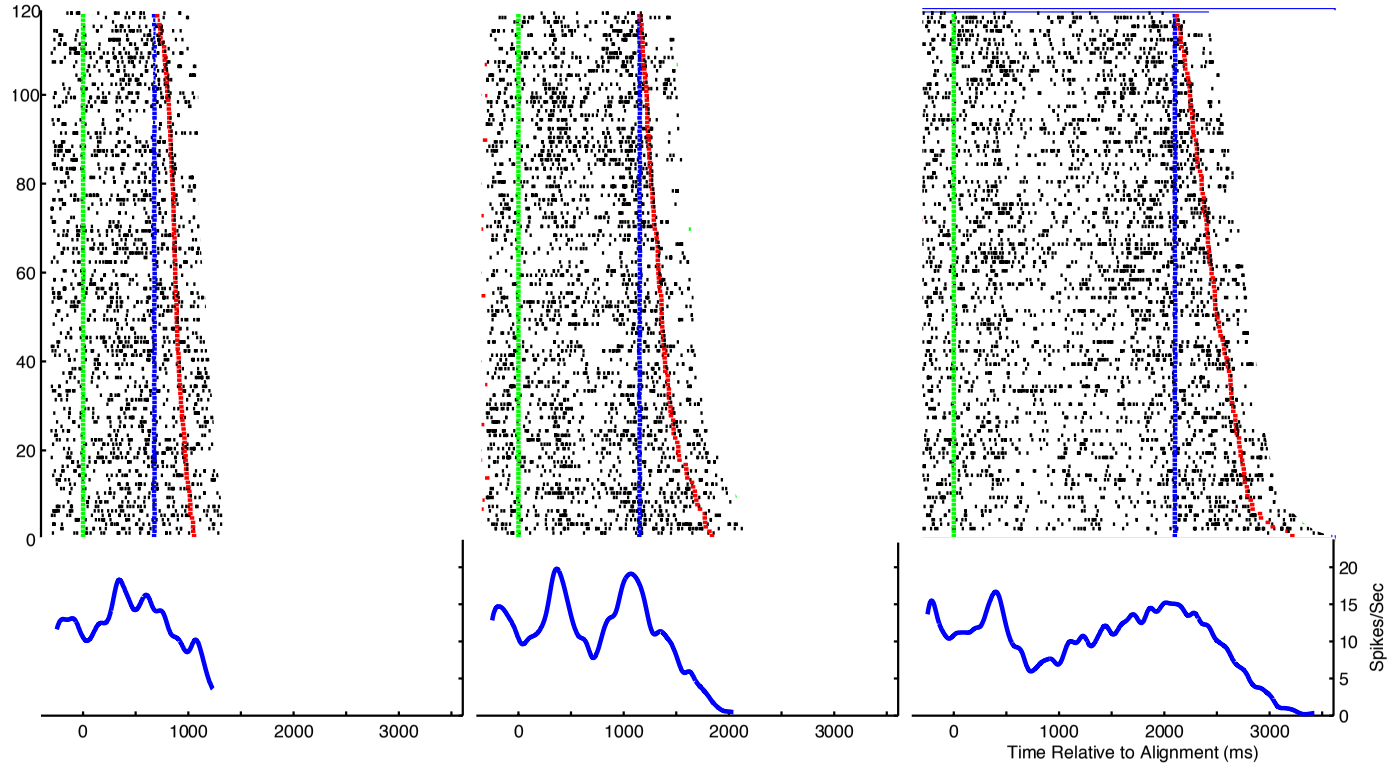

Figure 5A. A Second Ascending Neuron Modulated by Time. An example of a neuron in DLPFC (M2 060809 ch 18) showing neuronal activity selective for movement delay duration and sensitive to the passage of time. Raster displays and spike density functions depic average neuronal activity that peaked at the beginning and the end of the self-timed interval. (**A**) Neuronal activity decreases immediately upor entry into the target and then reaches a phasic peak 400 ms into the interval, 200ms after the duration cue appeared. Average activity then decreases again over 300 ms to a duration insensitive minimum.

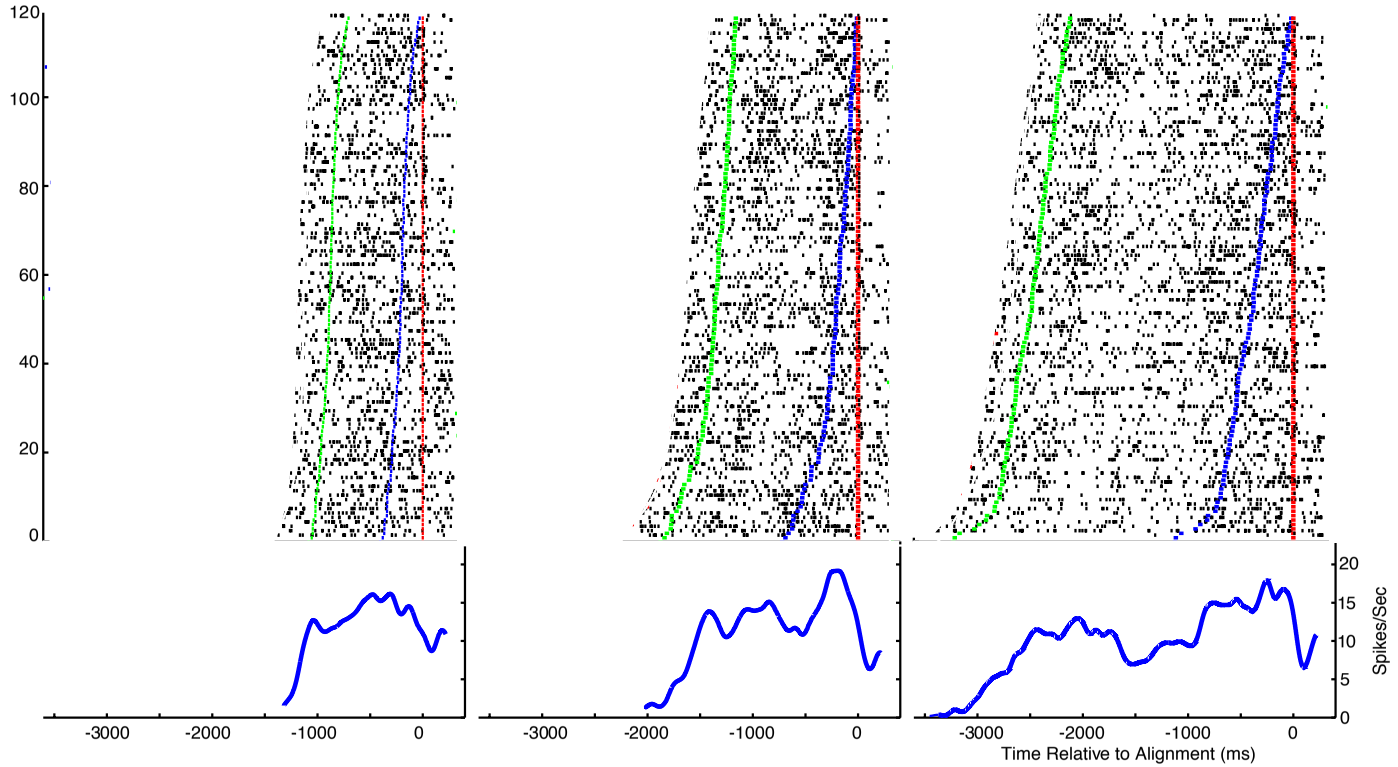

Figure 5B. The same neuron and formatting as is shown in 5A, except the activity is aligned to the end of the self-timed temporal intervals. The average neuronal activity steadily increases to a maxima about 300 ms before the movement ending the self-timed interval. Green lines indicate the start of the temporal interval. Blue lines indicate the minimum dwell time, and red lines indicate the moment the cursor exited the self-timed temporal interval target.

Many cells signaled the beginning and the end of the temporal interval with either two peaks (Figure 4) or two valleys (Figure 6). Figure 4 shows an example of a single neuron that signals the beginning and the end of the self-timed delay intervals with peaks in its discharge rate. The first phasic peak appears immediately after the vertical green line in Figure 4A, which indicates the moment that the cursor is moved into the delay target. 500 ms after the cursor entered the target, the activity reaches a minimum value, the 'reset', and then steadily builds up to a peak just before the exit movement, indicated by the red line in Figure 4B. Compression of the two peaks, and possibly two different underlying neural processes, is maximal during the 500ms delay interval, in which the reset does not reach the same low point observed during the 1000 and 2000 ms holds. Figure 5 shows another neuron that signals the beginning and the end of the self-timed delay intervals with peaks in its activity. In this case the start of the self-timed delay interval is signaled a bit later, at 400 ms into the interval, just after the appearance of the duration cue, at 200 ms. We also found decreasing activity related to ongoing time. Figure 6 shows neuronal activity that signaled the beginning and the end of the self-timed delay interval with firing rate minima. A phasic trough follows the entrance of the cursor into the target in Figure 6A, and then activity is 'reset' to a high level 500ms into the target. The neuronal activity then gradually decreases as the time to exit the target draws nearer.

The sign of the signal in the first phase was not always the same as the sign in the second phase. In Figure 7 the neuronal activity reaches a maximum at the start of the timing process, and then rather than resetting, it slowly descends to a minimum at the end of the temporal interval. Neuronal activity related to the passage of time was sometimes neither ascending nor descending, Figure 8 shows one neuron whose activity changed cyclically with the passage of time, or was related to the shorter duration intervals while the animal was performing the longer intervals.

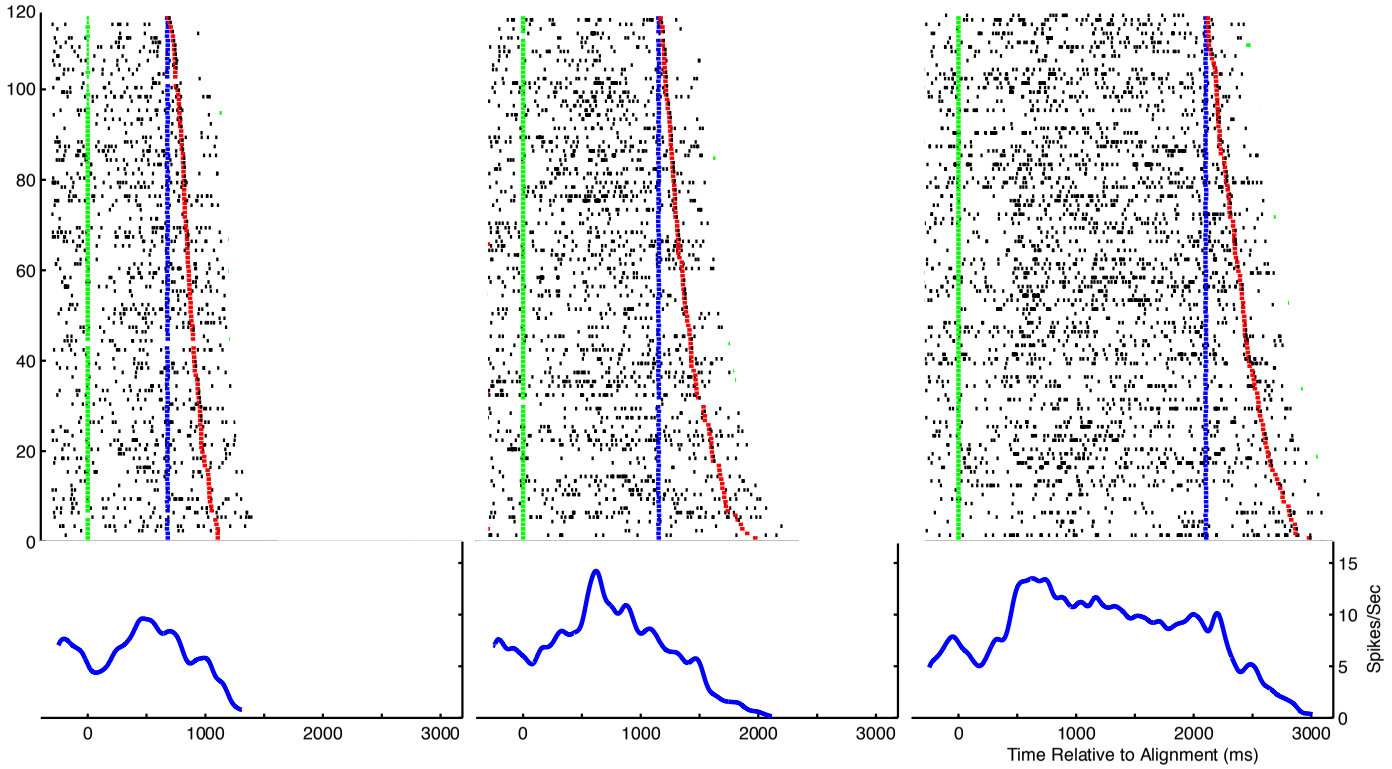

Figure 6A. A Descending Neuron Modulated by Time. An example neuron in DLPFC (M2_052909_29) showing neuronal activity whose rate of decrement depended on the self-timed delay duration. (**A**) A second neuron showing later activation of a timekeeping process. Neuronal activity drops to the first minima immediately after the start of the self-timed delay, then increases to a peak about 500 ms later, 300 ms after the duration cue appeared. (**B**) Neuronal activity steadily decreases to a non-zero threshold of about 5 Hz, similar to the first minima.

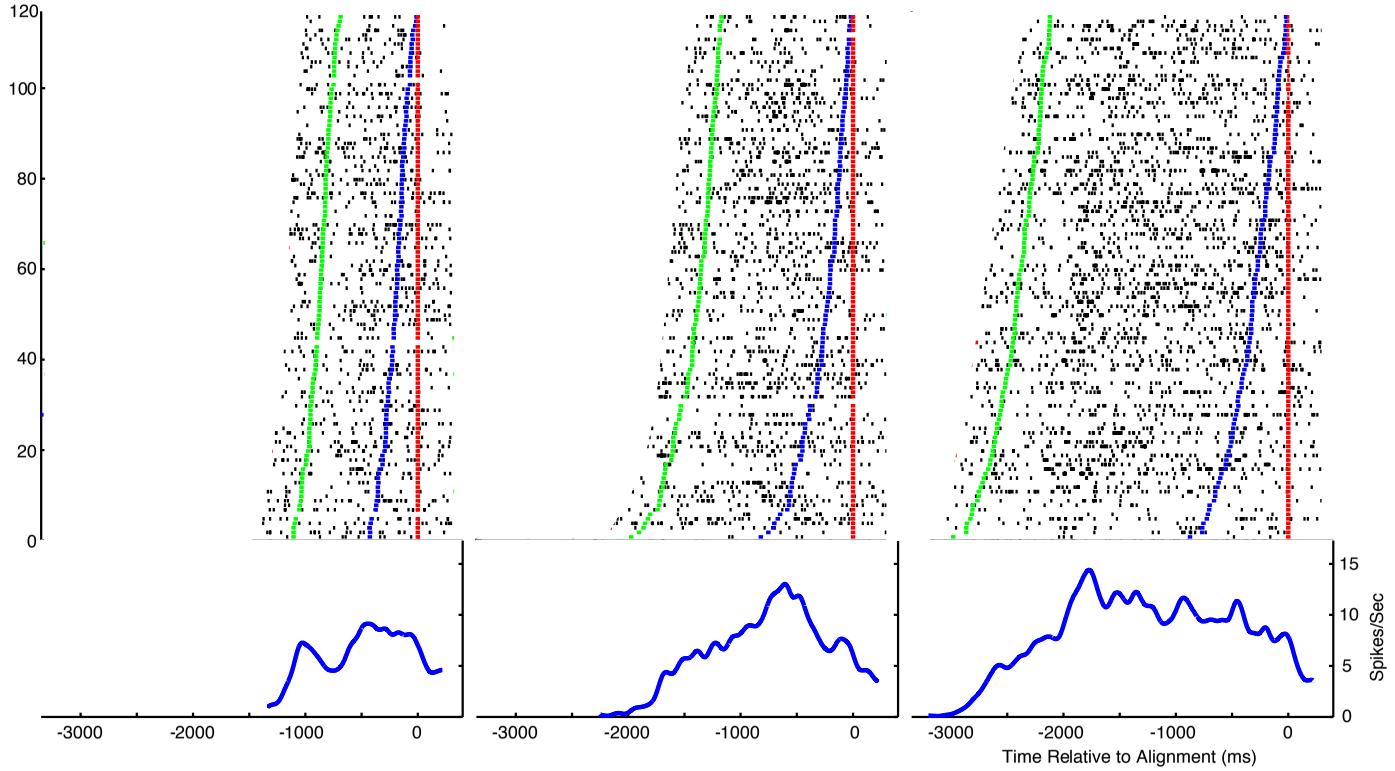

Figure 6B. The same neuron and formatting as is shown in 6A, except the activity is aligned to the end of the self-timed temporal intervals. (**B**) Neuronal activity steadily decreases to a non-zero threshold of about 5 Hz, similar to the first minima.

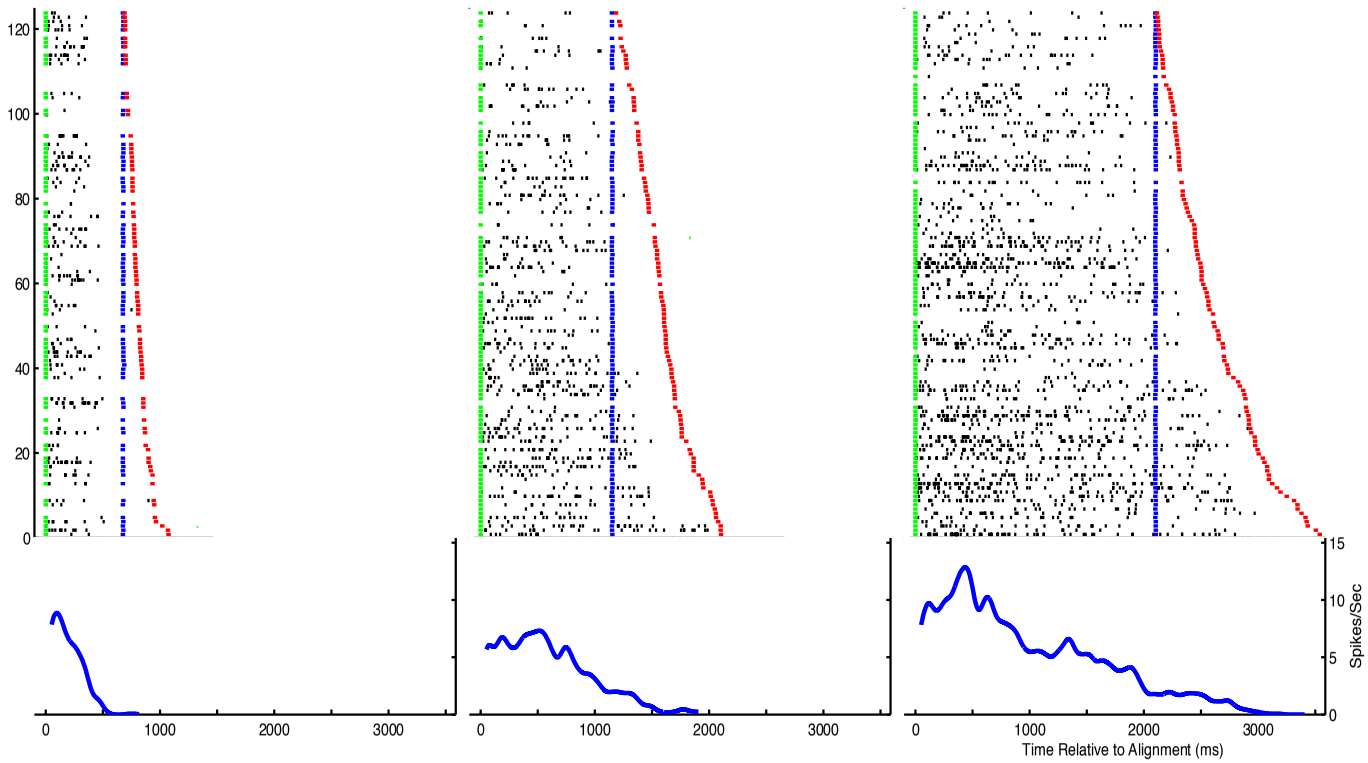

Figure 7A. A Second Descending Type Neuron Modulated by Time. Raster displays and spike density functions illustrate neuronal activity in DLPFC (M1_060210_13) whose rate of decrement depended on the self-timed delay duration. (**A**) the average neuronal activity reaches a peak during the first 500 ms of the delay, and then steadily decreases.

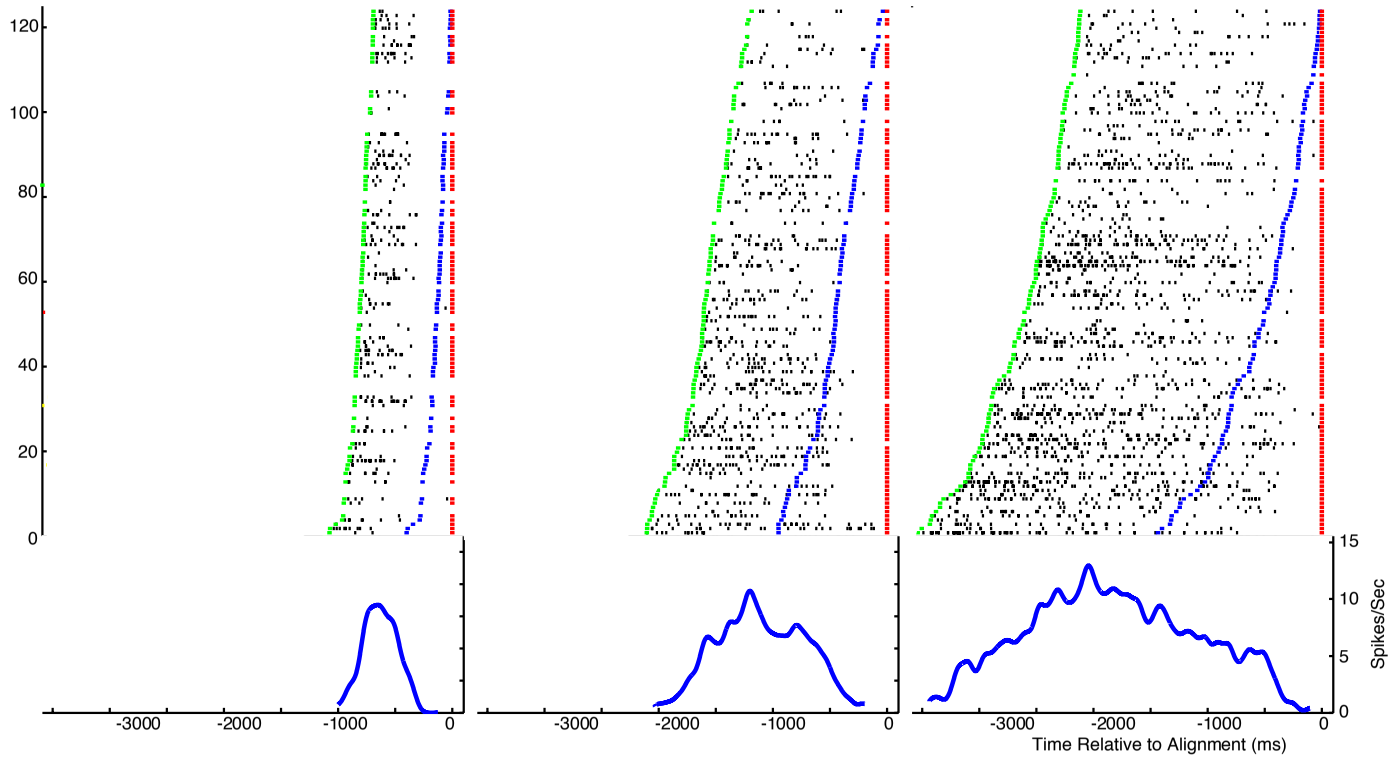

Figure 7B. The same neuron and formatting as is shown in 7A, except the activity is aligned to the end of the self-timed temporal interva
The neuronal discharge rate steadily drops, reaching zero spikes per second about 300 ms before the end of the self-timed temporal interv

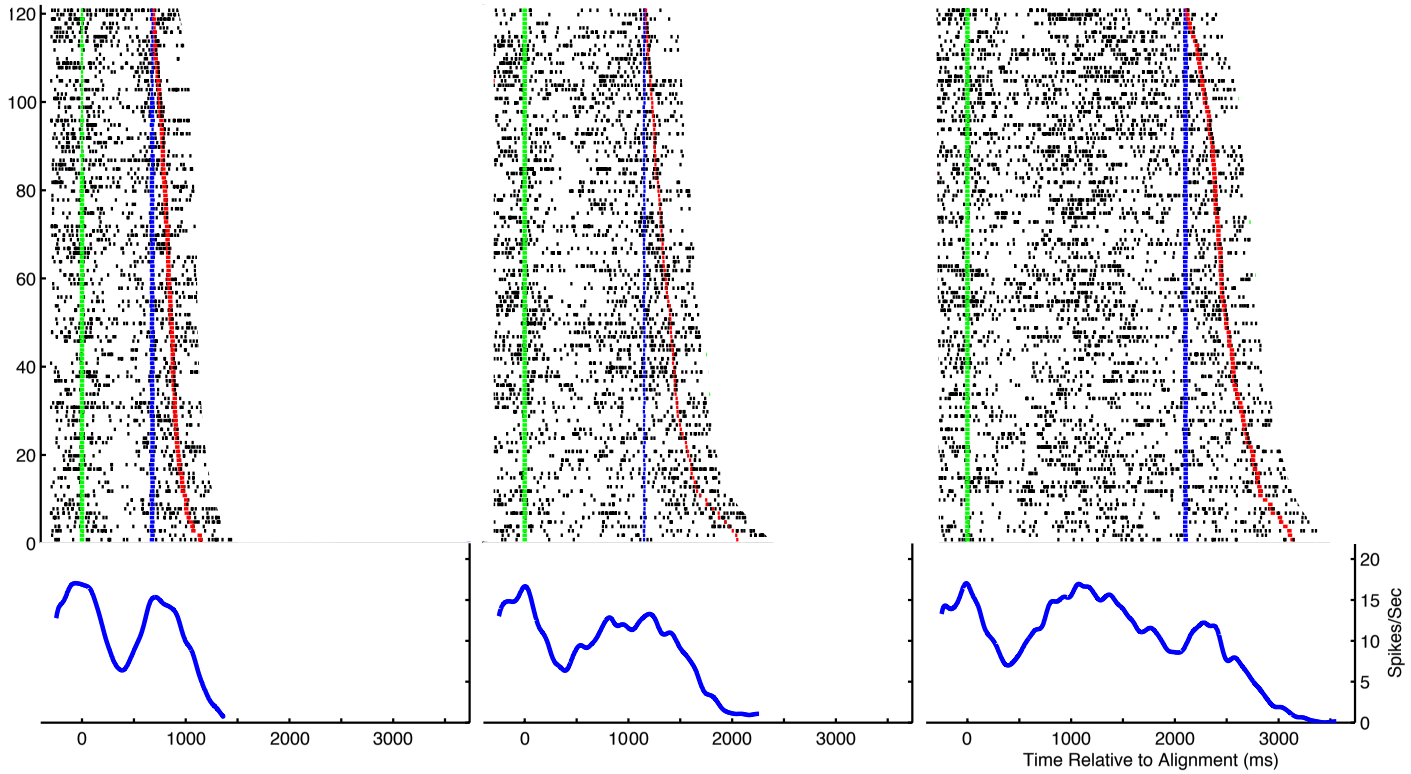

Figure 8A. An Example of Oscillating Neuronal Activity Sensitive to Ongoing Time. A neuron in DLPFC (M2_0528(showing cyclical activity sensitive to the passage of time. (**A & B**) Raster displays and spike density functions illustrate neuronal activity tha reaches a peak at the beginning and end of the self-timed delay. For delay durations greater than 500 ms a third peak at 1000 ms may be Cyclical activity changes or the partial activation of movements that were not performed might explain this activity.

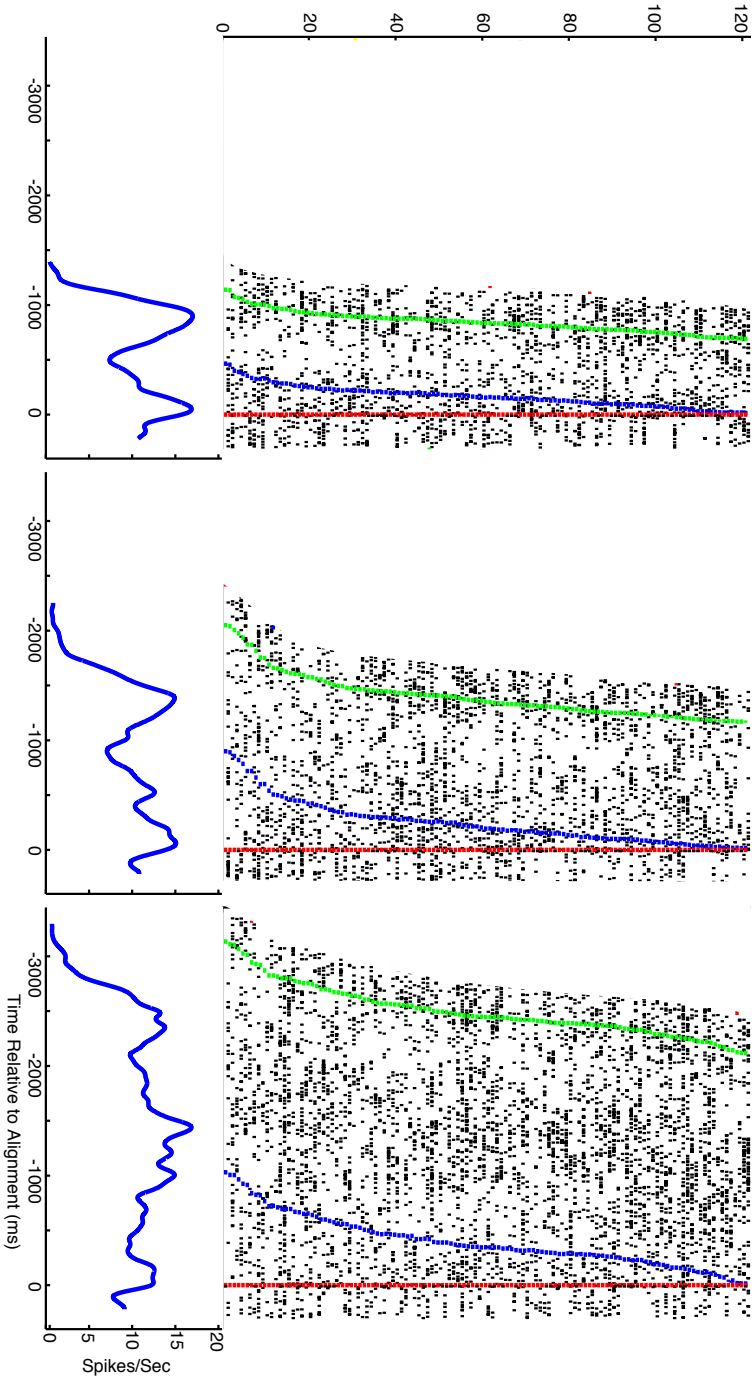

Figure 8B. The same neuron and formatting as is shown in 8A, except the activity is aligned to the end of the self-timed temporal interval

3.5: Neural Population Activity is Modulated By Temporal Interval Duration.

Following our observations of continuous time-sensitive activity modulations at the single cell level, we next examined the population response during the self-timed temporal intervals that were produced by the subjects. In order to characterize the population activity in DLPFC during the self-timed delay intervals, we first divided the neurons into subsets in which the change in activity was either an ascending or descending type, as these were the two most frequent activity patterns found amongst single neurons. We placed neurons into either ascending (the discharge rate was greatest at the end of the temporal interval) or descending (the discharge rate greatest at the beginning of the temporal interval) groups by determining if the firing rates during the first and last 300 milliseconds of each self-timed temporal interval were significantly different using one-tailed, two-way t-tests. This method found 85 (30%) and 33 (28%) neurons of an ascending type for subjects 1 and 2, and 77 (27%) and 37 (32%) neurons of a descending type in subjects 1 and 2. We also tested each temporal interval duration separately for ascending and descending type neurons, this yielded nearly the same populations, and did not reveal cells that displayed ascending activity for one temporal interval duration and descending activity for another.

We found that the ascending and descending neuronal populations were sensitive to the passage of time and the duration of the temporal interval. The slope of the continuous modulation of the population activity appeared to be tuned to the nominal self-timed temporal interval duration. This effect can be seen in the alignment to the start of the temporal interval (Figure 9, A1,3 ; Figure 10 D1,3), in which the population activity rises from the vertical blue and green lines, which indicate the start of the interval, to peak at the vertical red lines, which indicate the end of the intervals. Because the slopes of the activity modulations are different, the three population activity traces, related to the three different nominal delay durations, diverge between 0 ms and 300 ms. This shows

that the population activity was selective for interval duration early in the self-timed temporal interval. When aligned to the end of the delay (Figure 9, A2,4 ; figure 10 D2,4), the population activity slope and magnitude can be seen to diverge among the three nominal temporal interval durations. This shows that the representation of ongoing time was tuned to the planned duration.

The combined activity of the entire recorded population, for each monkey, is illustrated in Figures 11 and 12. Therefore, these activity traces include the ascending and descending neuronal populations, as well as neurons that did not fit into either of those categories. The combined activity in DLPFC generated a population signal that categorically differentiated between the different nominal target durations during the last 500 ms of the self-timed temporal intervals and responds at a time commensurate with initiating the movement that ends the self-timed delay. This can be seen in the clearly differentiated activity traces in the last 500 ms before the exit movement in Figure 11B and Figure 12B. Activity related to the self-timed exit from the short duration target was the greatest, the activity related to the 1000ms target was intermediate, and the activity preceding the exit to the 2000 ms target is lowest. Each peaks and then falls after the exit from the self-timed delay target. In contrast, the three traces can be seen to overlap when activity is averaged over movement direction, serial order, and screen position, namely before the target entrance (Figures 11A and 12A) and after the target exit (Figures 11B and 12B).

Figure 9. Ascending Neuronal Populations Modulated by Time.

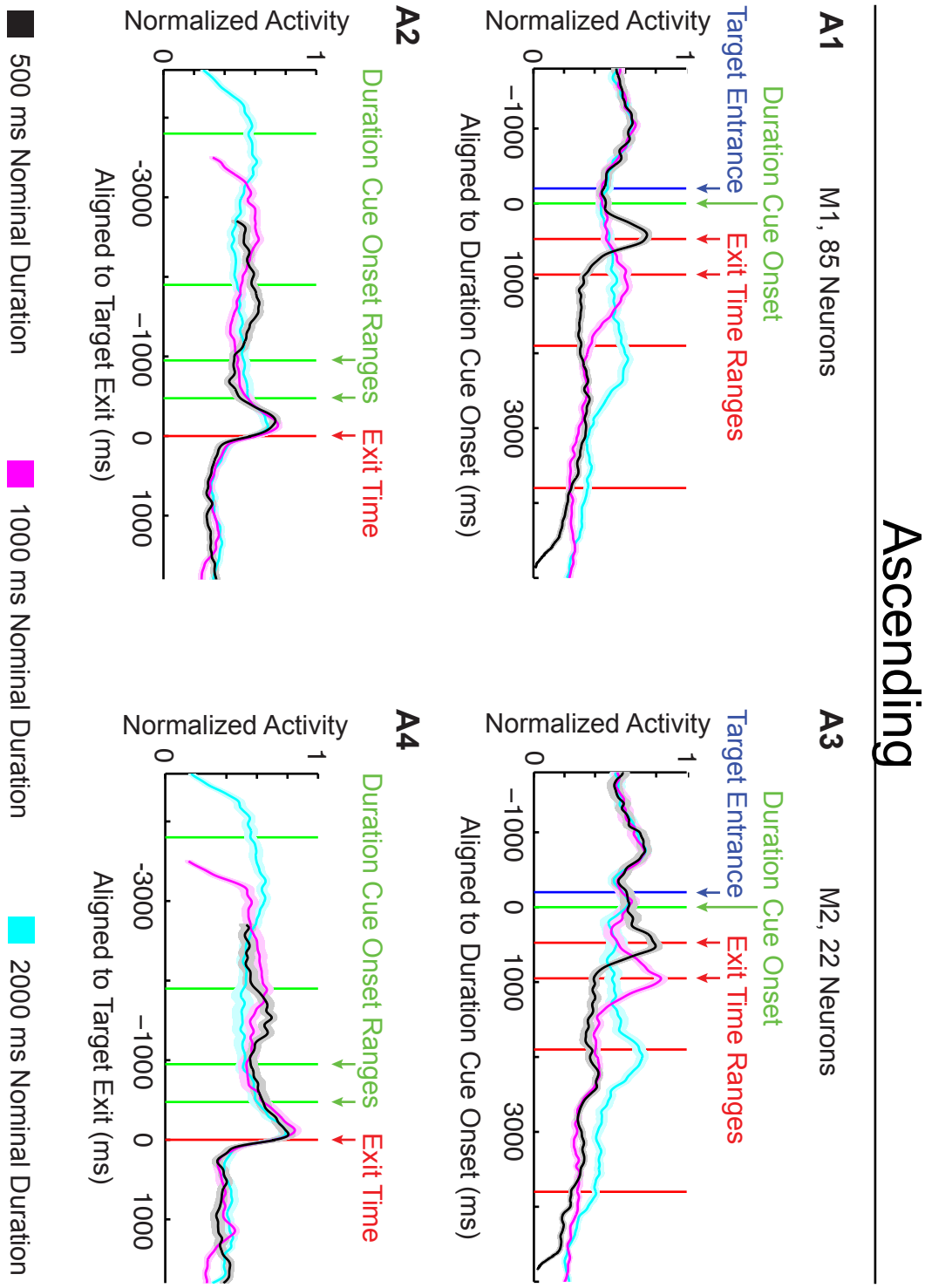

Figure 10. Descending Neuronal Populations Modulated by Time.

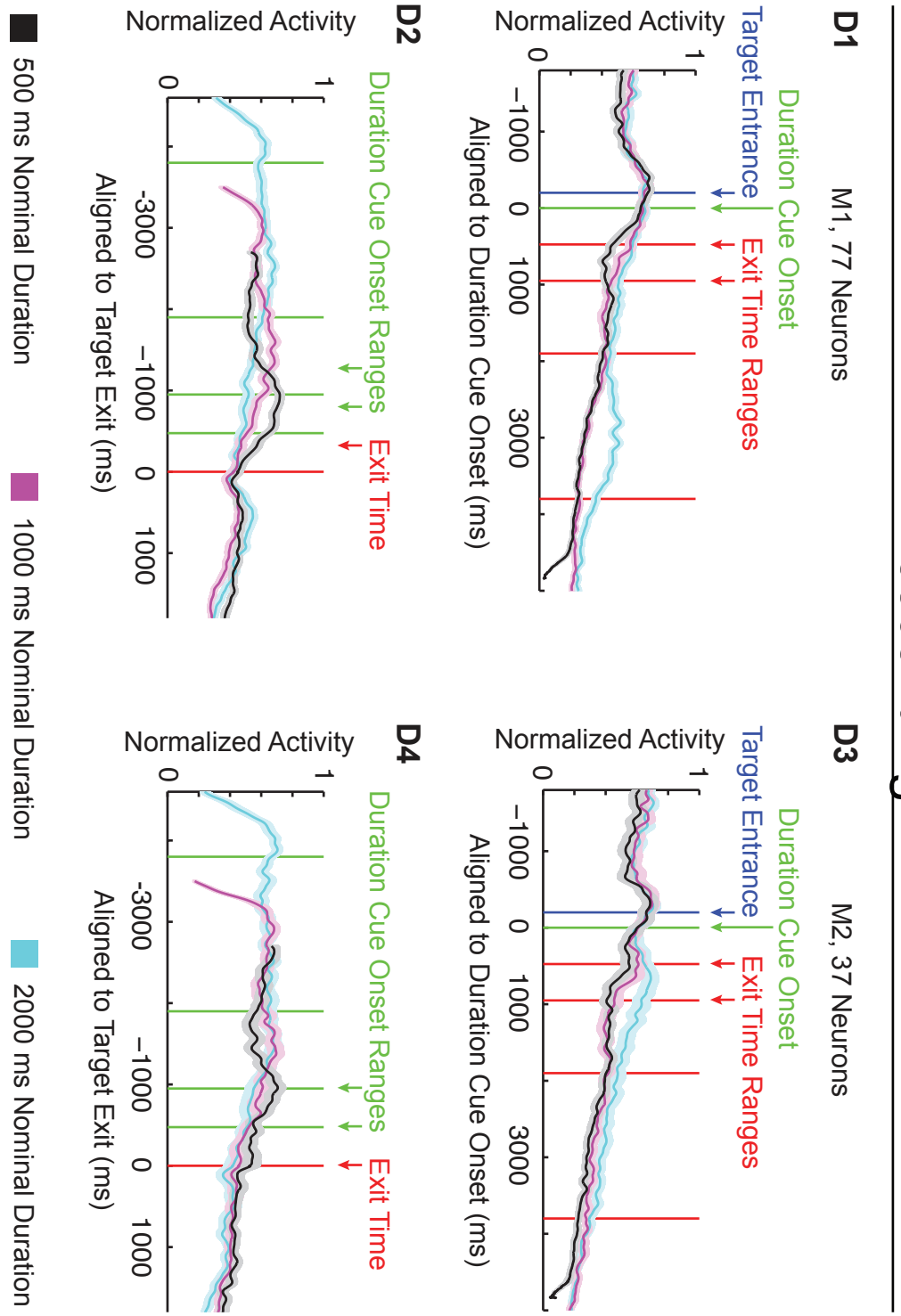

Figure 9. Illustrates the average normalized activity of ascending time-sensitive neuronal populations in each subject. (**A1, A3**) Ascending population activity with graded slope tuned to the self-timed duration is aligned to the start of the self-timed temporal interval. (**A2, A4**) Population activity is aligned to the movement ending the self-timed temporal interval. Shading indicates 95% confidence intervals based on the number of included neurons.

Figure 10. Illustrates the average normalized activity of dscending time-sensitive neuronal populations in each subject. (**D1, D3**) Descending population activity with graded slope tuned to the self-timed duration is aligned to the start of the self-timed temporal interval. (**D2, D4**) Population activity is aligned to the movement ending the self-timed temporal interval. Shading indicates 95% confidence intervals based on the number of included neurons.

Figure 11. Average normalized population activity of all recorded neurons during the self-timed delay durations for subject 1. (**A**) The population activity is plotted separately for each temporal interval duration and is aligned to the start of the self-timed delay. (**B**) The population activity is aligned to either the end of the self-timed delay. Shading indicates 95% confidence intervals.

Figure 12. Average normalized population activity of all recorded neurons during the self-timed delay durations for subject 2. (**A**) The population activity is plotted separately for each temporal interval duration and is aligned to the start of the self-timed delay. (**B**) The population activity is aligned to either the end of the self-timed delay. Shading indicates 95% confidence intervals.

Figure 11. Time Sensitive Modulation of All Neurons from Subject 1.

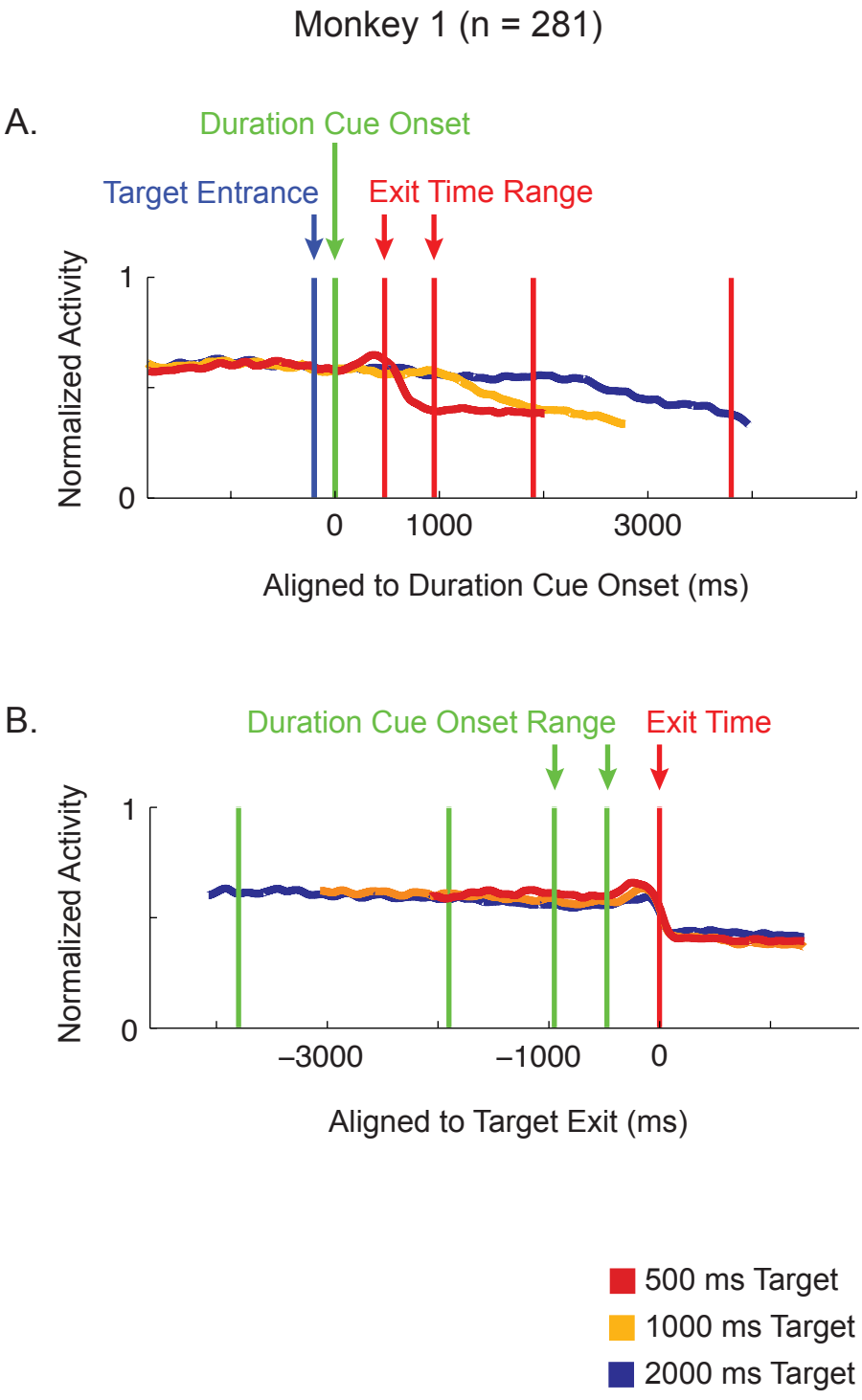

Figure 12. Time Sensitive Modulation of All Neurons from Subject 2

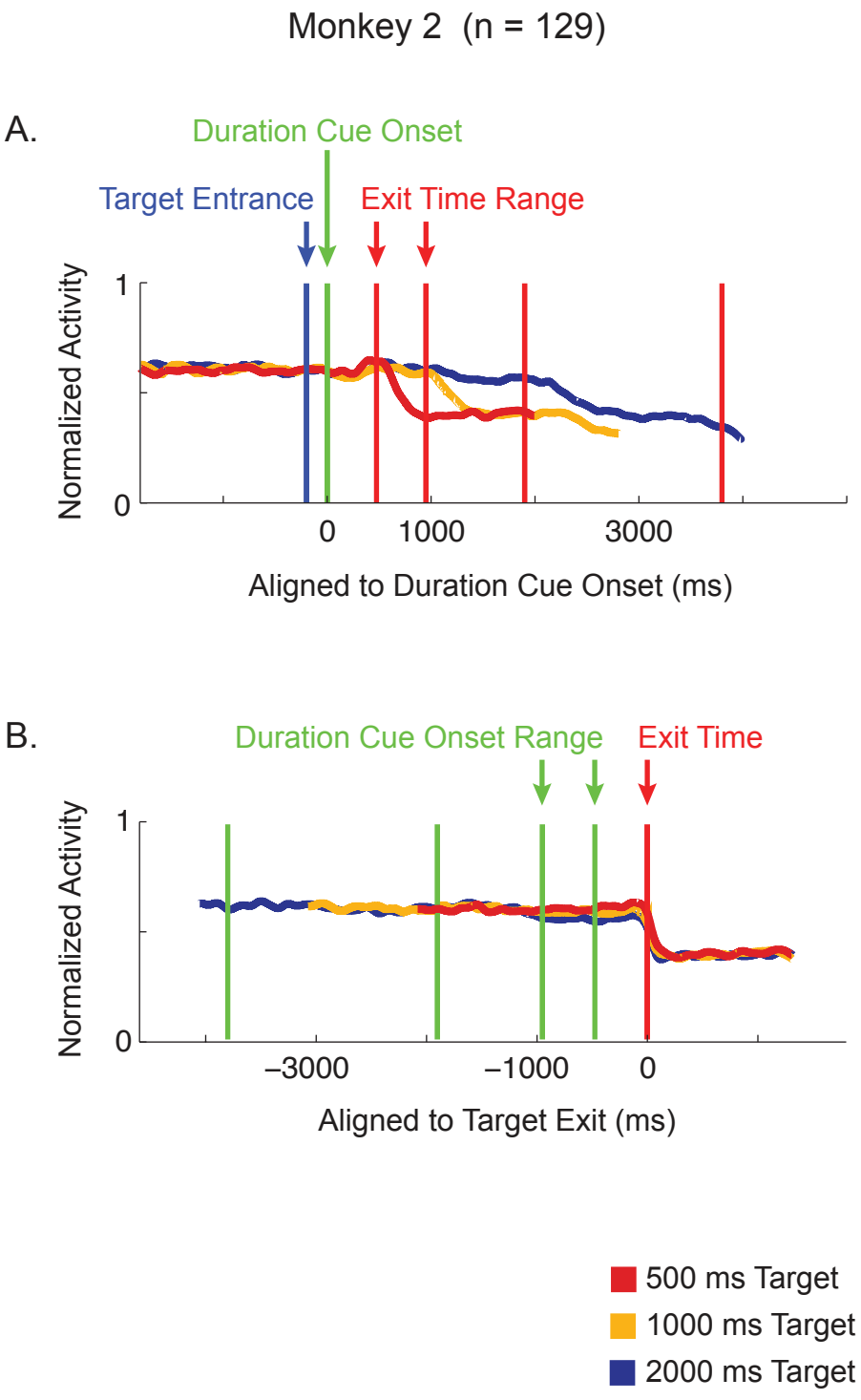

3.6: Discussion of Neuronal Modulations Related to Temporal Interval Production in Dorsolateral Prefrontal Cortex.

In this analysis, focused on neuronal modulations during the self-timed temporal intervals, five main findings emerged that were specifically related to movement timing. First, we found that the majority of the neurons in DLPFC carried information related to the passage of time: the activity of the entire recorded neuronal population differentiated between the three self-timed interval durations. Second, we found that neuronal activity modulated in relation to the passage of time displayed either ascending or descending ramps, which reached neural thresholds at consistent time points before movement initiation. Third, unlike most other studies, we found roughly equal numbers of ascending and descending type neurons encoding the time remaining during each self-timed-delay. Fourth, unlike previous reports in premotor cortex, we did not find that neurons in DLPFC were tuned to specific self-timed interval durations, instead, we found that the rate of change of activity, or ramp slope, varied to accommodate different interval durations. Finally, we found neurons that signaled the start of the self-timed temporal intervals: there was rapid modulation of neuronal activity immediately following the start of the interval that preceded continuous changes in activity related to ongoing time, but was not related to either interval duration or ongoing time.

3.7: Methodological Considerations Related to Behavior

The spatio-temporal sequence task required the NHP subjects to pause between sequential directional movements for temporal intervals of three different durations. The temporal intervals spanned a large range of durations, from 500 ms to well over 2000 ms. The task was challenging because both sequential movements and the production of temporal intervals are challenging in themselves, and require continuous concentration. The overall performance of

the subjects at ~42% correct reflected high level of task difficulty and the sustained concentration required during trials that lasted ~10 seconds.

The NHP subject's behavioral estimates of the temporal interval durations were sufficiently accurate and precise in the context of a challenging task. The animals clearly differentiated between the three durations: this can be seen in Figure 3, in which the interval estimate distributions related to each duration are uni-modal. Additionally, the distributions overlap only a small amount, and the majority of the temporal interval estimates (the exit-movement times) for both subjects lie well within the allowed limits for each duration. Because of the experimental design the correct response-time ranges for the different durations do not overlap(shown in gray in Figure 3). The duration distributions appear to be slightly skewed towards the minimum hold time, this might possibly reflect a strategy to reach the juice reward at the end of the sequence as quickly as possible. The 2000 ms duration delay is quite a long pause to time internally without the aid of an outside signal, such as a metronome. As might be expected, successful performance in both subjects was about 10 percentage points lower for the 2000ms self-timed delay than the 500ms delay.

3.8: Methodological Considerations Related to Neuronal Activity

During the self-timed delay intervals we observed neuronal signals that were related to a neural estimate of elapsing time and the production of a timed movement. Because the experimental design excluded any cues related to the passage of time we are confident these timing signals reflected the internal generation of an estimate of time by the subjects. In the dynamic behavior performed by the subjects, which was a series of movements punctuated by periods when the arm remained static, it was difficult for the animal subjects to know for each of the timed intervals when the estimation of time should begin; for example, the interval might begin when the cursor made contact with the visual

target, when more than half the cursor was within the visual target, or when the moving cursor had become stationary at the center of the target. To make the beginning of the estimate more explicit to the subject, a visual stimulus was displayed 200 ms after the cursor entered the target and remained static for the duration of the trial, and so it could not have been used to help the subject judge the amount of time remaining in the interval or signal the correct moment to perform the exit-movement. These stimuli served as a substitute for the tactile and auditory information that occurs during more natural behavior, such as when using a finger to strike a note on a musical instrument.

Because the self-timed temporal intervals were embedded in complex sequences, they were presented at various spatial locations, in various orders, and before and after each of the movement directions. Therefore we are confident that the signals related to duration were not confounded with the spatial position of the cursor, the spatial position of the stimuli, the retinal position of either, movement direction, or other stimuli. The task difficulty and sequential context required subjects to maintain continuous concentration on timing in the face of the other task requirements. This may have driven the unique timing representation that we observed in DLPFC, namely that single neurons signaled the start of the timing process, as well as the elapsing time leading up to the timed movement ending the interval.

Lighter and darker horizontal banding in the raster plots in Figures 4 through 8 depict trial-to-trial variability in the neuronal discharge rates that was not related to the passage of time. This variability may be discounted simply as noise, but might be better described as neuronal selectivity to additional ‘hidden’ variables. We take up analysis of simultaneous neuronal selectivity to additional movement features, such as ordinal position or movement direction in the next chapter. Here, we note that the general shapes of the spike density functions in these

figures seem to be conserved even when the presence of horizontal banding suggests a higher or lower mean activity rate.

Compression between the phasic neuronal activity indicating the start of the self-timed duration and the continuously modulated activity tracking ongoing time can be seen in the spike density functions during the 500ms nominal self-timed delay in Figures 4 & 5, A & C. If the overlap between these two signals is imagined to interfere with the neural timing process then the tendency for subjects to exit the 500 ms delay interval too late (Figure 3) supports the plausibility of their role in interval timing. The idea is that the 500 ms interval is too short for the full expression of the cortical timing process. The interference between the overlapping phasic start signal and continuous time-accumulation signal inhibits the accumulation signal from reaching it's full peak, which delays movement triggering. These observations also support the idea that timing on the scale of 10's to a few hundred milliseconds operates on different neural mechanisms and with less cortical involvement than timing in the range of seconds.

Subject 2 performed the experiment with pseudo-randomly assigned trial types after each correct trial, while Subject 1 was assigned trial types in a block (Methods 2.1). This would have made it more difficult for subject 2 to plan the correct sequences in advance (although some planning was still allowed as the trial type did not change after incorrect trails, thereby enabling a trial-and-error strategy). Therefore, subject 2 may have relied more heavily on a 'seat-of-the-pants' reaction to the duration stimulus at the start of each self-timed delay. This difference in task difficulty between subjects may account in part for differences in the subjects results, particularly in the neuronal population activity. The population activity for Subject 1 can be seen to begin and end each self-timed interval at about the same level, and reset just after the start of the interval (Fig 9, A1; Fig 10, D1). But for Subject 2, at the start of the self-timed interval the ascending population response is elevated for ~500 ms, centered between the

vertical blue and green lines (Fig 9, A3). The activity reset to baseline is occluded by the ascending ongoing-time signal for the 500 ms nominal delay interval, shown in black. The activity returns to baseline before ascending for the 1000 and 2000 ms nominal delay duration curves. Similarly, for Subject 2 the descending population activity contains an extra dip, this time centered just after the vertical green line (Fig. 10, D3). Baseline activity is high in the case, seen at the vertical blue line, and the time dependent population signal is only able to return to this level, before descending, for the 2000 ms nominal duration self-timed delay. This pattern of neuronal activity would be plausibly explained if Subject 2 placed a greater priority on incorporating a reaction to the duration cue into its initialization of the timing process.

3.9: Related Results from Macaque Neurophysiology

Many recent studies are dedicated to understanding the properties of conscious, attention-dependent timing tasks in the range of several hundred to a few thousand milliseconds, and their underlying neural mechanisms. Single neurons in several regions of macaque cortex have been observed to be modulated during an internally-generated neural estimate of ongoing time, or to represent that estimate directly including prefrontal cortex (Niki and Watanabe 1979, Kojima and Goldman-Rakic 1982, Vaadia, Kurata et al. 1988, Quintana and Fuster 1992, Goldman-Rakic 1995, Miller, Erickson et al. 1996, Kim and Shadlen 1999, Fuster 2001, Rainer and Miller 2002, Brody 2003, Lebedev, Messinger et al. 2004, Sakurai, Takahashi et al. 2004, Genovesio, Tsujimoto et al. 2006, Genovesio, Tsujimoto et al. 2009), premotor cortex (Weinrich and Wise 1982, Mauritz and Wise 1986, Romo and Schultz 1987, Crammond and Kalaska 2000, Lebedev and Wise 2000, Lucchetti, Ulrici et al. 2005, Ohmae, Lu et al. 2008, Mita, Mushiake et al. 2009, Merchant, Zarco et al. 2012, Merchant, perez et al. 2013), primary motor cortex (Roux, Boulanouar et al. 2003, Lebedev, O'Doherty

et al. 2008), and parietal cortex (Leon and Shadlen 2003, Janssen and Shadlen 2005, Maimon and Assad 2006, Schneider and Ghose 2012),

Dorsolateral prefrontal cortex (DLPFC) is known to represent, maintain, and anticipate task-related information while subjects make decisions and movements (Goldman-Rakic 1995, Miller, Erickson et al. 1996, Fuster 2001). Several earlier publications noted that the passage of time seemed to be convolved with the representation of the 'primary' mnemonic or attentional processes that was being studied. [See (Lebedev, Messinger et al. 2004), as well as (Niki and Watanabe 1979, Kojima and Goldman-Rakic 1982, Vaadia, Kurata et al. 1988, Quintana and Fuster 1992, Kim and Shadlen 1999, Rainer and Miller 2002, Brody 2003, Sakurai, Takahashi et al. 2004)]. In each of these reports time-dependent incrementing, or less often decrementing, neuronal activity can be seen that is very similar to the results obtained by later experiments in which time was an experimental variable, including our own. Recent experiments that studied the representation of time directly found that DLPFC encoded the duration of delay intervals prior to movement (Genovesio, Tsujimoto et al. 2006), and the duration of visual stimuli in conjunction with other stimulus properties (Genovesio, Tsujimoto et al. 2009). Specifically, during a temporal interval discrimination task that involved the serial presentation of two colored visual stimuli, (Genovesio, Tsujimoto et al. 2009) found that neuronal activity in DLPFC represented both the absolute and relative duration of the stimuli in conjunction with their color and ordinal position. Relative duration encoding was more prevalent, likely due to the subjects' need to report which stimulus had lasted longer in order to obtain a juice reward.

The activity of single neurons in primary motor and pre-motor cortices have also been shown to encode either elapsing time itself, or the amount of time remaining before an upcoming movement (Lebedev, O'Doherty et al. 2008, Ohmae, Lu et al. 2008, Mita, Mushiake et al. 2009, Merchant, Zarco et al. 2012,

Merchant, perez et al. 2013). Neuronal activity in the supplementary eye field varied systematically with the passage of time during the anticipation of a pseudo-randomly produced saccade, rather than the likelihood of the ‘go’ stimulus’ appearance (Ohmae, Lu et al. 2008). The medial prefrontal cortical areas (MPC) Pre-SMA and SMA contain neurons that encode the amount of time that passes between movements, as well as categories of temporal interval durations (Mita, Mushiake et al. 2009, Merchant, Zarco et al. 2012, Merchant, perez et al. 2013). In primary motor cortex (M1), and dorsal pre-motor cortex (PMd), neuronal activity was observed that represented the passage of time during a button press (of 2.5 to 4.5 seconds); population signals in each area were sufficient to decode the passage of time, and to predict the movement times bounding the button presses, however, these two features were encoded by separate populations of neurons (Lebedev, O'Doherty et al. 2008). Several recent neurophysiological reports have shown that the lateral intra-parietal area (LIP), in parietal cortex, encodes the salience of visual objects, and potentially visible objects, based on a neural estimate of elapsing time and other stimulus features (Leon and Shadlen 2003, Janssen and Shadlen 2005, Maimon and Assad 2006, Schneider and Ghose 2012).

In summary, two observations are common to the cortical encoding of duration summarized above. Time-related activity tends to be scalar, meaning that the pattern of activity appears as if it has been stretched to the length of each interval duration. The second prevalent feature is that some neurons have been found that are tuned to interval duration, meaning that their activity is graded from being most active during the preferred duration to being least active during the ‘anti-preferred’ duration. In M1 and LIP preferred durations have neither been reported nor disproved, as publications related to timing in these areas have so far focused on what information can be decoded from the neuronal activity, rather than which tuning curves might have been used to encode the information.

3.10: Comparing Our Results to the Related Results from Macaque Neurophysiology

From a general hypothetical perspective, the neural mechanisms for interval timing can be assumed to perform several critical functions. To time a temporal interval the timer must be started, then the elapsing time during the interval must be measured, and then the timer must be stopped. Temporal stimuli must be recognized and timed before being categorized according to their duration. For movements the decision about what duration is desired must be made before movements begin. The neural mechanisms for the starting, stopping, timekeeping, and decision phases of interval timing in the rage of hundreds to thousands of milliseconds are not well understood.

We have reported neural activity that was scaled to the length of the temporal intervals and encoded the passage of time by incremental modulation of the discharge rate. We did find that both the behavior and the neuronal activity were in accord with a scalar model of timing, in which the variability about the estimate grows linearly with the length of the estimated duration, as if measured with a rubber ruler. This scalar representation of time by single neurons in DLPFC corroborates the observations of scalar timing summarized above and found at the level of behavior. Our results extend the observations of previous publications by the observation of phasic activity modulations that appeared at the start of the timed interval and seem to initialize the timing process. Unlike many previous studies our task required subjects to produce the temporal intervals, and so this may have driven neurons in DLPFC to produce the ‘start’ signals.

Our results, in concert with those summarized above, are consistent with the idea that DLPFC participates in widely distributed neural networks that are recruited in order to perform interval timing behaviors. Our results do not speak directly to the various clock mechanisms that may or may not operate in the brain; the time-

dependent activity that we observed in DLPFC could rely on either regular oscillations or population dynamics. It is also possible that DLPFC could receive the timing related signals we observed as inputs, in this case DLPFC would be principally concerned with the decision and coordination processes related to timing, and might critically link the elements of the neural timer, namely the goal duration, the start signal, the passage of time during the interval, and the moment at which a movement had to be performed.

3.11: Conclusion: Temporal Interval Production and Neuronal Modulations Related to Elapsed Time in Dorsolateral Prefrontal Cortex

The dorsolateral prefrontal cortex links perception, goal selection, and attention to plan and prospectively encode actions. The role of the DLPFC is especially prominent when those actions must be performed after an intervening delay or in the face of other distractions. In this analysis, focused on neuronal modulations during the self-timed temporal intervals we found that activity of most of the recorded neurons in the DLPFC of non-human primates was related to the initialization and maintenance phases of an interval timing process during the production of self-timed temporal intervals. The neuronal discharge rate appeared to represent the passage of time, and its rate of change was tuned to the interval durations, and so repeatable thresholds were reached at the end of the self-timed intervals, consistent with the idea that DLFPC participates in the distributed neural mechanisms for interval timing. The threshold discharge rates that we observed were somewhat variable, in the next chapter we take up the analysis of the observed discharge rate variability and its relationship to other critical task variables, such as ordinal position and movement direction. The next chapter will also take up the issue of joint encoding of movement parameter conjunctions by DLPFC, which is related to the observations of conjunctive encoding related to stimulus features mentioned above (Genovesio, Tsujimoto et al. 2009).

Chapter 4: Results Related to Nonlinear Mixed Selectivity

4.1: Synergistic Encoding of Temporal Sequence Information in Monkey Dorso-Lateral Prefrontal Cortex.

We studied neuronal activity in the dorsolateral prefrontal cortex of two monkeys that were required to perform a series of three sequential movements separated by internally-timed temporal intervals. During the movements and internally-timed delays we observed neuronal selectivity for direction, temporal-interval duration, and serial order. Some neurons were simultaneously selective for two or three of these movement parameters. We then applied an information-theoretic analysis to partition the mutual information transmitted by single neurons into components related to direction, duration, serial order, or their overall spatio-temporal sequences. We found that single neurons simultaneously transmitted independently encoded information related to direction, duration, and serial order, as if in three separate channels. We also found that as many as 40% of the neurons encoded movement sequence information that was synergistically encoded in the dependent relationships between the three parameters. Our results show that neurons in DLPFC encode independent movement features in a way that supports the coordination of behavior during complex sequential movements.

4.2: Results Related to the Behavioral Performance

We have already presented the behavioral findings related to self-timed temporal interval duration; here, we focus on how the performance of the two NHP subjects was influenced by the sequential features of the task. The task comprised a sequence of three spatially distinct arm movements each followed by a self-timed delay interval of specific duration. The spatio-temporal sequence task included four movement directions and three temporal interval durations. These elements were organized into one of four spatial sequences, and one of

six temporal sequences, which were combined to form the twenty-four trial types (or unique spatial-temporal sequences) in the experiment. Animal 1 performed the task in a block design, with trial type changing between each block, while animal 2 was presented with a new trial type after each correct trial. For further description of the task refer to the task methods, section 2.1.

Both monkeys performed the task with an overall success rate per trial near 42% (Table 3). However, their success rate was not constant during each trial, the farther into a trial each subject progressed, the more likely they were to correctly complete the next segment. If an animal reached the third spatio-temporal segment, they performed it correctly 88% of the time, more often than for the earlier segments. We also note that NHP 2 was a little less likely to perform the first movement correctly, likely due to the presentation of new trial-type after each correct trial. To determine if serial order had a statistically significant effect on the likelihood of correct completion of each movement segment we performed a logistic regression using serial order and two other movement parameters applicable to each movement segment, the movement direction and the self-timed temporal delay duration. We found that all three parameters had an effect on the likelihood that a task segment was performed correctly (Table 4., $P < 0.001$). This is shown by the non-zero beta values shown in Table 4, which also indicated that that direction had the strongest consistent effect. In comparison to movement parameters that vary at each serial order position we also tested sequence categories. We also tested for effects of the spatial sequences, temporal sequences, and trial type (see methods) using a logistic regression, and found that these factors also had significant effects on the likelihood correct performance of task segments, but the beta value magnitudes were much smaller than those presented in Table 4; they ranged between 0.02 and 0.07 (data not shown).

Table 3.

Correct Behavior According to Movement Segment Serial Order Position				
	Monkey 1		**Monkey 2**	
	Total % Correct	Relative % Correct	Total % Correct	Relative % Correct
Center	85.0	-	78.2	-
First	56.9	66.9	54.6	69.8
Second	46.9	82.4	49.7	91.1
Third	41.5	88.6	43.8	88.2

Legend. Average behavioral performance for each segment of the spatio-temporal sequence task. The total percent correct shows the likelihood that a subject reaches each successive task segment and completes it correctly. The relative percent correct shows the likelihood that a segment is completed correctly, given that they have made it that far in the trial. Table 3 shows that the overall percent correct for each subject was below 44 %, and also that subjects were more likely to complete later ordinal positions if they were able to make it that far in the trial.

Table 4.

The Effect of Movement Segment Parameters on Correct Behavior				
	Direction (slope)	**Duration** (slope)	**Serial Order** (slope)	**Intercept**
Monkey 1	-0.41	-0.14	0.48[1]	2.16
Monkey 2	-0.43	-0.23	-0.12	2.85

Legend. Beta values from the logistic regression for the effect of movement parameters on behavioral performance during the spatio-temporal sequence task, ($P < 0.05$). The movement parameters direction, duration, and serial order all had significant effects on the likelihood of correct performance during the task. Beta value magnitude reflects the strength of each parameters influence on the correct completion of each movement segment.

4.3: Encoding of Sequential Movement Parameters During Spatio-Temporal Movement Sequences

As with the other analyses discussed above, we examined the activity of 397 neurons recorded in dorsolateral prefrontal cortex, 116 from monkey A and 281 from monkey B, that were found to be consistently active, fired on average more than 5 spikes per second, and did not present obvious signs of corruption from noise. All units were recorded during at least 5 repetitions of each of the 24 movement sequences, resulting in at least 120 trials per neuron.

There are many different parameters that might be chosen to describe the movements made during the spatio-temporal sequence task. The behavioral parameters include, but are not limited to, the direction of each movement between targets, the duration of each self-timed delay between movements, and the ordinal position of each of these elements during the trial. The movements can also be described according to the specific spatial sequence or temporal sequence into which they are organized, or the combination of these two sequences which we call the trial type. As a preliminary test to determine whether the movements were best encoded as elemental units or sequences we compared the performance of several different ANOVA's that modeled the behavior at different hierarchical levels of abstraction or conjugation. ANOVA 1 included the twenty-four possible trial types in the task as a single factor, see Figure 1 and Methods 2.1 and 2.4 for details. ANOVA 2 included two factors, the temporal and spatial sequences, which had six and four levels, respectively. ANOVA 3 included three main effects without interactions: movement direction, self-timed temporal interval duration, and ordinal position. The neuronal discharge rates and behavioral descriptors for the ANOVA's were collected from two epochs, the last 300 ms of the three movements, and a 300 ms epoch at the beginning of the self-timed delay periods (see Methods 2.4). Each epoch occurred three times per trial. ANOVA 3i was identical to ANOVA 3 but included the interactions between direction, duration, and serial order. Because direction

and serial order were correlated during the second segment of the task only data from the first and third ordinal positions of the task were included in ANOVA3i (see Methods 2.7).

Table 5.

The Number of Neurons with Significant Effects for Three Sequence-Based ANOVA Models.

		ANOVA 1	ANOVA 2	ANOVA 3	ANOVA 3i
M1 (n=281)	**Self-Delay**	181	216	136	205
	Movement	191	211	134	208
M2 (n=116)	**Self-Delay**	20	39	59	68
	Movement	21	51	71	74

Legend. The three ANOVA's were based on either trial type, sequence type, and movement type, which represent different levels of abstraction or conjunction of the movement sequences. ANOVA 3i is the only model to include the interactions between the main effects; data from the second segment of the task was excluded to remove correlation between movement direction and serial order.

Taken as a whole, the ANOVA results suggest that mixed selectivity for the three sequential movement parameters enabled most of the neurons in DLPFC to be selective for all of the tested factors. We found that the residual ranges from each ANOVA were largely overlapping for both NHP subjects (data not shown), indicating that the explanatory power of the different movement descriptors for the neuronal activity were approximately the same. However, the number of neurons captured by each ANOVA differed, particularly across the two subjects. The ANOVA models based on sequences (ANOVA 1 and 2) found few significant

neurons in NHP subject 2. This is likely due to the properties of the experimental design which differed for each animal; in subject 1, the trials were presented pseudorandomly across spatial sequences within blocks organized by spatial sequence category, a strategy which likely made the sequential organization more explicit for the subject; by contrast, Subject 2 was presented with a new trial type chosen pseudorandomly after each correct trial which may have had the effect of making sequence-related modulation much less common in the population of neurons we studies. ANOVA 3i captured the highest percentage of the neurons in both subjects. Because this model better captured the patterns of activity in both subjects, we show its results in greater detail in Table 6.

ANOVA 3i includes the main effects of direction, duration, and serial order, along with their interactions, which originate in the movement sequences. Thus we are able to count how many neurons were selective for single elemental movement parameters, such as direction and differentiate them from neurons that were selective to aspects of the movement sequences, such as the interaction between direction and serial order. The most prevalent main effect, and the only main effect that was observed in isolation, was direction ($P<0.05$), shown in the left hand column of Table 6. Main effects of both serial order and temporal interval duration were also observed, but not in the absence of other main effects, shown in columns 4 – 7 of Table 6. Direction and serial order were the most frequent main effect pair, shown in column 5. Main effects of all three factors were less common than pairs. Interactions between both direction and duration with serial order were frequent in Subject 1.

For Subject 2 the most frequent significant interaction was between direction and serial order. Significant interactions between all three terms were infrequent for both subjects. These results clearly indicate that the firing rates of many neurons in DLPFC were modulated by the movement sequences present in the spatio-temporal sequence task, and that their activity pattern was resolved by the

elemental movement parameters and interactions used in ANOVA 3i. The observed mixed selectivity for the factors in ANOVA 3i indicated that the neuronal firing rates encoded some information that was directly related to the movement direction, the self-timed movement delay duration, and their serial order, and some information that was related to the movement sequences that contextualized the elements.

Table 6.

The Number of Neurons with Significant Effects in ANOVA 3i.

		Main Effects							Interactions			
		Direction	Duration	Serial Order	Dir & Dur	Dir & SO	Dur & SO	Dir & Dur & SO	Dir x Dur	Dir x SO	Dur x SO	Dir x Dur x SO
M1	**Self-Delay**	43	0	0	10	18	25	4	10	33	92	4
	Movement	47	0	0	12	20	19	4	20	56	88	4
M2	**Self-Delay**	25	0	0	2	11	5	1	5	10	5	1
	Movement	39	0	0	1	14	3	0	1	21	3	0

Legend. Numbers of neurons with the noted effects during the spatio-temporal sequence task in the ANOVA 3i model ($P < 0.05$). ANOVA 3i recognizes the main effects and interactions between the elemental movement parameters: movement direction, self-timed temporal interval duration, and serial order position. There are two sections of Table 6, the Main Effects and the Interactions. Within each section a neuron may only add to the count for one column at a time. For instance, the 43 neurons found at the top of column 1 do not contribute to the counts for columns 2 – 7, but might contribute to one of the interaction counts, columns 8 – 11. Significance was obtained at the level of $P<0.05$.

4.4: Neuronal Activity is Widely Tuned to Sequential Movement Parameters

To examine the influence of the three elemental movement parameters – direction, duration, and serial order – on the neural activity during the spatio-temporal sequence task we first identified neurons carrying signals related to each of these three factors. We then constructed spike density functions for each population signal, with the activity in each ranked according to each neurons preference amongst the levels of each factor. To define a population of neurons selective for movement direction on neural activity after movement initiation we used a one-way ANOVA ($P<.05$). We found that the majority of neurons in DLPFC were modulated by the direction of the movement: 110 (95%) and 256 (91%) neurons in monkeys 1 and 2, respectively. We examined the effect of direction at the population level by constructing preferred direction spike density functions (SDF's). For all of the neurons with a significant effect of duration, described above, we ranked their activity according to their preferences for the four directions and then averaged the corresponding normalized SDF's. The peak of the normalized average population response for preferred direction (Figure 13), occurred 301 ms before the target entrance in subject A, and 365 before in subject B. The trough of the anti-preferred directions occurred 274 ms and 339 ms before the target entrances. Ninety five percent of the movements made by the monkeys during the task lasted between 300 and 600 ms. The average population activity clearly differentiates between movement in the four directions during motion, as well as before and after the movements.

To define a population of neurons selective for the instructed self-timed temporal interval duration during the initiation of self-timed movements we used a one-way ANOVA ($P<. 05$) on the last 300 ms of the self-timed delays. We found 30 (26%) and 49 (17%) neurons were tuned to the instructed temporal interval duration. The normalized average SDF's (Figure 13 C&D) show this effect in the population of cells. Peak firing rates for the preferred duration, shown in red,

occurred 124 ms and 212 ms before the end of the self-timed duration for animals A and B.

To define a population of neurons selective for the serial order of the spatio-temporal segment we used a one-way ANOVA ($P<.05$) on firing rates during the same epoch at the end of the first three movements used for direction. We found 66 (57%) neurons in monkey 1 and 98 (35%) neurons in monkey 2 that were selective for serial order position. To examine neural tuning to serial order in this population we constructed preferred serial order SDF's. In Figure 13 E&F, the average normalized neural activity of the population is clearly graded depending on the serial order position, reflecting the wide tuning to serial order of the individual neurons. The graded selectivity for serial order stretched from the movement period well into the self-timed delay period. The zero alignment point indicates the entrance of the cursor into the self-timed delay targets. The peaks of the preferred serial order SDF's are found at 23 ms and 61 ms after the cursor had entered the subsequent target for animals 1 and 2.

Figure 13. Average normalized activity of direction, duration, and serial order selective neuronal populations. **A.** Average normalized population activity during movement illustrates direction selectivity. The red line corresponds to the direction with the highest firing rate, the 'preferred direction'. The blue line corresponds to the direction with the lowest firing rate, the 'anti-preferred direction'. Yellow and green lines indicate directions of intermediate rank. The zero point indicates alignment to the end of the movements, ie the entrance of the cursor into the three self-timed delay targets. **B**. Same as (**A**) except data shown is from monkey 2. **C** & **D**. Average normalized population activity during movement initiation illustrates duration selectivity. Alignment is to the actual movement time concluding the three self-timed delay durations. **E** & **F**. Average normalized population activity illustrates selectivity to serial order position. Alignment is the same as in (**A**). Shading indicates 95% confidence interval in all plots.

Figure 13. Neuronal Populations Tuned to Movement Parameters

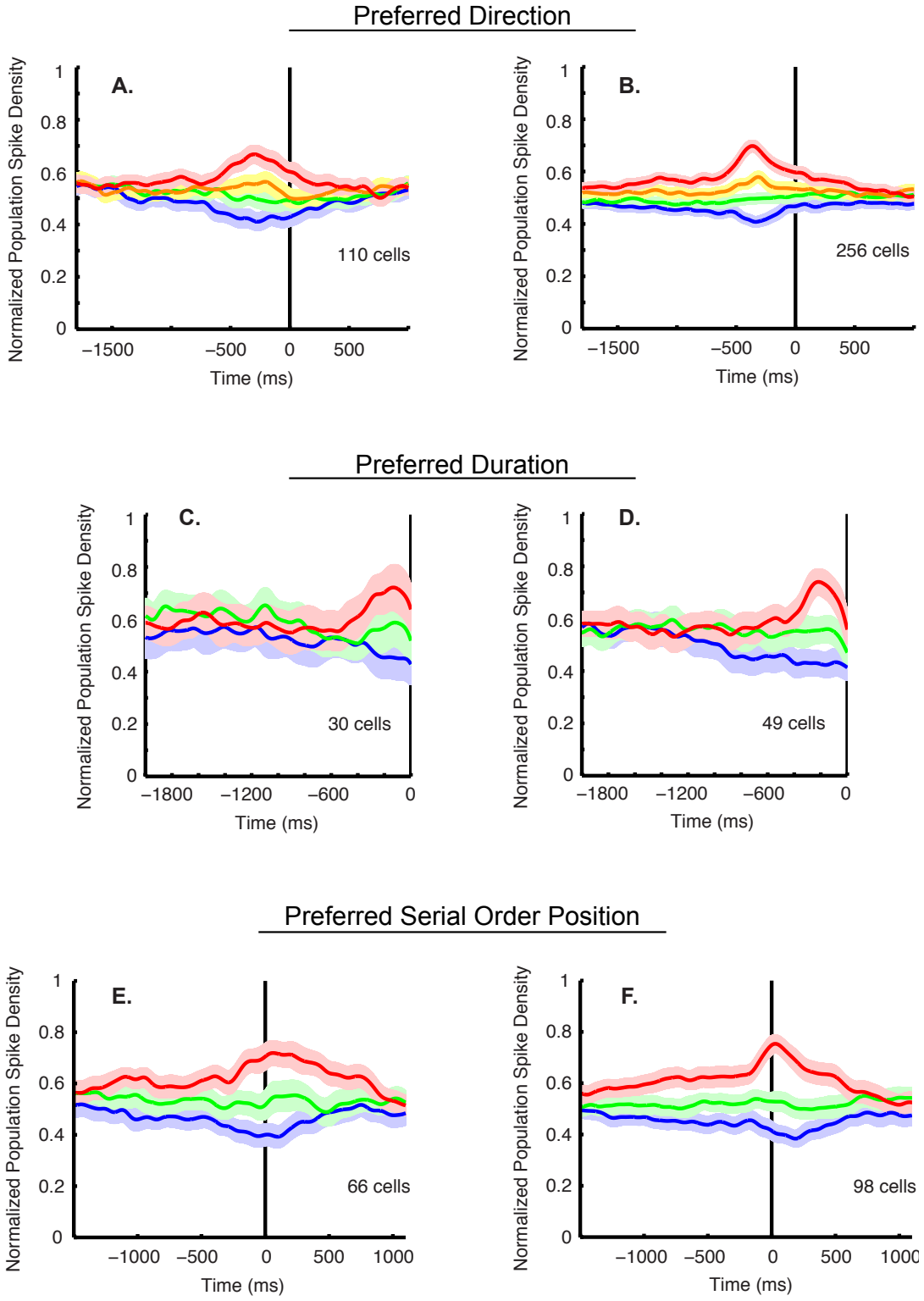

The population spike density functions exhibited graded activity according to the level of each of the three elemental movement parameters, indicating the presence of widely tuned distributed encoding of the sequential parameters in DLPFC. Using classical neurophysiological methods we found clear neuronal tuning to each of the three tested sequential movement factors, movement direction, self-timed delay duration, and serial order during the behavioral task.

4.5: Mixed Selectivity for Sequential Movement Parameters

In the previous section we constructed population spike density functions, which illustrated that neuronal activity in DLPFC was widely tuned for the three single task parameters. However we also found evidence of mixed selectivity amongst the neurons in DLPFC. Here we refer to simultaneous selectivity for multiple task variables, in which multiplicative or other nonlinear gain adjustments set the response rates, by using the term ‘mixed selectivity’ (Rigotti, Barak et al. 2013). Figure 14 shows one neuron selective for the second and fourth spatial sequences (right ordinate axis) during the planning delay prior to the first movement. But, one can also see that during spatial sequences two and four the neuron is selective for the second temporal sequence (second white band from the bottom of each spatial sequence). A few hundred milliseconds later the pattern changes, the neuron is more active during the first and fourth temporal sequences, but only for the fourth spatial sequence. Even ignoring the changing moment-to-moment preferences of this cell, the complex selectivity observed here might be better described by trial type than either spatial or temporal sequences. Another possible explanation for this neurons selectivity is that it relates events that occur at a certain time and place, which are only common to only a few trial, and in that case rather than being described as selectivity for whole trial types, the selectivity would be best described by the interactions between serial order, movement direction, and self-timed delay duration. Whatever the explanation, patterns of this nature were also common during the execution phase of the task.

Figure 14. Spatial Sequence Selectivity During Planning.

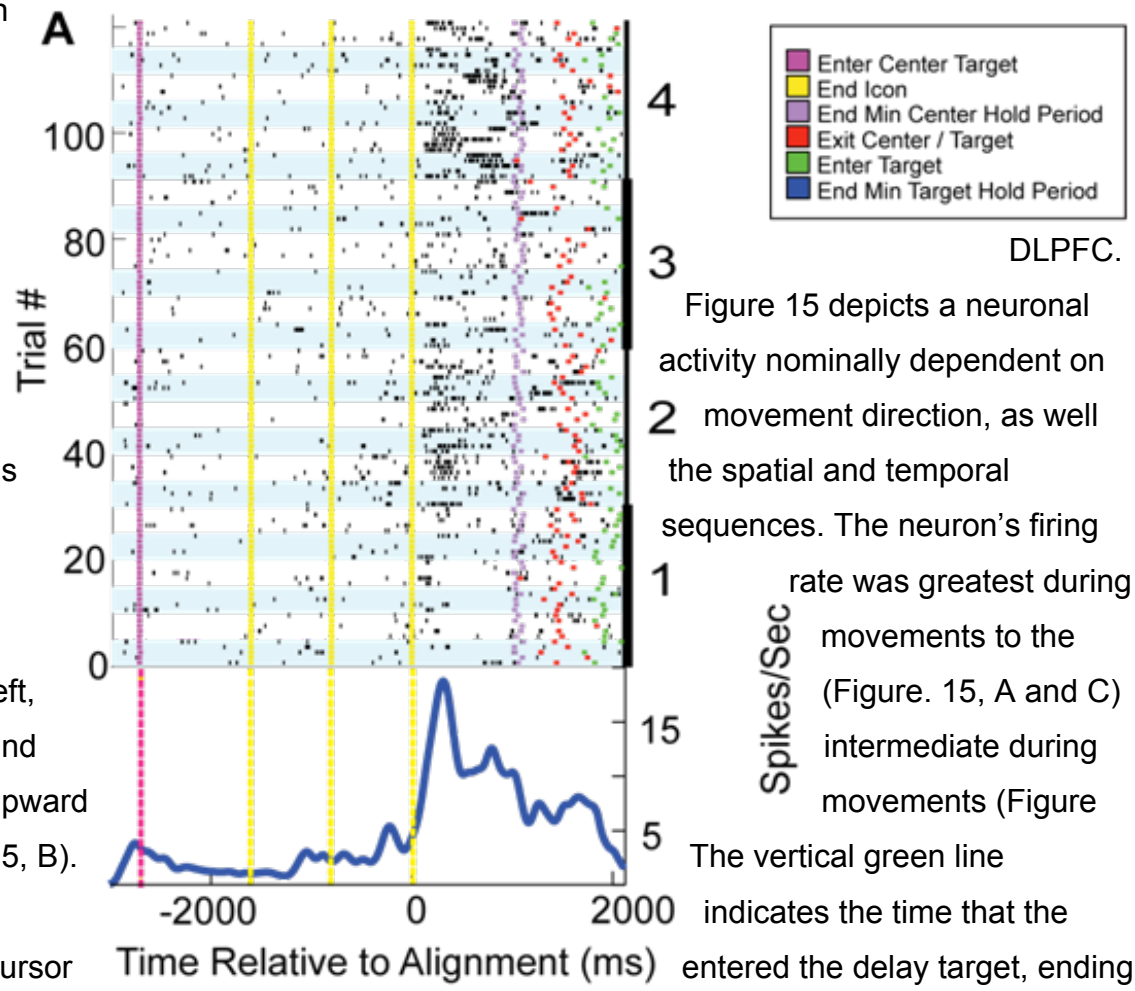

During the movement phases of the task, direction was the most prevalent signal in DLPFC. Figure 15 depicts a neuronal activity nominally dependent on movement direction, as well as the spatial and temporal sequences. The neuron's firing rate was greatest during movements to the left, (Figure. 15, A and C) and intermediate during upward movements (Figure 15, B). The vertical green line indicates the time that the cursor entered the delay target, ending

Legend. Raster plots and spike density functions depict one example of neuronal activity selective for trial type, the combination of the upcoming spatial and temporal sequences, during the planning stages of the task. (M2, 052709_9) The third vertical yellow line marks the beginning of the computer controlled delay period prior to movement during a trial. The far right ordinate axis indicates the four spatial sequences. Blue and white banding indicates the six temporal sequences that were combined with each spatial sequence. This neuron is clearly selective for second and fourth spatial sequence, but can also be seen to be more active for the second temporal sequence, or a few hundred milliseconds later it is more active during the fourth temporal sequence.

the movement phase. The brisk increases in activity begin several hundred ms after movement initiation and persist as the cursor is driven into the subsequent self-timed delay target, indicated by the vertical green line. The effect of serial order was small, but clearly movements to the left during the third task segment draw higher discharge rates than the first segment especially early in the movement. Critically, we draw your attention to the neuron's discharge rate after the entrance into the third target, when it is clearly sensitive to spatial and temporal sequence. The firing rates are elevated during the first spatial sequence 1 and temporal sequences 1,3,4 and 5 (Figure 15 C, left and right ordinate axes), and are unlikely to be caused by neuronal variability alone.

We next show two examples in which serial order adjusted the gain of selectivity for direction or self-timed interval duration. Figure 16 shows a gain-like adjustment of direction selectivity by serial order; recall that this was the most common interaction from ANOVA 3i. Data aligned to the movement phase of the behavioral task; it shows a neuron that prefers movements to the left, especially during the third task segment. The effect of serial order on direction selectivity is consistent with a gain-like multiplicative factor; serial order boosts the activity during the third segment by a roughly equal percentage whether movements are in the preferred or non-preferred direction. The relationship between serial order and self-timed interval duration is shown in Figure 17; as serial order progresses from the first to third task segment, the magnitude of the neuronal activity associated with the 500 ms interval is enhanced, while the activity associated with the 1000 and 2000 ms intervals is diminished.

Figure 15. Neuronal Populations Tuned to Movement Parameters

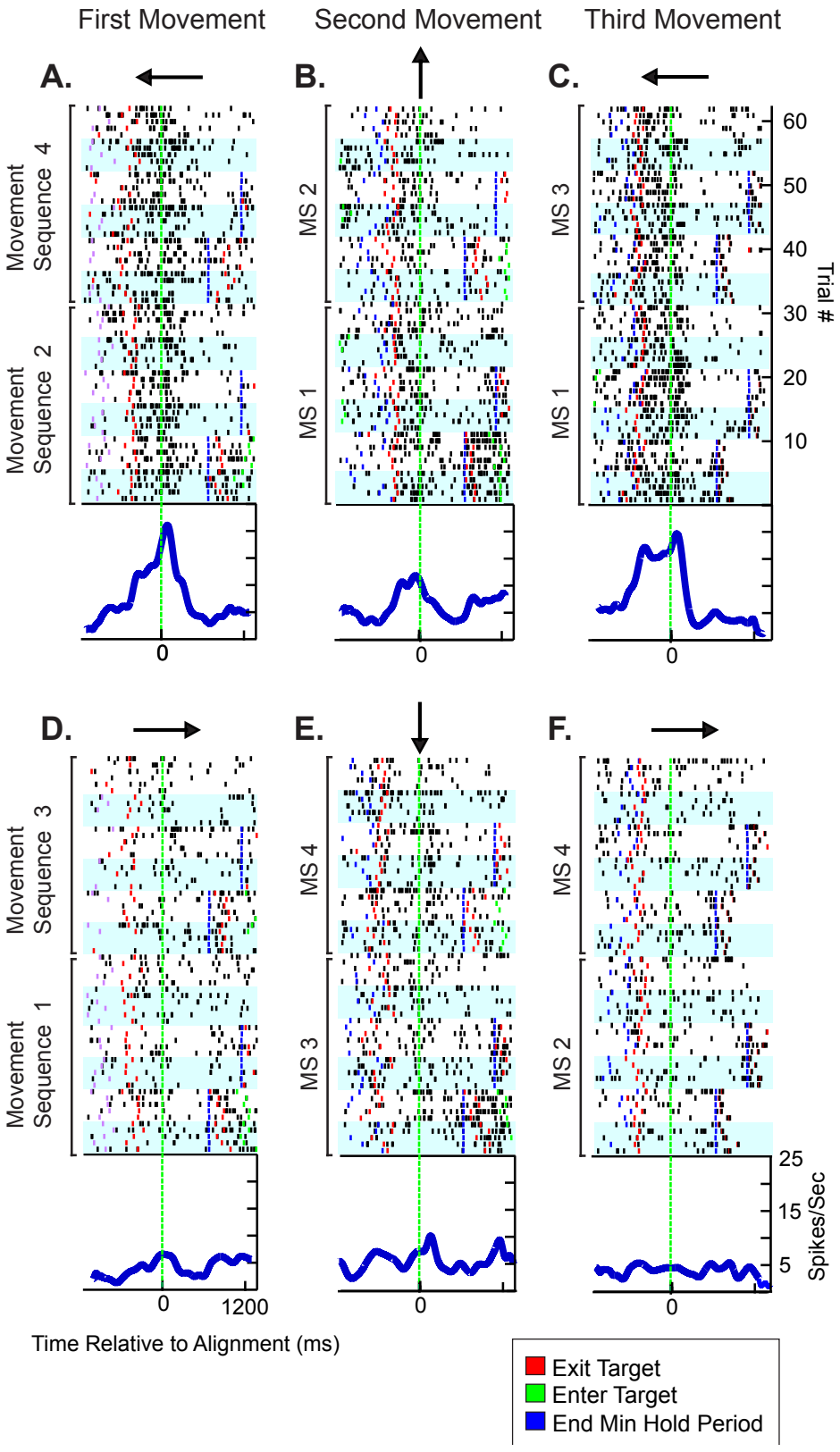

Figure 15. An example of directional selectivity after movement initiation. Raster displays and spike density functions from one cell in DLPFC illustrate neuronal activity that was highest during movements to the left (**A** & **C**), and moderate during upward movements (**B**). The vertical green line shows the alignment to the end of the movement, when the cursor entered the subsequent target. Neural activity selective for direction is consistent across serial order, particularly at the end of the movement after the target is entered.

Figure 16. An Example of Neuronal Activity that Illustrates Serial Order and Direction Dependent Gain Adjustment.

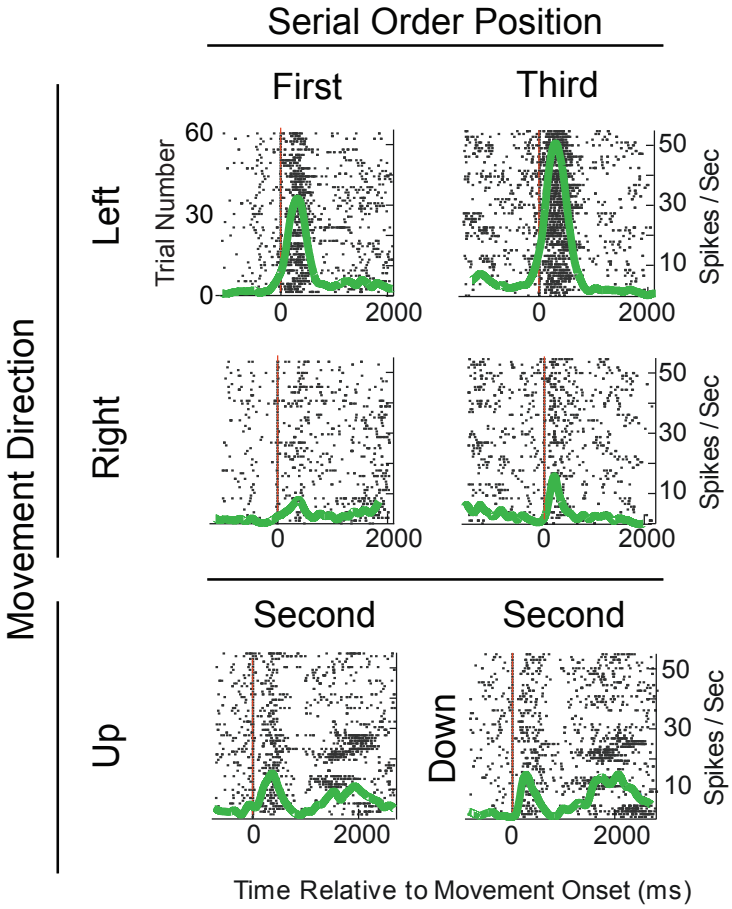

Legend. Raster plots and overlaid spike density functions depict neuronal activity whose discharge rate is strongly modulated by the direction and serial order of the movements of the cursor. Neuronal activity is aligned to the start of the movement. The vertical red line indicates the moment the cursor exits the previous target.

Figure 17. An Example of Neuronal Activity that Illustrates Serial Order and Duration Dependent Gain Adjustment.

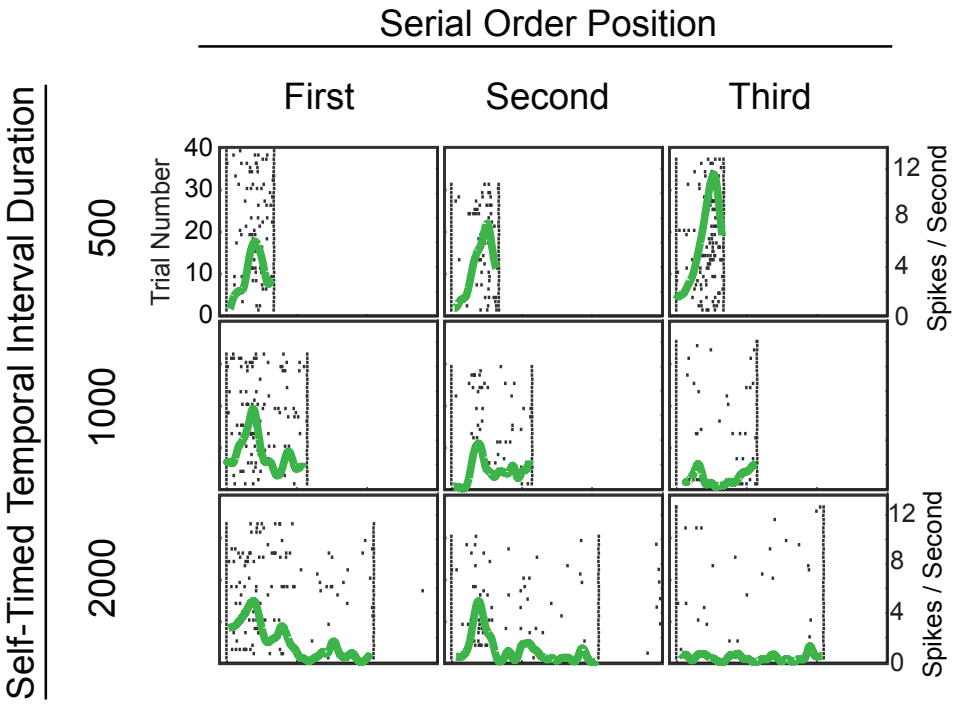

Legend. Raster plots and overlaid spike density functions depict neuronal activity whose discharge rate is strongly modulated by the duration and serial order of the self-timed temporal intervals. Neuronal activity is aligned to the beginning of the self-timed temporal intervals. Vertical dotted black lines indicate the beginning and the end of the instructed temporal intervals.

4.6: Measuring Mixed Selectivity Using Information Theory

We observed mixed selectivity for sequential movement parameters in dorso-lateral prefrontal cortex. We then modified the direct method of mutual information estimation to measure the information encoded by spike trains of this type. This analysis included four parallel computations using the same data that measured to information related to each of the three movement parameters direction, duration, and serial order (MI_{DIR}, MI_{DUR}, MI_{SO}), as well as the overall amount of information related to the three movement parameters and their interactions, (MI_{JOINT}) (Figure 18, Methods 2.7). As with the ANOVA analysis outlined above, all computations were performed using the average activity during the last 300ms of the movements and the first 300ms of the self-timed delays, beginning with the appearance of the duration cue. We sampled the neuronal activity by simply taking the firing rate for each trial from each epoch listed above, and report information estimates in bits. All reported information results were first corrected for positive bias twice, and then determined to be significantly greater than could be expected by chance ($P<0.05$, Methods 2.8). The computations were performed using custom code and the information breakdown toolbox (Magri, Whittingstall et al. 2009).

Figure 18. Information Theoretic Analysis: Individual and Joint Terms

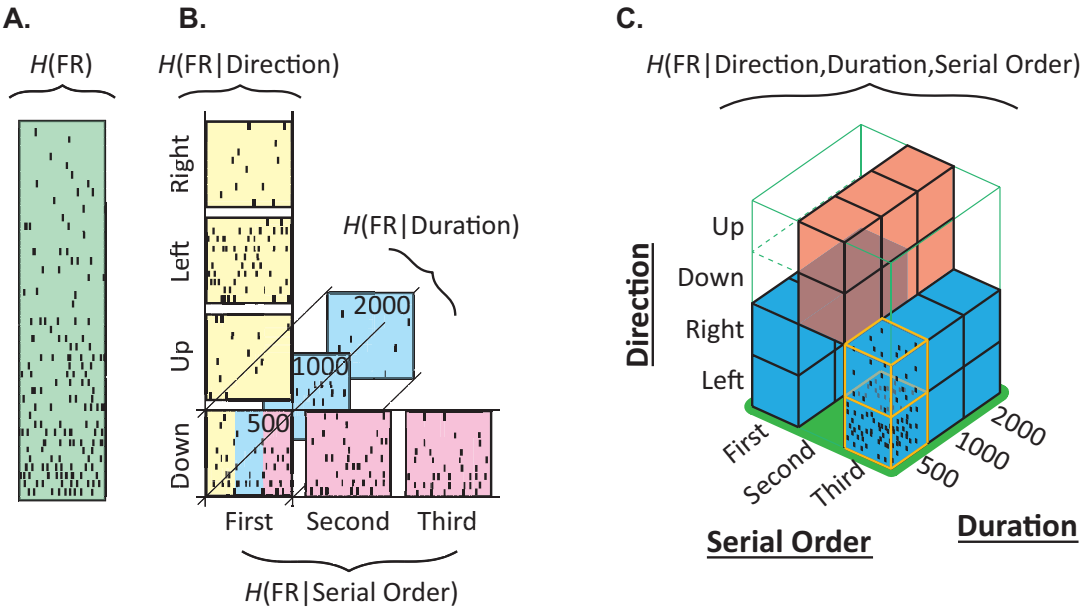

$MI_{\text{Direction}} = H(\text{FR}) - H(\text{FR} \mid \text{Direction})$
$MI_{\text{Duration}} = H(\text{FR}) - H(\text{FR} \mid \text{Duration})$
$MI_{\text{Serial Order}} = H(\text{FR}) - H(\text{FR} \mid \text{Serial Order})$

$MI_{\text{Joint}} = H(\text{FR}) - H(\text{F R} \mid \text{DIR,DUR,SO})$

Legend. These illustrations depict the methods used to sample the activity of single neurons and estimate the amount of transmitted mutual information that was related to three aspects of the behavior, movement direction, duration, and serial order. **A)** The raster plot depicts a hypothetical neuron that fires action potentials at various rates during some epoch of the behavior. The total entropy of these firing rates, $H(\text{FR})$, is directly related to the total number of different neuronal responses (we used firing rates exclusively) and represents the maximum amount of information that could be sent by the neuron. **B)** This Illustration depicts three parallel samplings of the neural data in A, which enable separate measurement of the firing rate entropy related to each behavioral variable. The amount of mutual information related to behavioral parameter X (MI_X), is equal to the difference between the total entropy $H(\text{FR})$ and the entropy that remains given the possible states of parameter X, $H(\text{FR}|\text{X})$, the so-called 'noise entropy'. This method enables us to separately measure how much mutual information was encoded about each behavioral parameter. **C)** This illustration depicts the fourth sampling of the neural data, which was used to measure the joint mutual information, (MI_{Joint}). Joint information refers to the total information related to direction, duration, and serial order, including their interactions. The position of each cube in the matrix is dependent on each movement parameter. Because each cube contains some distribution of firing rates, the joint entropy of all three parameters may be calculated, $H(\text{FR}|\text{XYZ})$, and used to calculate the MI_{Joint}. ***Importantly***, in order to ensure the statistical independence of the three movement parameters and to enable fair comparison of the individual and joint terms, our results were generated without the data from second ordinal position.

Figure 19 shows an illustration of how neuronal activity dependent on the elemental movement parameters and their interactions is captured by the information theoretic analysis. Each cube (in each matrix) represents the average firing rate during 1 of the 18 possible task states specified by the three movement parameters (Methods 2.7). The average activity across either the vertical, horizontal, or z-axis plane illustrates selectivity related to a single movement parameter. The horizontal plane at the top of each matrix represents firing rates during upward movements; and contains the highest activity levels. Comparison of the four horizontal planes illustrates graded activity related to movement direction. The independent parameter terms (MI_{DIR}, MI_{DUR}, MI_{SO}) are designed to measure the information contained in neuronal selectivity of this type. The average activity of the example neuron in Figure 19 was also dependent on the interactions between the movement parameters. By looking at the single cubes within each matrix, one can see that the neuronal activity was modulated in concert with the state of all three elemental movement parameters. For instance, in panel B, during the first self-timed temporal interval, the average response was greatest following leftward movements. Further, still during the first self-timed interval and following leftward movements, graded activity increases from a minimum during the 500 ms delay interval to a maximum during the 2000 ms delay interval. Thus, for some neurons, response variability within one state of one parameter (e.g. first) encodes the state of one or both of the other two parameters (e.g. left, 2000ms). This means that the variability in the activity of some directionally selective neurons is not noise, it in fact encodes serial order or temporal interval duration or both. The Joint term (MI_{JOINT}) is designed to measure the information contained in any neuronal selectivity that appears as a pattern in this matrix.

Figure 19. An Example of Average Neuronal Activity Selective for Multiple Parameters as Captured by the Joint Term.

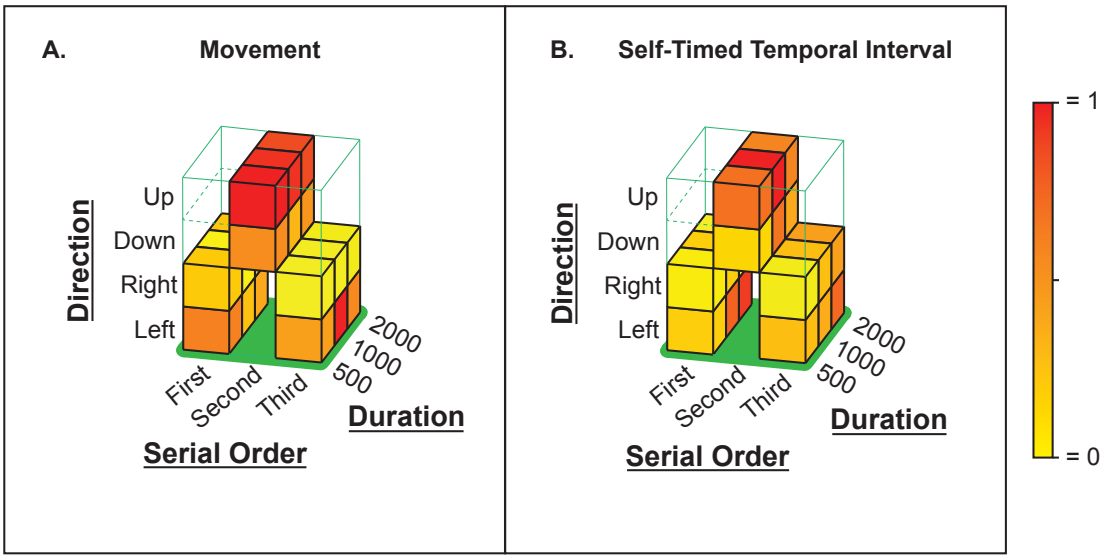

Legend. The average activity of a single neuron that was dependent on direction, duration, and serial order, is shown by a color-coded illustration of the joint term matrix. **A**. Normalized average activity matrix for one neuron during the last 300 ms of the three movement epochs. **B**. Normalized average activity matrix for the same neuron during 300 ms of the self-timed temporal interval epochs, beginning with the appearance of the duration cue. Matrices were colored according to the normalized average firing rate. See Methods for additional details related to the construction of the joint input matrix, which was not normalized and excluded the second serial order position.

Figure 20 summarizes the magnitude and prevalence of task related mutual information transmitted by single neurons during two epochs of the behavior. Significant information related to each term is shown separately for neurons in each monkey during both the movement and the self-timed delay epochs of the task. Significance was determined separately for each of the four terms (Methods 2.8). Cells that simultaneously encoded multiple movement parameters better than chance contributed to more than one distribution. Bits are a $\log_2$ unit, thus the distributions of information magnitudes shown are characteristically skewed. We found that the amount of MI_{JOINT} was significantly different from the three single parameter results (paired Kolmogorov-Smirnov test, $p < .05$). This is to be expected, as the Joint term quantifies information related to all three parameters. We found that the direction information distribution was significantly different from both the duration and serial order information distributions during the movement epoch for monkey 1. We also found that the duration distribution was significantly different from the direction and serial order distributions during the self-timed delay epoch, again for monkey 2 only.

Figure 20: Mutual information related to three statistically independent movement parameters. Boxplots illustrate separate distributions of mutual information (bits) related to the direction, duration, serial order, or joint direction-duration-serial order terms. Information was estimated from the discharge rates of single neurons; each population of neurons comprises all the neurons that encoded significantly more mutual information than would be expected by chance (see Methods for greater detail). Horizontal red lines represent the median, boxes represent the interquartile range, whiskers represent the 5%—25% and 75%—95% ranges, and red crosses represent outliers. **A**&**B**. Results from the last 300 ms of the first and third movements (Methods) for non-human primate subjects 1 and 2. **C**&**D**. Results from a 300 ms epoch beginning with the appearance of the duration cue in the first and third self-timed temporal interval targets for NHP subjects 1 and 2.

Figure 20. Simultaneous Representations of Direction, Duration, and Serial Order.

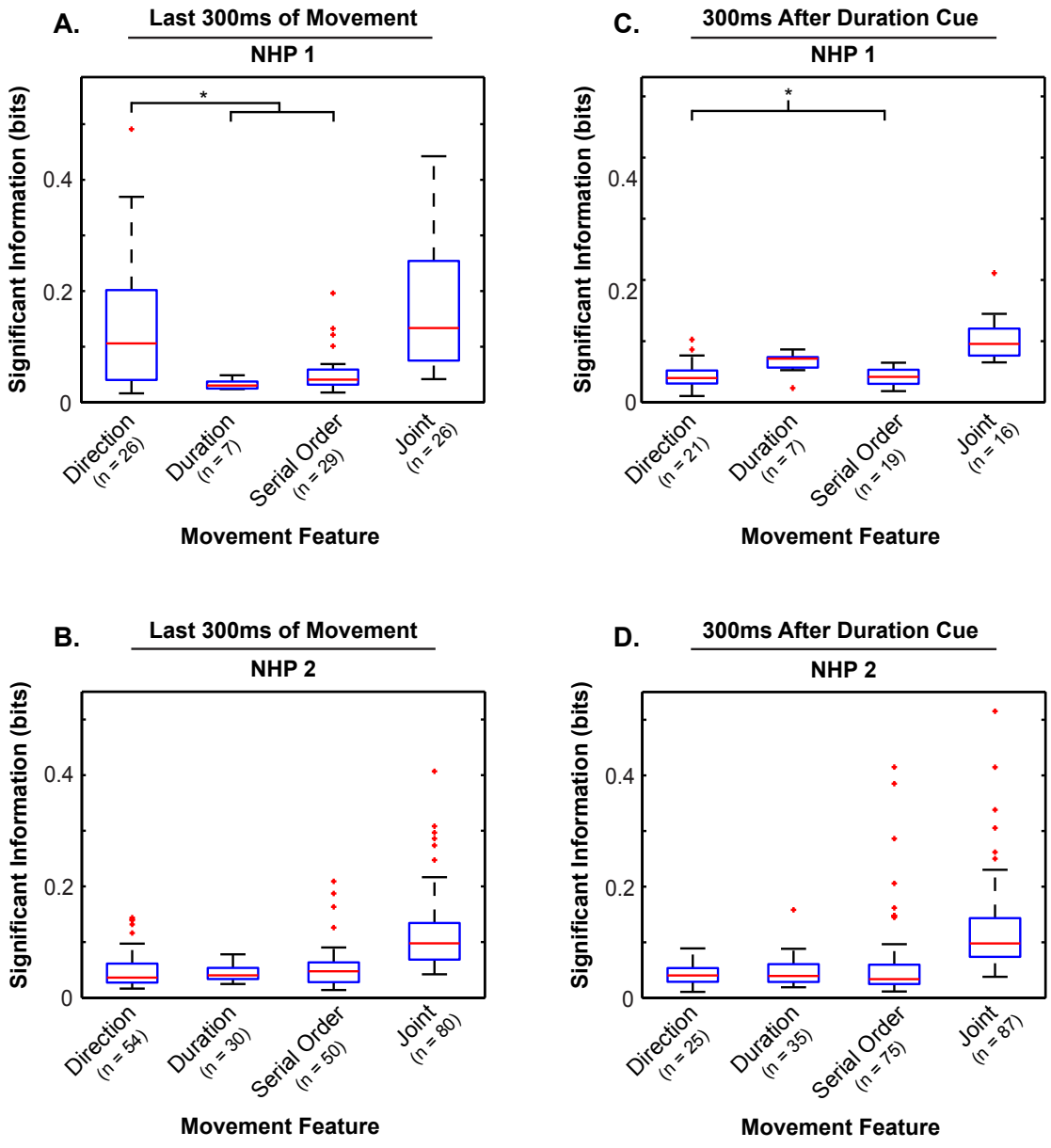

4.7: Proportion of Neural Bandwidth Used For Individual and Joint Movement Parameter Representations.

Next, we explored the relation between the total parameter information and the three movement parameter fractions. Importantly, we left the second serial order position out of the information theoretic analysis in order to calculate the information exclusively related to each single parameter, which we refer to as *independent* information (Figure 18, Methods 2.7). The difference between the joint information and the sum of the three independent terms is equal to the *synergistic* information. Synergistic information is simultaneously related to the state of more than one parameter and cannot reduce ones uncertainty about the state of any isolated parameter, and is derived from dependencies between the elemental parameters created by the movement sequences. Synergistic information may be found by this subtraction provided that there is no influence from experimental or 'real-world' correlations between the parameters, such as would be created by using terms such as force and acceleration. Any deterministic relationship between the elemental parameters will introduce redundant information, which inflates the Joint information but not the independent fractions, and so interferes with a simple calculation of the synergy. Figure 19 also serves as an illustration of our method to separate the information related to the independent movement parameters from the information related to their interactions. By subtracting the sum of the information resolved only by the x, y, & z axes (i.e. the independent movement parameter terms) from the information resolved by the whole matrix (i.e. the joint term), we were able to separate the synergistic information from the independently encoded movement parameter information. Unlike this illustration, the computations we employed do not use average activity; the firing rate variability from trial-to-trial is critical for mutual information estimates.

Figure 21. Independent and Synergistic Encoding of Direction, Duration, and Serial Order.

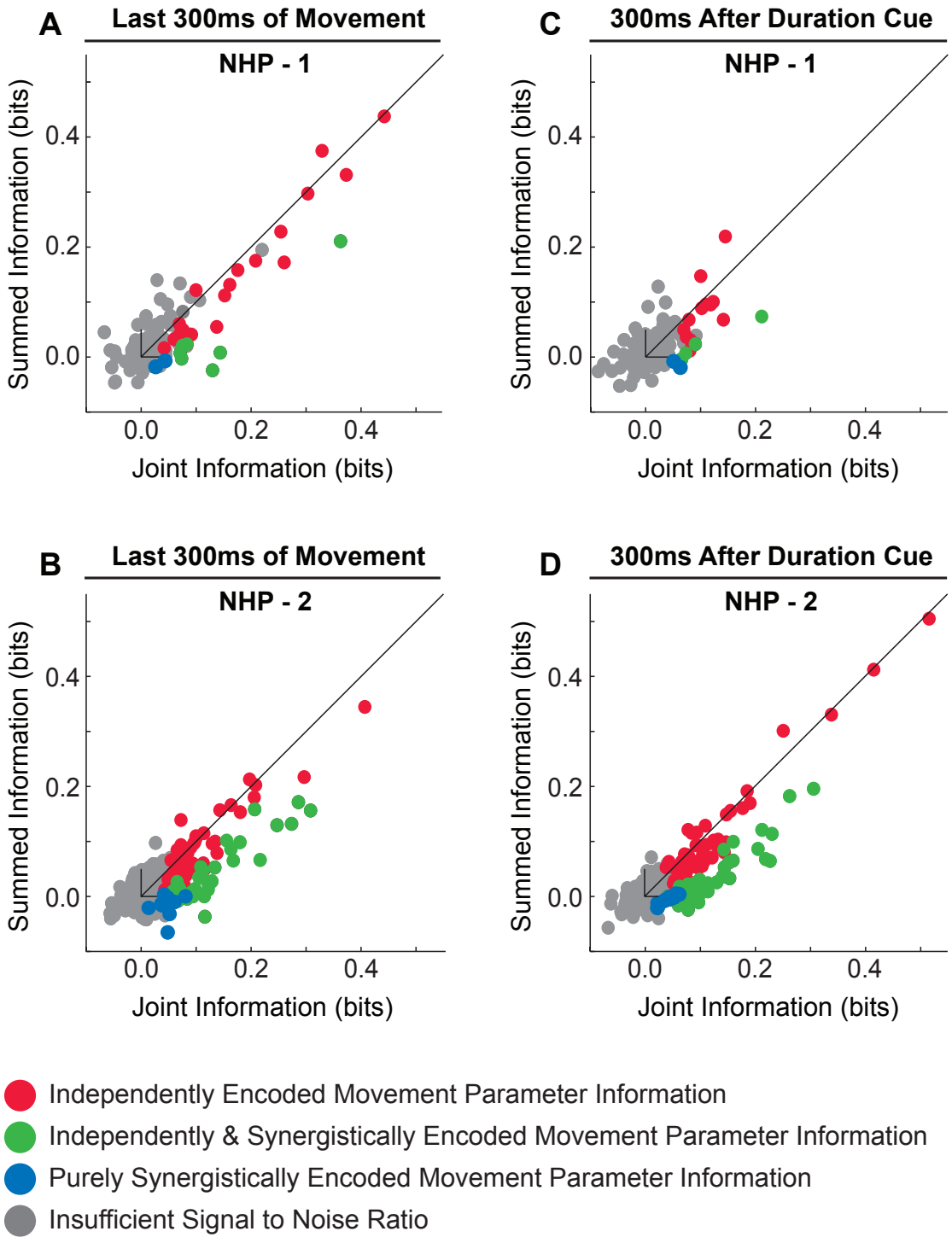

The scatterplots in Figure 21 illustrate information estimates with and without sequence-based interactions among the parameter terms. We did not observe redundant information, instead, we found that all the cells that carried statistically significant joint information, shown in red and green, lie along or below unity. Cells shown in red transmitted information about one or more movement parameters simultaneously and independently. We also found large amounts of synergistically encoded information, indicated by the distance of a dot below unity. Green dots represent neurons that encoded more synergistic information than would be expected by chance ($P < 0.05$, Methods 2.8). We found that the amount of synergy did not appear to depend on the total amount of information encoded. This can be seen in the population of green cells, they lie in a linear orientation parallel to the line of unity. If synergy varied as a function of information magnitude then the slope of the green dots especially, and also the red, would have deviated from 1. Red dots that lie above the line reflect inherent noise in the information-estimation procedure, rather than the presence of redundancy. Gray dots in Figure 21 represent neurons that did not transmit statistically significant joint information. These cells do not encode the movement parameters well, and their positions reflect noise in both the signal and the analysis (see page 118). The gray dots lie in a cloud around the point (0,0), negative data points are caused by our stringent positive bias correction, information estimates are greater than or equal to zero (Methods 2.6, 2.8).

Figure 21: **Independent and Synergistic Encoding of Direction, Duration and Serial Order.** Scatterplots depict the amount of information (bits) resolved by the joint term (MI_{Joint}) on the abscissa, and the sum of the direction, duration and serial order terms (MI_{SUM}) on the ordinate. Each dot represents the results from one neuron. Red dots indicate the MI_{Joint} was significantly greater than would be expected by chance. Green dots indicate that the amount of MI_{Joint} and synergistically encoded movement parameter information were greater than chance. Blue dots indicate the presence of significant synergy but lack significant MI_{Joint}. Gray dots indicate MI_{Joint} was not significant. Diagonal black lines represent unity. **A**&**B**. Results from the movement epochs. **C**&**D**. Results from the self-timed temporal interval epochs.

In this analysis, redundant information greater than our measurement error is not possible. Redundant information occurs if the sum of the independent terms is greater that the joint term. This does not occur because any direction information will contribute to the MI_{DIR} and MI_{JOINT} equally, except that MI_{JOINT} will be able to resolve any interactions involving direction. The same is true for duration and serial order. Thus, overall MI_{JOINT} cannot really be smaller than the sum of the independent terms: $MI_{DIR,}$ MI_{DUR}, MI_{SO}. Redundant information is excluded because the independent terms are truly statistically independent. A population of neurons may transmit redundant information about some stimulus (Reich, Mechler et al. 2001), or a single neuron could transmit redundant information about statistically dependent variables, such as whether or not a stop sign is octagonal or red, but a single neuron cannot transmit redundant information about two statistically independent variables. We measured the uncertainty in our MI estimates by plotting 95% confidence intervals (made using the shuffled-data MI distributions) on each point in Figure 21, and found that the uncertainty for each point above the unity line stretched well below the unity line (data not shown). (for further discussion see Methods 2.7, (Reich, Mechler et al. 2001, Panzeri, Senatore et al. 2007))

We next examined the relative neuronal sensitivity to the movement parameters by plotting the fractional breakdown of the total information for each cell. Figure 22 shows the synergistic (MI_{SYN}) and independent fractions (MI_{SUM}, MI_{DIR}, MI_{DUR}, and MI_{SO}) of the total movement parameter information (MI_{TOTAL}) for single neurons. In each panel neurons were sorted from left to right according to the proportion of their total information that was encoded independently. We found that the relative size of the independent information fractions varied as a function of task epoch. As we would expect, the information related to movement direction, shown in cyan, occupies the greatest fraction of the independent information during the movement epoch, shown in Figure 22, A and B. One can see that the cyan area is diminished in the self-timed delay epoch. The

proportions of independent serial order and duration information are largest during the self-timed duration epoch.

We found that about half of the neurons encoded more than 50% of their parameter information independently, and about half of the neurons encoded more than 50% of their parameter information synergistically. This finding is depicted by the white line, which represents the sum of the independent fractions; it runs diagonally across each panel from a value of 1 to a value of 0 and passes near to the center. The green area above the line represents the synergistically encoded information. The area below the white line represents the independently encoded portion. We found that 26% and 22% of the neurons in monkeys 1 and 2 independently encoded greater than 90% of their transmitted information during behavior. These cells are found on the far left of each panel in Figure 22. This result is possible if the parameters are encoded without cross talk or interference, as if they are in three separate channels. At the other extreme, about 14% and 9% of the cells synergistically encoded more than 90% or their transmitted information.

We did not find that the number of parameters encoded by individual neurons varies as a function of the percent bandwidth devoted to synergy. Neurons that represented one, two, or three parameters were not more likely to form clusters according to the percentage of their signal devoted to synergy. For neurons that mainly encoded one parameter in their independent portion, the parameter type did not vary as a function of the percent synergy. We also did not find that the percent synergy predicted which parameters might be encoded. For example, within any single panel of Figure 22, the proportion of the independent information related to direction did not vary as a function of the percent synergy.

Figure 22. Independent and Synergistic Fractions of the Total Information

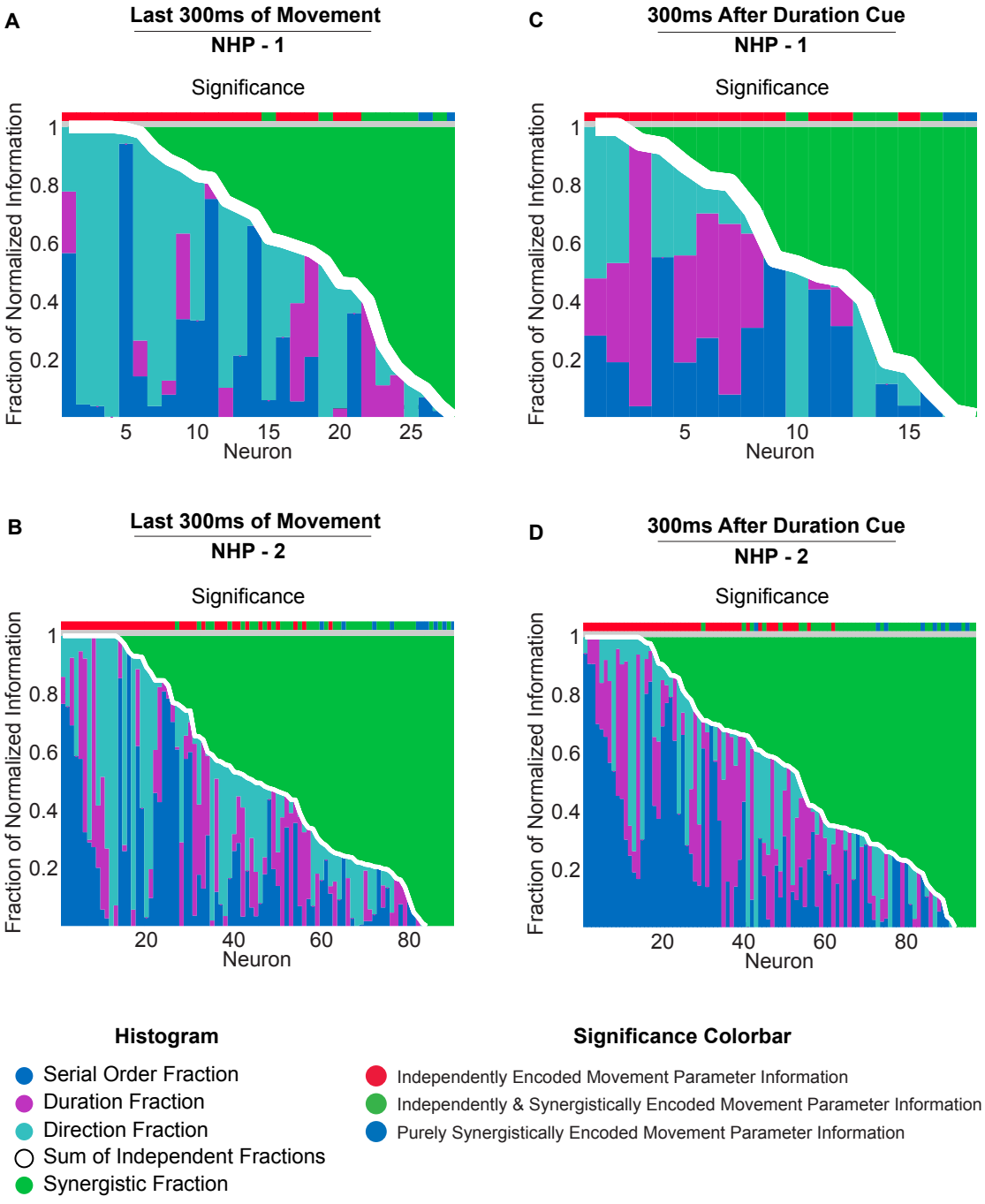

Legend: Normalized cumulative histograms plot the MI_{SO}, MI_{DUR}, and MI_{DIR} as fractions of the MI_{TOTAL} for each neuron with significant joint or synergistic information. Plots illustrate that the percent synergy varies continuously from 100 to 0 across the population, and that the differential composition of the independent portions between the two task epochs.

4.8: Discussion of Synergistic Encoding of Temporal Sequence Information in Monkey Dorso-Lateral Prefrontal Cortex.

In Chapter 4 our analysis focused on neuronal activity related to the direction of movement and the length of the self-timed delay intervals at each ordinal position in the sequential behavior, and yielded five principle findings. Our primary observation was of broadly tuned neuronal selectivity for the three elemental movement parameters during the execution of the behavior, in contrast to more abstract selectivity for sequences categories or goal positions. Second, we found that variability in activity related to single parameters reflected additional selectivity to other movement parameters, notably serial order. Third, using an information theoretic analysis we showed that neurons in DLPFC transmitted information related to direction, duration, and serial order independently, as if in three separate channels. Fourth, We found that the mixed selectivity for the movement parameters resulted in a separate fraction of synergistically encoded information that was related to the spatio-temporal sequences in as many as 40% of the neurons. Finally, we found that the synergistic fraction of the total parameter information varied continuously across the population of recorded neurons, between zero and 100 percent synergy.

Single neurons in the PFC are highly adaptive to behavioral variables, and may represent them via mixed selectivity. We found that broadly tuned neurons in DLPFC transmitted a signal that simultaneously and separately encoded movement parameters and their contextual relationships during a complex, timed sequential behavior. This unified representation of the behavior originated in the mixed selectivity of neurons in DLPFC, and should enable downstream targets to operate on the behavioral elements to which they are tuned as well as integrate them with the rest of the behavior. Thus, we believe that mixed selectivity is not only a product of the widely distributed connections and associative processing within PFC, but also important for encoding a signal sufficient to provide top-down coordination of complex behaviors.

4.9: Preferred Parameter Spike Density Functions

We found neural populations preferentially tuned to each of three elemental movement parameters. For example, a directionally tuned neuron may fire more spikes before and during all movements, but its peak firing rate amplitude will be highest for movement in its 'preferred' direction. Movements in a direction near to the preferred one will have an intermediate firing rate, and movements in the anti-preferred direction will have the lowest peak firing rate, or in some cases a firing rate below baseline. We did not explicitly test for cosine tuning, its existence is well known and not central to our results.

Within Figure 13, a single level of direction includes firing rates associated with all levels of duration and all levels of serial order. However, the movement directions up and down only occur in the second serial order position. We have not controlled for this correlation in these population spike density functions. To execute the information theoretic analysis described below we took great care to exclude this experimental correlations as it would be a source of redundant information.

4.10.1: Information Theoretic Analysis: The Effects of Epoch Width on the Sampling of Neuronal Activity Modulations

Our results were obtained using the firing rates obtained during 300ms wide epochs. In unpublished observations, we found that epoch width was not a strong predictor of the amount of encoded information. Epochs of 100 ms in width typically resolved more than 50% of the information resolved by epochs 600 ms in width. Epoch placement, however, was very important. If a bin of any size (greater than ~50 or 100 ms) encompasses the right moment in time, then it will resolve the information encoded there well. This is because neurons in DLPFC tended to be most highly modulated at precise and reliable moments during the behavior; but between neurons we observed great heterogeneity in when that moment happened to be. (As described in detail in the results above,

we also observed great heterogeneity in the preferences of cells for certain combinations of the movement parameters.) Thus, the most important difference between narrow and wide epochs was the likelihood that they contained the moment when a particular cell was most highly modulated.

We chose to use 300 ms wide sampling epochs because this was the largest size still compatible with the time scales of movement during the behavioral task (90% of the cursor movements during the task were between 300 and 600 ms in duration). Correct performance on the shortest self-timed delay required that movements be made between 475 ms and 950 ms after the appearance of the duration cue. Thus, using a window more than 300 ms wide was more likely to confound the interpretation of the results by including features of behavior beyond those of interest in a particular epoch; for example, delay timing during what was supposed to be a movement, or movement planning during was supposed to be a self-timed delay period.

4.10.2: Information Theoretic Analysis: Information Estimates as Minima

The mutual information estimates reported here are the minimum amounts of information that neurons in the DLPFC could have transmitted about the behavior. In fact, information estimates from any neuroscience experiment should be treated as minima. This is because information theory cannot be used to recover information that isn't there, and given that whatever information *is* recovered from the brain is done using many assumptions and very limited data, there must be at least that much information actually encoded, and in all likelihood, there is more. For instance, our analysis is based on the independent movement parameters direction, duration, and serial order; and will be blind to any aspects of the behavior that are not captured by these parameters (or their conjunctions). Secondly, we chose to use a rate code as a simple place to begin, but not in any way to preclude other metrics by which neuronal action potentials may be used to transmit information.

Another reason that information theoretic results should be regarded as minima is related to the estimation process itself. Information theory was developed to measure information transmitted through man-made communication channels, in which the probabilities of all possible output states given all possible input states can be known, either *a priori* or through collection of very large amounts of data (Shannon 1948). During actual biological experiments data are limited. Thus the probability distributions for the set of neural responses, and the set of neural responses given each stimulus, must be estimated (Borst and Theunisson 1999, Panzeri, Senatore et al. 2007, Quian Quiroga and Panzeri 2009, Rolls and Treves 2011). Because the set of neural responses during each stimulus (or movement in our case) is necessarily more under-sampled than the total set of neural responses, information estimates can become positively biased. Rigorous correction of the positive bias is necessary, but the result is that the neuron may encode more information than we can resolve without risk of an overly optimistic estimate.

Rigorous study has shown that most of the information neurons encode can be found in their firing rates (Rolls and Treves 2011). This is corroborated by experimental studies that have made only incremental improvements to neuronal information estimates by incorporating spike timing and other more specialized codes (Chase and Young 2006, Victor and Purpura 2010). Therefore, minimum mutual information estimates based on a rate code serve as a useful quantification that can be used to compare different encoding schemes. The comparison of different encoding schemes forms the basis for our modification of the direct method; we determined the synergistic portion of the information by comparing the sum of separate calculations of three independent terms to the value of a joint term incorporating all three. As described in the methods, uniform discretization of the responses ensured that all four terms were set on a level playing field prior to our comparison.

4.10.3: Information Theoretic Analysis: Elemental Parameters and Synergy

We used mutual information as a metric for the relative neuronal sensitivity to direction, duration, and serial order during movement sequences. The results of the information theoretic analysis support our assumption that these terms are indivisible and sufficient to capture all the sequential information encoded by the neurons. Many of the neurons that we recorded from in DLPFC encoded information related to the direction, duration, and serial order terms without a significant synergistic component, and are shown in red in Figures 21 and 22. The prevalence of these 'independent' encoders is evidence of the validity of these variables as elemental parameters. This is because if neurons in DLPFC were primarily concerned with more differentiated parameters, such as position, the movement parameters we chose would not have resolved much information. For instance, because the direction and duration especially, as well as ordinal position, were presented at many positions on the screen, then these terms would either fail to resolve neuronal selectivity related to cursor position, or possibly turn some up in the synergistic fraction. Secondly, if more abstract movement parameters were principally encoded by many neurons, such as trial type, spatial sequence, or goal positions, then that selectivity would be best resolved by the joint term, and would show up as synergy. We certainly observed synergistic encoding, but about half of the neurons with significant task-related information were independent encoders, and so we would not expect to find that much independently encoded direction, duration, and serial order information if more abstract movement parameters were a primary component of the neural signals we observed. In addition, more abstract sequential or goal selective activity should have been visible in the rasters and spike density functions plotted in Figures 4 through 8 and 15 through 17. Because we find the direction, duration, and serial order terms to provide a believable basis for neuronal encoding of the sequential behavior, and because synergistically encoded movement parameter information was observed in about half of the neurons with significant task related information, we are convinced that synergy is a realistic

description of how DLPFC encoded the sequential context that links the elemental parameters.

We did not see evidence that the size of the synergistic information fraction was related to how many single parameters were encoded by a single cell, seen in Figure 22. In the decerebrate cat inferior colliculus, synergistic information related to auditory stimuli was maximal when neurons encoded multiple acoustic cues (Chase and Young 2005). This was interpreted to reflect the inefficiency in encoding multiple cues with a rate code. The fact that we did not observe that the synergistic information percentage is influenced by either the identity or number of movement parameters encoded, combined with our observation that the percent of the total information that was synergistic varied as a continuous function from zero to one hundred percent, suggested to us that the presence of synergy is not related to a neuronal inability to multiplex movement parameters in a rate code. Rather, we suspect that the movement sequences were encoded by successful multiplexing of four information channels, three independent parameters and one synergistic channel relating them all.

4.11: Comparison to the Most Relevant Previous Literature.

The analytical approach of Reich et al. (2001) inspired our breakdown of neuronal information into separate fractions related to individual movement parameters and their synergistic interactions. We next revisit their findings and some others, and then consider the implications of our results in light of this previous literature. Reich et al. recorded neuronal responses in macaque V1 during the presentation of visual stimuli defined by two visual features, contrast and spatio-temporal sequence (Reich, Mechler et al. 2001). The authors found that V1 neurons encoded the stimulus features independently and simultaneously. The authors also found that a fraction of the total information transmitted about contrast and spatio-temporal pattern could not be unambiguously assigned to either category. We have termed this fraction of the

information, here related to the interaction between contrast and spatio-temporal pattern, synergistic, and have suggested that it may serve to enable combination of these features in downstream neural processing.

Chase and Young (Chase and Young 2005) investigated neuronal responses to auditory localization cues in the inferior colliculus (IC) of decerebrated cats. Using a similar information theoretic analysis, the authors found that IC neurons encoded the auditory stimulus cues independently and simultaneously. They also found that although the overt neuronal responses appeared to support unique differential sensitivity for the localization cues, the transmitted information did not. Neither the absolute nor relative amounts of information separately encoded about the localization cues could be used to discriminate between the three cell types. The authors next investigated whether the addition of a spike timing code could eliminate the synergistically encoded portion of the information (Chase and Young 2006). They found that incorporating spike timing improved the information recovered about two of the three cues, but did not eliminate the fraction of information not attributable to a single cue type.

(Nishikawa, Okada et al. 2008) approached the issue of encoding movement sequences in the anesthetized zebra finch brain, and have reported results similar to our own. They recorded from neurons in premotor nucleus HVC, while anesthetized birds listened to permutations of pairs of their own song syllables. The authors observed broad neuronal tuning to these short sequences, even to syllable pairs the animals never actual sang. They also found both independently and synergistically encoded information related to the syllable pairs.

In addition to our own, we interpret these results to indicate that synergy is a real facet of neural information processing, rather than a consequence of less than ideal measurement of either neural information transmission by our experiments, or stimulus measurement by single neurons in the brain. We have suggested that

the synergistically encoded information fraction may help downstream targets coordinate the signal's independent aspects. In relation to our information theoretic analysis; direction, duration, and serial order are statistically independent and sufficient to specify the entire behavior, and so the synergistically encoded fraction related to their dependent interactions are related to the movement sequences, the context in which each parameter may be specified.

4.12: Conclusion: Synergistic Encoding of Temporal Sequence Information Based on Mixed Selectivity in Monkey Dorso-Lateral Prefrontal Cortex.

The dorsolateral prefrontal cortex represents the goals of action, including sequences, sets, and categories of both high-dimensional and abstract goals. DLPFC is able to assemble these goals thought associative processing that combines the incoming dorsal visual stream, which provides information about space, time, and order, with intrinsic connections to orbitofrontal and medial PFC, which encode recent outcomes and rewards, sensory context, and motivational state. DLPFC is then able to contribute towards the achievement of action goals through connections with the medial and lateral premotor cortices and movement planning areas in the posterior parietal cortex. We found that during the spatio-temporal sequence task, neurons in DLPFC represented movement goals in a manner best described as the high-dimensional conjunction of abstract movement parameters. Before the sequential movements began, neuronal activity signaled which of the 24 possible movement sequences the animal should perform; while during the execution of the movement sequences, neuronal activity in DLPFC simultaneously encoded the direction, duration, and serial order of each movement. The neuronal activity that we recorded displayed nonlinear sensitivity to the three movement parameters, which produced the observed simultaneous joint representation of the movement parameters. Because these three elemental parameters are sufficient to reconstitute the full behavior, especially in conjunction with the synergistic component of the signal, which encodes the interactions between the parameters, we conclude that the movement goal signal transmitted by DLPFC seems ideally suited for translation into movement metrics by pre-motor areas. The premotor area's Pre-SMA and SMA are known to encode both serial order and specific transitions during sequential movements, and so seem ideally suited to receive and implement this goal signal.

4.13.1: Overview: Timed Movement Sequences and Macaque DLPFC

In this thesis I have provided a general introduction to the anatomy and physiology of the primate prefrontal cortex, and shown that the PFC is required for primates to behave in an intelligent, well-organized manner. I have provided short reviews of the neural control of interval timing and sequential movements, each with a focus on neurophysiology performed in non-human primates, and the special contributions made by neurons in the dorsolateral prefrontal cortex. I have also provided an introduction to using mutual information to quantify the information contained in neuronal spike trains.

4.13.2: Summary of the Introduction

I have described what is known about the distributed neural mechanisms of interval timing, and how they enable humans and other animals to judge interval durations and produce timed movements in the range of hundreds to thousands of milliseconds. I hope I have convinced the reader that the conscious control subjects can exert over their interval timing seems to come at the price of precision, and with a requirement for sustained attention, especially for intervals greater than 1000 ms in duration.

I have also described the properties that define sequential behaviors, and paid particular attention to the contributions made by the DLPFC, Pre-SMA, and SMA. I hope to have convinced the reader that the DLPFC is importantly engaged in the control of movement sequences, especially at the level of goals, while the Pre-SMA and SMA have been shown to represent the actions that should occur in a sequence and their ordinal position.

In regards the DLPFC, above all else, I hope I have convinced the reader that the neurons therein are extremely adaptable, simultaneously sensitive to multiple features of their current behavioral context, and known to exhibit persistent firing during the recall and maintenance of information. I have reviewed the massively

parallel intrinsic and distributed reciprocal connections to the PFC, and how they sub-serve both the adaptability of the neurons located therein, and the distribution of top-down control from the PFC to other structures. I also hope I have convinced the reader that there is strong evidence for sustained, attention-directed bias signals that descend from the PFC and are able to entrain distant neural processes and thereby coordinate brain-wide activity.

I have reviewed the basic computations used to estimate the mutual information encoded in spike trains, as well as the preliminary considerations that should be taken to ensure an estimate is accurate, and more importantly, useful. I hope I have convinced the reader that mutual information is an appropriate metric for neural coding, especially in the case of nonlinear mixed selectivity by single neurons, which is an important aspect of neuronal activity in DLPFC and directly related to one of our primary results. I have also reviewed the small group of computational publications that set the stage for our own results.

4.13.3: Summary of the Experimental Results

In this thesis I have described the results of our experiments related to the neural control of actions during the spatio-temporal sequence task. Chapter 3 focused on the neuronal activity related to interval timing. We found that an incremental modulation of the discharge rate encoded the passage of time during the self-timed intervals. We also found that both the behavior and the neuronal activity were in accord with a scalar model of timing, in which the variability about the estimate grows linearly with the length of the estimated duration, as if measured with a rubber ruler. Our results extended the observations of previous publications with a description of phasic activity modulations that seem to initialize the timing process. Unlike many previous studies our task required subjects to produce the temporal intervals, and so this may have driven neurons in DLPFC to produce the ‘start’ signals.

In Chapter 4 our primary observation was of broad tuning and nonlinear mixed selectivity of single neurons in DLPFC for three elemental movement parameters during the execution of the behavior: the direction, duration, and ordinal position of individual movements during the spatio-temporal sequence task. We used an information theoretic analysis to show information related to direction, duration, and serial order was transmitted independently, as if in three separate channels, by single neurons in DLPFC. We also found that the nonlinear mixed selectivity resulted in a separate fraction of synergistically encoded information that was related to the interactions between the movement parameters and rooted in the spatio-temporal movement sequences themselves.

The dorsolateral prefrontal cortex links perception, goal selection, and attention to plan and prospectively encode actions. The role of the DLPFC is especially prominent when those actions must be performed after an intervening delay or in the face of other distractions. On the whole, our results indicate that activity in DLPFC seems related to the sustained attention required by this difficult task. During interval timing or sequential behaviors distraction can easily cause errors. Our first results section seems related to the decision and coordination processes related to timing, and might critically link the elements of the neural timer, namely the goal duration, the start signal, the passage of time during the interval, and the moment at which a movement had to be performed. Similarly, the simultaneous representation of the elemental movement parameters seems related to the decision and coordination processes related to the sequential aspects of the task. Our results suggest that during this complex task DLPFC is primarily recruited in order to provide organizational control by way of encoding the movement goals and the related passage of time.

In regards to the observed nonlinear mixed selectivity for movement parameters, it seems that synergy is a real facet of neural information processing, rather than a consequence of less than ideal measurement of either neural information

transmission by our experiments, or stimulus measurement by single neurons in the brain. We have suggested that the synergistically encoded information fraction may help downstream targets coordinate the signal's independent aspects.

REFERENCES

Averbeck, B. B., M. V. Chafee, D. A. Crowe and A. P. Georgopoulos (2002). "Parallel processing of serial movements in prefrontal cortex." Proc Natl Acad Sci U S A 99(20): 13172-13177.

Averbeck, B. B., P. E. Latham and A. Pouget (2006). "Neural correlations, population coding and computation." Nat Rev Neurosci 7(5): 358-366.

Averbeck, B. B. and D. Lee (2003). "Neural Noise and Movement-Related Codes in the Macaque Supplementary Motor Area." J Neurosci 23(20): 12.

Averbeck, B. B. and D. Lee (2007). "Prefrontal neural correlates of memory for sequences." J Neurosci 27(9): 2204-2211.

Averbeck, B. B., J. W. Sohn and D. Lee (2006). "Activity in prefrontal cortex during dynamic selection of action sequences." Nat Neurosci 9(2): 276-282.

Badre, D. (2008). "Cognitive control, hierarchy, and the rostro-caudal organization of the frontal lobes." Trends Cogn Sci 12(5): 193-200.

Barone, P. and J.-P. Joseph (1989). "Prefrontal cortex and spatial sequencing in macaque monkey." Experimental Brain Research 78(3): 447-464.

Borst, A. and F. E. Theunisson (1999). "Information theory and neural coding." Nat Neurosci 2(11): 11.

Botvinick, M. M. (2007). "Multilevel structure in behaviour and in the brain: a model of Fuster's hierarchy." Philos Trans R Soc Lond B Biol Sci 362(1485): 1615-1626.

Botvinick, M. M. (2008). "Hierarchical models of behavior and prefrontal function." Trends Cogn Sci 12(5): 201-208.

Brody, C. D. (2003). "Timing and Neural Encoding of Somatosensory Parametric Working Memory in Macaque Prefrontal Cortex." Cerebral Cortex 13(11): 1196-1207.

Brown, T. G. (1914). "On the nature of the fundamental activity of the nervous centres; together with an analysis of the conditioning of rhythmic activity in progression, and a theory of the evolution of function in the nervous system." The Journal of Physiology 48(1): 18-46.

Buhusi, C. V. and W. H. Meck (2005). "What makes us tick? Functional and neural mechanisms of interval timing." Nat Rev Neurosci 6(10): 755-765.

Bullock, D. (2004). "Adaptive neural models of queuing and timing in fluent action." Trends Cogn Sci 8(9): 426-433.

Buonomano, D. V. and U. R. Karmarkar (2002). "Book Review: How Do We Tell Time?" The Neuroscientist 8(1): 42-51.

Buonomano, D. V. and R. Laje (2010). "Population clocks: motor timing with neural dynamics." Trends Cogn Sci 14(12): 520-527.

Buonomano, D. V. and W. Maass (2009). "State-dependent computations: spatiotemporal processing in cortical networks." Nat Rev Neurosci 10(2): 113-125.

Buonomano, D. V. and M. M. Merzenich (1995). "Temporal information transformed into a spatial code by a neural network with realistic properties." SCIENCE-NEW YORK THEN WASHINGTON-: 1028-1028.

Buschman, T. J. and E. K. Miller (2007). "Top-down versus bottom-up control of attention in the prefrontal and posterior parietal cortices." Science 315(5820): 1860-1862.

Carpenter, A. F., A. P. Georgopoulos and G. Pellizzer (1999). "Motor Cortical Encoding of Serial Order in a Context-Recall Task." Science 283(5408): 1752-1757.

Chase, S. M. and E. D. Young (2005). "Limited segregation of different types of sound localization information among classes of units in the inferior colliculus." J Neurosci 25(33): 7575-7585.

Chase, S. M. and E. D. Young (2006). "Spike-timing codes enhance the representation of multiple simultaneous sound-localization cues in the inferior colliculus." J Neurosci 26(15): 3889-3898.

Crammond, D. J. and J. F. Kalaska (2000). "Prior information in motor and premotor cortex: activity during the delay period and effect on pre-movement activity." Journal of Neurophysiology 84(2): 986-1005.

Duncan, J. (2001). "AN ADAPTIVE CODING MODEL OF NEURAL FUNCTION IN PREFRONTAL CORTEX." Nature Reviews 2: 10.

Fuster, J. M. (2001). "The Prefrontal Cortex—An Update: Time Is of the Essence." Neuron 30: 319-333.

Fuster, J. M., M. Bodner and J. K. Kroger (2000). "Cross-modal and cross-temporal association in neurons of frontal cortex." Nature 405.

Gabbiani, F., H. G. Krapp, C. Koch and G. Laurent (2002). "Multiplicative computation in a visual neuron sensitive to looming." Nature 420(6913): 320-324.

Genovesio, A., S. Tsujimoto and S. P. Wise (2006). "Neuronal activity related to elapsed time in prefrontal cortex." J Neurophysiol 95(5): 3281-3285.

Genovesio, A., S. Tsujimoto and S. P. Wise (2009). "Feature- and order-based timing representations in the frontal cortex." Neuron 63(2): 254-266.

Genovesio, A., S. Tsujimoto and S. P. Wise (2011). "Prefrontal cortex activity during the discrimination of relative distance." J Neurosci 31(11): 3968-3980.

Genovesio, A., S. Tsujimoto and S. P. Wise (2012). "Encoding goals but not abstract magnitude in the primate prefrontal cortex." Neuron 74(4): 656-662.

Gibbon, J., C. Malapani, D. L. Dale and C. R. Gallistel (1997). "Toward a neurobiology of temporal cognition: advances and challenges." Cog Neuro: 15.
Goldman-Rakic, P. (1995). "Cellular basis of working memory." Neuron 14(3): 477-485.

Grillner, S., P. Wallén, K. Saitoh, A. Kozlov and B. Robertson (2008). "Neural bases of goal-directed locomotion in vertebrates—an overview." Brain research reviews 57(1): 2-12.

Hoshi, E. and J. Tanji (2004). "Differential roles of neuronal activity in the supplementary and presupplementary motor areas: from information retrieval to motor planning and execution." J Neurophysiol 92(6): 3482-3499.

Ivry, R. B. and R. M. Spencer (2004). "The neural representation of time." Curr Opin Neurobiol 14(2): 225-232.

Janssen, P. and M. N. Shadlen (2005). "A representation of the hazard rate of elapsed time in macaque area LIP." Nat Neurosci 8(2): 234-241.

Jazayeri, M. and M. N. Shadlen (2010). "Temporal context calibrates interval timing." Nat Neurosci 13(8): 1020-1026.

Kim, J.-N. and M. N. Shadlen (1999). "Neural correlates of a decision in the dorsolateral prefrontal cortex of the macaque." Nature neuroscience 2(2): 176-185.

Koechlin, E., C. Ody and F. Kouneiher (2003). "The architecture of cognitive control in the human prefrontal cortex." Science 302(5648): 1181-1185.

Kojima, S. and P. S. Goldman-Rakic (1982). "Delay-related activity of prefrontal neurons in rhesus monkeys performing delayed response." Brain research 248(1): 43-50.

Lashley, K. S. (1951). "The Problem of Serial Order in Behavior."
Latham, P. E. and S. Nirenberg (2005). "Synergy, redundancy, and independence in population codes, revisited." The Journal of neuroscience 25(21): 5195-5206.

Lebedev, M. and S. Wise (2000). "Oscillations in the premotor cortex: single-unit activity from awake, behaving monkeys." Experimental brain research 130(2): 195-215.

Lebedev, M. A., A. Messinger, J. D. Kralik and S. P. Wise (2004). "Representation of attended versus remembered locations in prefrontal cortex." PLoS biology 2(11): e365.

Lebedev, M. A., J. E. O'Doherty and M. A. Nicolelis (2008). "Decoding of temporal intervals from cortical ensemble activity." J Neurophysiol 99(1): 166-186.

Leon, M. I. and M. N. Shadlen (2003). "Representation of Time by Neurons in the Posterior Parietal Cortex of the Macaque." neuron 38: 20.

Levy, R. and P. S. Goldman-Rakic (1999). "Association of storage and processing functions in the dorsolateral prefrontal cortex of the nonhuman primate." The Journal of neuroscience 19(12): 5149-5158.

Lewis, P. A. and R. C. Miall (2006). "Remembering the time: a continuous clock." Trends Cogn Sci 10(9): 401-406.

Lewis, P. A. and R. C. Miall (2009). "The precision of temporal judgement: milliseconds, many minutes, and beyond." Philos Trans R Soc Lond B Biol Sci 364(1525): 1897-1905.

Lucchetti, C. and L. Bon (2001). "Time-modulated neuronal activity in the premotor cortex of macaque monkeys." Experimental brain research 141(2): 254-260.

Lucchetti, C., A. Ulrici and L. Bon (2005). "Dorsal premotor areas of nonhuman primate: functional flexibility in time domain." Eur J Appl Physiol 95(2-3): 121-130.

Magri, C., K. Whittingstall, V. Singh, N. K. Logothetis and S. Panzeri (2009). "A toolbox for the fast information analysis of multiple-site LFP, EEG and spike train recordings." BMC Neurosci 10: 81.

Maimon, G. and J. A. Assad (2006). "A cognitive signal for the proactive timing of action in macaque LIP." Nat Neurosci 9(7): 948-955.

Maimon, G. and J. A. Assad (2006). "Parietal area 5 and the initiation of self-timed movements versus simple reactions." J Neurosci 26(9): 2487-2498.

Marder, E. and D. Bucher (2001). "Central pattern generators and the control of rhythmic movements." Current biology 11(23): R986-R996.

Matsuzaka, Y., H. Aizawa and J. Tanji (1992). "A Motor Area Rostra1 to the Supplementary Motor Area (Presupplementary Motor Area) in the Monkey: Neuronal Activity During a Learned Motor Task." J Neurophysiol 68(3): 10.

Mauk, M. D. and D. V. Buonomano (2004). "The neural basis of temporal processing." Annu Rev Neurosci 27: 307-340.

Mauritz, K.-H. and S. Wise (1986). "Premotor cortex of the rhesus monkey: neuronal activity in anticipation of predictable environmental events." Experimental Brain Research 61(2): 229-244.

Merchant, H., O. perez, W. Zarco and J. Gamez (2013). "Interval Tuning in the Primate Medial Premotor Cortex as a General Timing Mechanism." J Neurosci 33(21): 9082–9096.

Merchant, H., W. Zarco, O. perez and R. Bartolo (2012). "Measuring time with different neural chronometers during a synchronization-continuation task." Proc Natl Acad Sci U S A 108(49): 5.

Miller, E. K. and J. D. Cohen (2001). "AN INTEGRATIVE THEORY OF PREFRONTAL CORTEX FUNCTION." Annu Rev Neurosci 24: 167-202.

Miller, E. K., C. A. Erickson and R. Desimone (1996). "Neural mechanisms of visual working memory in prefrontal cortex of the macaque." The Journal of Neuroscience 16(16): 5154-5167.

Mita, A., H. Mushiake, K. Shima, Y. Matsuzaka and J. Tanji (2009). "Interval time coding by neurons in the presupplementary and supplementary motor areas." Nat Neurosci 12(4): 502-507.

Mushiake, H., M. Inase and J. Tanji (1990). "Selective coding of motor sequence in the supplementary motor area of the monkey cerebral cortex." Experimental Brain Research 82(1): 208-210.

Mushiake, H., N. Saito, K. Sakamoto, Y. Itoyama and J. Tanji (2006). "Activity in the lateral prefrontal cortex reflects multiple steps of future events in action plans." Neuron 50(4): 631-641.

Nakajima, T., R. Hosaka, H. Mushiake and J. Tanji (2009). "Covert representation of second-next movement in the pre-supplementary motor area of monkeys." J Neurophysiol 101(4): 1883-1889.

Nemenman, I., W. Bialek and R. de Ruyter van Steveninck (2004). "Entropy and information in neural spike trains: Progress on the sampling problem." Physical Review E 69(5).

Nieder, A. (2005). "Counting on neurons: the neurobiology of numerical competence." Nat Rev Neurosci 6(3): 177-190.

Niki, H. and M. Watanabe (1979). "Prefrontal and cingulate unit activity during timing behavior in the monkey." Brain research 171(2): 213-224.

Ninokura, Y., H. Mushiake and J. Tanji (2004). "Integration of temporal order and object information in the monkey lateral prefrontal cortex." J Neurophysiol 91(1): 555-560.

Nishikawa, J., M. Okada and K. Okanoya (2008). "Population coding of song element sequence in the Bengalese finch HVC." Eur J Neurosci 27(12): 3273-3283.

Ohmae, S., X. Lu, T. Takahashi, Y. Uchida and S. Kitazawa (2008). "Neuronal activity related to anticipated and elapsed time in macaque supplementary eye field." Exp Brain Res 184(4): 593-598.

Onoe, H., M. Komori, K. Onoe, H. Takechi, H. Tsukada and Y. Watanabe (2001). "Cortical networks recruited for time perception: a monkey positron emission tomography (PET) study." Neuroimage 13(1): 37-45.

Oshio, K. i., A. Chiba and M. Inase (2006). "Delay period activity of monkey prefrontal neurones during duration-discrimination task." European Journal of Neuroscience 23(10): 2779-2790.

Panzeri, S., R. Senatore, M. A. Montemurro and R. S. Petersen (2007). "Correcting for the sampling bias problem in spike train information measures." J Neurophysiol 98(3): 1064-1072.
Passingham, R. E. and S. P. Wise (2012). "The Neurobiology of the Prefrontal cortex: Anatomy, Evolution, and the Origin of Insight." Oxford University Press.

Paxinos, G., X.-F. Huang and A. W. Toga (1999). "The rhesus monkey brain in stereotaxic coordinates."

Pena, J. L. and M. Konishi (2001). "Auditory spatial receptive fields created by multiplication." Science 292(5515): 249-252.

Petrides, M. (1991). "Functional specialization within the dorsolateral frontal cortex for serial order memory." Proc Biol Sci 246(1317): 299-306.

Petrides, M. (2000). The role of the mid-dorsolateral prefrontal cortex in working memory. Executive Control and the Frontal Lobe: Current Issues, Springer: 44-54.

Petrides, M., B. Alivisatos and A. C. EvANs (1995). "Functional activation of the human ventrolateral frontal cortex during mnemonic retrieval of verbal information." Proceedings of the national academy of sciences 92(13): 5803-5807.

Quian Quiroga, R. and S. Panzeri (2009). "Extracting information from neuronal populations: information theory and decoding approaches." Nat Rev Neurosci 10(3): 173-185.

Quintana, J. and J. M. Fuster (1992). "Mnemonic and predictive functions of cortical neurons in a memory task." Neuroreport 3(8): 721-724.

Rainer, G. and E. K. Miller (2002). "Timecourse of object-related neural activity in the primate prefrontal cortex during a short-term memory task." European Journal of Neuroscience 15(7): 1244-1254.

Rammsayer, T. and W. Classen (1997). "Impaired Temporal Discrimination in Parkinson'sDisease: Temporal Processing of Brief Durations as an Indicator of Degeneration of Dopaminergic Neurons in the Basal Ganglia." Intern. J. Neuroscience 91(1-2): 45-55.

Rammsayer, T. and S. D. Lima (1991). "Duration discrimination of filled and empty auditory intervals: Cognitive and perceptual factors." Perception & Psychophysics 50(6): 565-574.

Rammsayer, T. and R. Ulrich (2005). "No evidence for qualitative differences in the processing of short and long temporal intervals." Acta Psychol (Amst) 120(2): 141-171.

Rammsayer, T. H. (1999). "Neuropharmacological evidence for different timing mechanisms in humans." Q J Exp Psychol B 52(3): 273-286.

**Reich, D. S., F. Mechler and J. D. Victor (2001). "Formal and Attribute-Specific Information in Primary
Visual Cortex." J Neurophysiol 85: 14.**

Reich, D. S., F. Mechler and J. D. Victor (2001). "Independent and redundant information in nearby cortical neurons." Science 294(5551): 2566-2568.

Rigotti, M., O. Barak, M. R. Warden, X.-J. Wang, N. D. Daw, E. K. Miller and S. Fusi (2013). "The importance of mixed selectivity in complex cognitive tasks." Nature.

Roesch, M. R. and C. R. Olson (2005). "Neuronal activity in primate orbitofrontal cortex reflects the value of time." Journal of Neurophysiology 94(4): 2457-2471.

Rolls, E. T. and A. Treves (2011). "The neuronal encoding of information in the brain." Prog Neurobiol 95(3): 448-490.

Romo, R. and W. Schultz (1987). "Neuronal activity preceding self-initiated or externally timed arm movements in area 6 of monkey cortex." Experimental brain research 67(3): 656-662.

Roux, F.-E., K. Boulanouar, J.-A. Lotterie, M. Mejdoubi, J. P. LeSage and I. Berry (2003). "Language functional magnetic resonance imaging in preoperative assessment of language areas: correlation with direct cortical stimulation." Neurosurgery 52(6): 1335-1347.

Saga, Y., M. Iba, J. Tanji and E. Hoshi (2011). "Development of multidimensional representations of task phases in the lateral prefrontal cortex." J Neurosci 31(29): 10648-10665.

Saito, N., H. Mushiake, K. Sakamoto, Y. Itoyama and J. Tanji (2005). "Representation of immediate and final behavioral goals in the monkey prefrontal cortex during an instructed delay period." Cereb Cortex 15(10): 1535-1546.

Sakamoto, K., H. Mushiake, N. Saito, K. Aihara, M. Yano and J. Tanji (2008). "Discharge synchrony during the transition of behavioral goal representations encoded by discharge rates of prefrontal neurons." Cereb Cortex 18(9): 2036-2045.

Sakurai, Y., S. Takahashi and M. Inoue (2004). "Stimulus duration in working memory is represented by neuronal activity in the monkey prefrontal cortex." European Journal of Neuroscience 20(4): 1069-1080.
Salinas, E. (2009). "Rank-order-selective neurons form a temporal basis set for the generation of motor sequences." J Neurosci 29(14): 4369-4380.

Schneider, B. A. and G. M. Ghose (2012). "Temporal production signals in parietal cortex." PLoS Biol 10(10): e1001413.

Shadlen, M. N. and W. T. Newsome (1998). "The Variable Discharge of Cortical Neurons: Implications for Connectivity, Computation, and Information Coding." J Neurosci 18(19): 27.

Shallice, T. (1982). "Specific impairments of planning." Philosophical Transactions of the Royal Society of London. B, Biological Sciences 298(1089): 199-209.

Shannon, C. E. (1948). "A Mathematical Theory of Communication." The Bell System Technical Journal 27: 55.

Shima, K., M. Isoda, H. Mushiake and J. Tanji (2007). "Categorization of behavioural sequences in the prefrontal cortex." Nature 445(7125): 315-318.

Shima, K. and J. Tanji (1998). "Both Supplementary and Presupplementary Motor Areas Are Crucial for the Temporal Organization of Multiple Movements." J Neurosci 80: 14.

Shima, K. and J. Tanji (2000). "Neuronal Activity in the Supplementary and Presupplementary Motor Areas for Temporal Organization of Multiple Movements." J Neurophysiol 84: 12.

Soechting, J. and M. Flanders (1992). "Moving in three-dimensional space: frames of reference, vectors, and coordinate systems." Annual review of neuroscience 15(1): 167-191.

Strong, S. P., R. R. de Ruyter van Steveninck and R. Koberle (1998). "On the Application of Information Theory to Neural Spike Trains." Phys. Rev. Lett 80.
Tanji, J. (2001). "SEQUENTIAL ORGANIZATION OF MULTIPLE MOVEMENTS: Involvement of Cortical Motor Areas." Annu Rev Neurosci 24(631): 20.

Tanji, J. and E. Hoshi (2008). "Role of the Lateral Prefrontal Cortex in Executive Behavioral Control." Physiol Rev 88: 20.

Tsujimoto, S. and T. Sawaguchi (2007). "Prediction of relative and absolute time of reward in monkey prefrontal neurons." Neuroreport 18(7): 703-707.
Vaadia, E., K. Kurata and S. P. Wise (1988). "Neuronal activity preceding directional and nondirectional cues in the premotor cortex of rhesus monkeys." Somatosensory & motor research 6(2): 207-230.

Victor, J. D. (2006). "Approaches to Information-Theoretic Analysis of Neural Activity." Biol Theory 1(3): 14.

Victor, J. D. and K. P. Purpura (1996). "Nature and Precision of Temporal Coding in Visual Cortex: A Metric-Space Analysis." J Neurophysiol 76(2): 17.

Victor, J. D. and K. P. Purpura (2010). "Spike Metrics." 129-156.

Weinrich, M. and S. P. Wise (1982). "The premotor cortex of the monkey." The Journal of Neuroscience 2(9): 1329-1345.

Wise, S. P. (2008). "Forward frontal fields: phylogeny and fundamental function." Trends Neurosci 31(12): 599-608.